6-25-2021 1:00 PM

The effects of decellularized adipose tissue constructs on mesenchymal stromal/stem cell phenotype and pro-angiogenic secretory function.

Yehia Moharrem, *The University of Western Ontario*

Supervisor: Hess, David, *The University of Western Ontario*
Co-Supervisor: Flynn, Lauren, *Univeristy of Western Ontario*
A thesis submitted in partial fulfillment of the requirements for the Master of Science degree in Physiology and Pharmacology

Abstract

Due to limited treatment options for critical limb ischemia (CLI), cellular-based therapies have been investigated to induce blood vessel regeneration. Bone marrow-mesenchymal stromal/stem cells (BM-MSC) have shown pre-clinical success in animal models of CLI as they possess pro-angiogenic and immunomodulatory functions. However, clinical translation has been hindered by inadequate expansion and delivery strategies. This project aimed to characterize the phenotype and pro-angiogenic secretory function of BM-MSC on decellularized adipose tissue (DAT) bioscaffolds as expansion platforms. Compared to cells grown on tissue-culture plastic, DAT substrates supported BM-MSC growth, regenerative marker expression, and pro-angiogenic secretory function. Conditioned media generated by BM-MSC cultured on DAT coatings were enriched with factors associated with wound healing and significantly increased human endothelial cell survival under serum-free conditions *in vitro*. Overall, these studies show that DAT constructs present a promising tissue engineering approach to expand MSC while enhancing regenerative potential.

Keywords: Lower Extremity Arterial Disease, Angiogenesis, Cellular-based Therapies, Mesenchymal Stromal/Stem Cells, Biomaterials, Decellularized Adipose Tissue

Summary for Lay Audience

Lower Extremity Arterial Disease (LEAD), also known as Peripheral Artery Disease (PAD), is caused by plaque accumulation in the blood vessels to the limbs, leading to reduced blood supply to the lower limbs. If the blood supply is reduced enough, patients will develop the most severe form of PAD known as critical limb ischemia (CLI). Patients with CLI present with resting limb pain, non-healing ulcers, and gangrene. Unfortunately, due to limited treatment options, many patients may require limb amputation and face a very high mortality rate. As a result, there has been interest in cellular-based therapies to regenerate new blood vessels in ischemic limbs. Bone marrow-derived mesenchymal stromal/stem cells (BM-MSC) are regenerative cells that have demonstrated promising therapeutic results in stimulating blood vessel formation in animal models of CLI. However, this benefit has not yet been translated clinically, as challenges with cell expansion and survival after injection have limited clinical progress. Generating enough cells for clinical use is a challenge as expanded cells lose regenerative abilities. Cell delivery is also difficult, with poor cell retention and survival after injection into the affected limbs. This project aimed to improve BM-MSC expansion by investigating alternative culturing methods using human fat-derived bioscaffolds. Compared to conventional culturing on plastic, fat-derived bioscaffolds increased the yield of viable BM-MSC and retention of cell markers associated with enhanced regenerative capacity. Additionally, culturing BM-MSC on fat-derived bioscaffolds enhanced their secretory abilities and their capacity to promote endothelial cell survival *in vitro*. Overall, this study aimed to enhance BM-MSC culture using biomaterials to improve MSC-based CLI therapies.

Co-authorship Statement

All work presented in this thesis was performed by Yehia Moharrem, co-supervised by Dr. Lauren Flynn and Dr. David Hess. Dr. Tyler Cooper from Dr. Gilles Lajoie's lab performed the proteomic analyses. Gillian Bell assisted with animal surgeries and care. Dr. Lauren Flynn and Dr. David Hess contributed to the design and interpretation of all experiments.

Acknowledgements

First and foremost, I'd like to thank my supervisors and mentors, Dr. Lauren Flynn and Dr. David Hess. Your immense support, encouragement, and guidance was integral to the progression of this project, and this thesis is an accumulation of both your mentorships. You were extremely supportive both inside and outside the lab setting and fostered a positive environment that would encourage any student to grow as a researcher and as a person. Thank you for providing me the independence to explore different directions for my project, while guiding me towards progress. Your ongoing patience and support have been instrumental to my development as a scientist, and the lessons learned under your mentorship will forever be with me.

I would also like to thank my advisory committee members, Dr. Rob Gros and Dr. Lina Dagnino. Your insight and expertise were paramount to the progression of this project, and your passion for research pushed me to grow and expand my skills as a researcher.

To all members of the Flynn and Hess labs, thank you for your support and warm welcome since I started, you made my experience very memorable and I will forever be grateful. I would like to thank Gillian Bell, for all your training, expertise, and encouragement, with many skills that were valuable for this project. You always made the lab environment positive, fun, and supportive; it made my experience at the lab truly rewarding. A special thank you to Brianna Ananthan, Chris Leclerc, Naz Rasiwala, Fiona Serack, Anna Kornmuller, for being amazing friends, mentors, and colleagues. Your support and contributions directly lead to the progression of this thesis, thank you.

Finally, I would like to thank my parents and brothers, Yusuf and Omar, thank you for always listening and being supportive. Your support through this journey through the ups and downs was integral to my development as a person as well as the completion of this thesis. To my very close friends Hashir, Aboudie, Omar, and Umar, thank you for making this an effortless journey and pretending to understand what my work is on. Although you could not directly help run experiments, the phone calls, food, walks, bonfires, and long drives were more helpful than you can imagine. This thesis is the result of all your support and encouragement. I love you all.

Table of Contents

List of Figures

List of Tables

List of Appendices

List of Abbreviations

7-AAD – 7-aminoactinomycin D

ABAM – Antibiotic antimycotic

AMBIC – Ammonium bicarbonate

ABI – Ankle-Brachial Index

ACN - Acetontirile

ALDH – Aldehyde dehydrogenase

ANG-1,2 – Angiopoeitin (isoforms 1 and 2)

ANOVA – Analysis of variance

ASC – Adipose-derived stromal cells

BCA – Bicinchoninic acid assay

BDNF – Brain-derived neutrotrophin factor

bFGF – Basic fibroblast growth factor

BM –Bone marrow

CdM – Conditioned media

CFU-F – Colony forming unit - fibroblast

CLI – Critical limb ischemia

CVD – Cardiovascular disease

DAT – Decellularized adipose tissue

DDR – Discoidin domain receptor

DEAB – N,N-diethylaminobenzaldehyde

DIVAA – Directed in vivo angiogenesis assay

DRAQ5 – 1,5-bis2-(di-methylamino) ethylamino-4, 8-dihydroxyanthracene-9,10-dione

DTT - Dithiothreitol

EBM – Endothelial basal media

EC – Endothelial cell

ECM – Extracellular matrix

EdU - 5-Ethynyl-2′-deoxyuridine

EGF – Epidermal growth factor

EGM – Endothelial growth media

EPC - Endothelial progenitor cell

EPO - Erythropoetin

EV – Extracellular vesicles

FA – Formic acid

FAL – Femoral artery ligation

FBS – Fetal bovine serum

FDR – False discovery rate

FMO – Fluorescence minus one

GAG - Glycosaminoglycans

G-CSF – Granulocyte – Colony stimulating factor

GVHD – Graft-vs-host disease

HGF – Hepatocyte growth factor

HIF-1α – Hypoxia inducible factor - 1α

HLA – Human leukocyte antigen

HMVEC – Human microvascular endothelial cells

HPC – Human progenitor cells

HSC – Hematopoietic stem cells

IDO – Indolamine 2,3-dioxygenase

IGF-1 – Insulin-like growth factor-1

IL-6 – Interleukin 6

ISCT – International society for cell & gene therapy

IT - Intrathecal

IV - Intravenous

LDL – Low-density lipoprotein

LNGFR – Low-affinity nerve growth factor receptor

LRFCF – London regional flow cytometry facility

MCP-1 – Monocyte chemoattractant protein-1

miR – micro RNA

MMP – Matrix metalloproteinases

MNC – Mononuclear cells

MS - Mass spectrometry

MSC – Mesenchymal stromal/stem cells

NGF – Nerve growth factor

NO – Nitric oxide

NOD – Non-obese diabetic

NT - Neutrotrophin

PAD – Peripheral artery disease

PBS – Phosphate buffered solution

PDGF – Platelet-derived growth factor

PGE-2 – Prostaglandin E2

PHD – Prolyhydroxylase

ROS – Reactive oxygen species

RT – Room temperature

RTK – Receptor tyrosine kinase

SCID – Severe combined immunodeficient mice

SDF-1 – Stromal derived factor-1

SDS – Sodium dodecyl sulfate

SMC – Smooth muscle cell

TCP – Tissue-culture plastic

TF – Tissue factor

TFA – Trifluoric acid

TGF-β – Transformation growth factor-β

TIMPs – Tissue inhibitor of metalloproteinases

TNF-α – Tumor necrosis factor-α

UPLC – Ultra performance liquid chromatography

VEGF-A – Vascular endothelial growth factor - A

VEGFR2 – Vascular endothelial growth factor receptor 2

vWF - Von Willebrand factor

Chapter 1.0 Introduction

1.1 Ischemic Cardiovascular Disease

The cardiovascular system plays an integral role in the circulation of blood throughout the body in order to deliver vital nutrients and oxygen and to remove cellular waste from metabolic activity[1]. This is achieved through a complex network of arteries, veins, and capillaries. Lining the walls of blood vessels is an interconnected system of endothelial cells (EC) that act as a barrier between blood circulation and tissues[1,2]. The endothelium serves to regulate vascular tone, blood flow, and platelet function[3–5]. Dysfunction of the endothelium is a major contributor to cardiovascular disease (CVD) which refers to any condition affecting the heart or vascular system[3,6]. Ischemic CVD are often complications of atherosclerotic plaque accumulation in the blood vessel walls, which impairs blood flow to target organs[7–9] and leads to myocardial infarction, coronary artery disease, peripheral artery disease, and stroke[1,6,7,10]. Collectively, CVD remains the leading cause of death worldwide, claiming 17.9 million lives in 2017[6,11]. In the last two decades, the incidence of CVD has grown by > 120% and is expected to continue to grow over the next decade[12,13]. In addition to high rates of morbidity and mortality, CVD also places a tremendous economic burden on the health care system, costing $213 billion per year in the United States alone[11,14].

1.2 Blood Vessel Structure and Function

The anatomy of blood vessels generally consists of EC, smooth muscle cells (SMC), pericytes, fibroblasts, and extracellular matrix (ECM) consisting of elastin, collagen, and glycosaminoglycans[3,15]. The vessel wall is comprised of three major layers that can be histologically distinguished in large vessels[16]. The outermost layer consists of the tunica adventitia, providing shape and structural integrity through collagen-rich connective tissue and fibroblasts[15]. The middle layer is the tunica media, composed of collagen and smooth muscle tissue, which regulates artery diameter through muscle contractions, playing a crucial role in regulating blood flow[4,16]. Lastly, the innermost layer, the tunica intima, consists of a single-cell endothelial lining that provides a pathway for blood to travel[4,15]. Within each layer, the relative composition of muscle and collagen content differ depending on the size and location of the blood

vessels. This ensures vessels are suited for unique physiological roles throughout the body. Large blood vessels such as the aorta contain high elastin content and have relatively low smooth muscle to withstand the great pressure generated by powerful contractions of the heart[1,15]. As vessels leave the heart and bifurcate into smaller arterioles, smooth muscle content increases to allow for spatial control over blood velocity through inner diameter regulation[17]. Vessels eventually bifurcate into small capillaries, composed of a single EC layer attached to a basal lamina[1,3]. Here nutrients, metabolites, and gases are exchanged to feed the target tissue and eliminate cellular waste, with the thin walls allowing for efficient diffusion[18]. Surrounding the single endothelial cell layers are supportive cells called pericytes, which wrap around and stabilize the vessels[19].

1.2.1 Endothelial Cell Homeostasis

The role of EC in vascular homeostasis was first described in detail by Furchgott & Zawadzki in 1980[20]. EC are found in all the blood vessels lining the inner tunica intima, and are heavily involved in regulating blood flow, formation of new blood vessels, and site-specific infiltration of immune cells[20,21]. In the arterioles, EC regulate vasomotor tone through complex chemical communication with SMC to regulate vessel diameter. EC predominantly achieve this through nitric oxide (NO) production and release in response to chemical or physical cues from the surrounding tissues, inducing local vasorelaxation[4,20,22,23]. EC also regulate immune cell infiltration through locally secreted inflammatory cytokines following tissue injury to initiate repair. EC recruit immune cells by upregulating expression of adhesion molecules, such as vascular endothelial adhesion molecule-1 (VCAM-1) to bind circulating immune cells and initiate infiltration into the injured tissue[23–25]. EC also secrete enzymes to control coagulation following tissue injury to prevent blood loss[3,21,23]. Following tissue injury, a chain of pro-inflammatory and regenerative processes are triggered. First, sub-endothelial collagen fibers are exposed to circulating blood, which activates EC and promotes adhesion of circulating platelets through von Willebrand Factor (vWF), initiating the clotting process[21,26]. Activated EC also express tissue factor (TF), which proteolytically cleaves a series of inactive coagulation factors to ultimately produce thrombin[27]. Thrombin activates adhered platelets to form platelet aggregates, further activating other pro-coagulation factors[21,27]. Finally, thrombin also generates insoluble fibrin through a cross-linked fibrin mesh, and together the platelet aggregates and fibrin networks form a stable clot to prevent blood loss[21,23,26].

1.2.2 Atherosclerosis

Atherosclerosis is the most frequent initiator of CVD, characterized by the accumulation of plaque consisting of lipids, calcium, and fibrin[28]. Atherosclerotic plaque also has cellular components consisting of EC, leukocytes, and SMC[28]. As the plaque accumulates, it thickens the blood vessel wall, greatly obstructing blood flow to the target tissue[28]. Ultimately, atherosclerosis is the result of chronic inflammation associated with the accumulation of lipid molecules[9]. Although the direct cause remains controversial, factors such as elevated plasma cholesterol levels, hypertension, diabetes, smoking, and physical inactivity are among the greatest risk factors[12,29].

Not all arteries are equally susceptible to atherogenesis, and it has been shown that areas with lower laminar flow are more susceptible[30]. Due to effects on gene expression, cytoskeletal arrangement, leukocyte adhesion, and inflammation[28,30], an accumulation of these factors leads to EC dysfunction resulting in low-density lipoprotein (LDL) extravasating through the leaky and defective endothelium in the tunica intima layer of the artery[9,28]. Although still controversial, the LDL-oxidation hypothesis has been under investigation as a major cause for atherogenesis[9,28]. More specifically, following deposition, LDL particles interact with subendothelial ECM and are exposed to cell-derived oxidants, forming oxidized LDL[28,31]. LDL oxidation is also mediated by resident inflammatory cells[31], myeloperoxidase[32], lipoxygenase[33], and/or reactive oxygen species (ROS)[9]. The pro-inflammatory environment also activates EC[28], which recruit circulating leukocytes through upregulation of VCAM-1, E-selectin, and P-selectin[9,24]. During atherogenesis circulating monocytes are predominantly recruited and to a lesser extent, T-lymphocytes. Chemotaxis occurs by oxidized LDL and other pro-inflammatory cytokines, which facilitates leukocyte trans-endothelial migration[9]. Macrophages will uptake LDL particles through scavenger receptors and become lipid-filled foam cells and continue to uptake LDL until apoptosis or necrosis occurs, forming a soft and destabilized lipid-rich atherosclerotic core[9,28,34,35].

The inflammatory environment that is filled with apoptotic and necrotic immune cells stimulates SMC from the tunica media to migrate and proliferate to repair the injury[28,36]. This initiates a fibroproliferative response resulting in ECM deposition over the growing plaque to form a fibrous cap, which is susceptible to rupture[34]. Atherosclerotic plaque alone can greatly reduce blood flow, however in advanced stages the plaque can rupture and turn into a thrombus. The thrombotic-rich plaque can enter the circulation and rapidly coagulate to form an atherothrombotic clot[28]. The atherothrombotic clot can dislodge downstream

in a narrower vessel, causing a complete blockage and depending on the location, can present with a life-threatening event such as a myocardial infarction or stroke[28,29].

1.2.3 Peripheral Artery Disease

Peripheral artery disease (PAD) is characterized by the atherosclerotic narrowing of the arteries, where plaque accumulation in the extremities results in reduced blood flow to the limbs[37]. Lower extremity arterial disease (LEAD) is generally encompassed within the more general term of PAD that can affect any non-cardiac and non-intracranial arteries. PAD impacts more than 200 million individuals worldwide and places tremendous morbidity, mortality, and economic burdens on the health care system[37]. In the United States alone, it is estimated that PAD costs in excess of $21 billion according to 2016 estimates, a number that is projected to rise as the population ages[37].

Occlusions in LEAD are generally classified into two subtypes: proximal disease, resulting from obstruction in the aortoiliac and femoropopliteal locations and distal disease, involving the infrapopliteal location[37]. During the early stages of LEAD, patients can be asymptomatic. As such, many patients are underdiagnosed and undertreated, however, when luminal occlusion of the vessel is >50%, patients will begin reporting intermittent claudication and discomfort[38]. Hemodynamic analysis of blood flow in the limbs can be performed to screen for LEAD, by using laser-doppler imaging or ankle-brachial pressure (ABI) index[37]. The reduced blood supply creates a shortage of nutrient and oxygen delivery to tissues and if the occlusion progresses, patients will enter late-stage LEAD, known as critical limb ischemia (CLI)[37,38]. The reduced blood supply creates a cascade of pathophysiological events that results in patients presenting with resting limb pain, non-healing ulcers, and gangrene[37–39].

In response to ischemia, EC respond through vasodilation and arteriogenesis, thereby increasing blood supply through activation of pre-existing arteriole collaterals[40]. Arterioles eventually reach maximal vasodilation and become insensitive to pro-vasodilatory stimuli, ultimately failing to supply adequate blood to the limb[37,40,41]. Additionally, vessels affected in CLI have decreased wall thickness, decreased cross-sectional area, and decreased wall-to-lumen ratio, leading to increased fluid extravasation of fluid and subsequent edema[41]. The influx of fluid into the interstitial compartments of the limb increases the hydrostatic pressure, further impairing oxygen and nutrient diffusion to the limb[37,41].

In addition to macrovascular pathologies, microvascular pathologies also develop as the chronic ischemia leads to EC dysfunction[41]. Increased ROS production within the EC and surrounding tissues creates a highly inflammatory environment and results in inappropriate platelet activation, immune cell infiltration, and unregulated vasomotor control[10,21,41]. Collectively, these pathological factors lead to microthrombi formation, effectively impeding oxygen and nutrient exchange at the capillary level[39].

1.2.4 Current Therapeutic Approaches for CLI

Following diagnosis, the goal of treatment plans are to relieve ischemic pain, heal ischemic ulcers, prevent limb amputation, improve patient function and quality-of-life[37,38]. Revascularization bypass and endovascular catheterization procedures are employed to restore blood flow and salvage the limb[42]. Although these procedures are successful in improving quality-of-life, amputation and mortality rates remain high for individuals living with CLI[37]. Further, it is estimated that > 50% of patients do not qualify for surgical intervention due to diffuse blockages and various comorbidities[39]. Pharmacological interventions are also used, mainly to treat cardiovascular risks including medications to treat hypertension, hyperlipidemia, and diabetes, as well as antiplatelet agents to prevent clotting[37]. Due to limited treatment options, amputation is required in approximately 20% of patients and CLI has a mortality rate of up to 27% at 1-year post-diagnosis[43].

1.3 Blood Vessel Regeneration

During physiological development and in various pathologies, the body utilizes complex processes to generate new blood vessels to various organ systems[44]. This predominantly occurs through angiogenesis, vasculogenesis, and arteriogenesis, a series of complex processes that rely on the orchestration of many cells, chemical, and mechanical cues (Figure. 1.1)[45]. Angiogenesis and arteriogenesis are the predominant processes that occur in the adult organism and are in response to mechanical cues or tissue hypoxia to supply ischemic areas with essential oxygen and nutrients[44,45]. Oxygen and hemodynamic factors are thus crucial in regulating blood vessel regeneration. In the past 50 years, therapeutic control of angiogenesis has gained tremendous interest, as stimulating angiogenesis can be therapeutic in PAD and wound healing, while inhibiting angiogenesis can be therapeutic in cancer[46]

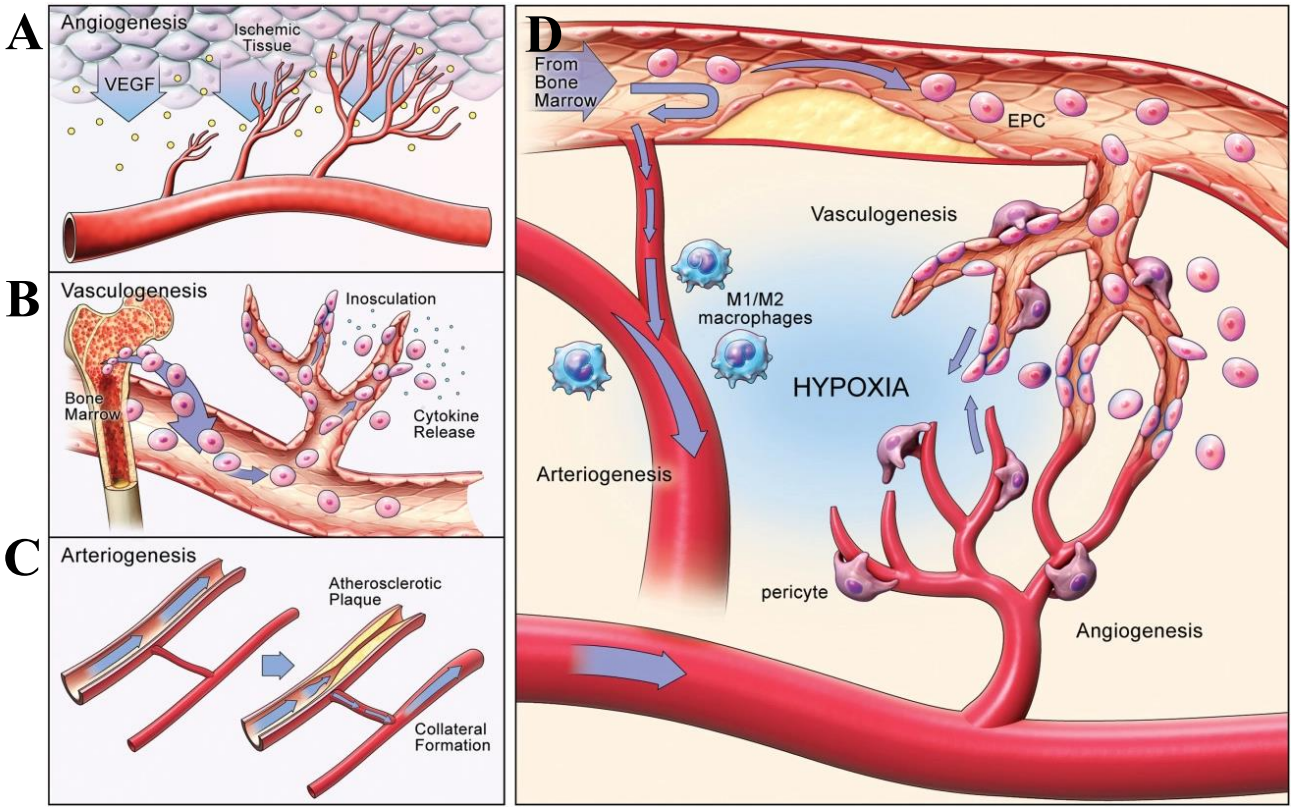

Figure 1.1 Overview of mechanisms for blood vessel regeneration. (A) *Angiogenesis,* the formation of new blood vessels from pre-existing vessels through sprouting or intussusception[17]. **(B)** *Vasculogenesis,* the de novo synthesis of new blood vessels from BM-derived endothelial progenitor cells[47]. **(C)** *Arteriogenesis,* shear stress induces remodelling of already existing collateral vessels that act as an alternative route for blood flow[48]. **(D)** All of these processes occur in concert and are crucial for vascular repair and regeneration. Figure adopted with permission[49].

1.3.1 Angiogenesis

The formation of new blood vessels from pre-existing vessels is termed angiogenesis, a complex multi-step process that is mediated by cytokines secreted from vessel-resident EC[44]. There are two types of angiogenesis, sprouting and intussusceptive angiogenesis[45,46]. The latter is also referred to as splitting angiogenesis, as it involves the formation of an intraluminal tissue pillar inside the vessel followed by

splitting into two separate conduits[50]. Intussusceptive angiogenesis occurs relatively quickly, as it does not require EC proliferation or migration, only reorganization of existing EC[51].

Hypoxia is the major driving force in stimulating sprouting angiogenesis, where cellular oxygen sensing mechanisms trigger new blood vessel formation to satisfy metabolic demands[46]. Hypoxia-inducible factor 1-α (HIF1-α) is a master regulator of oxygen homeostasis. Under normoxic conditions, proline residues of HIF1-α are marked for degradation through hydroxylation by prolyl-4-hydroxylase (PHDs) using oxygen as a co-factor, leading to ubiquitination and proteasomal degradation of HIF1-α[46,52]. Under hypoxic conditions, the activity of PHD is decreased, and HIF1-α translocates into the nucleus to bind HIF1-β. Together this heteromeric dimer induces the transcription of various proangiogenic factors such as vascular endothelial growth factor-A (VEGF-A), transforming growth factor-β (TGF-β), erythropoietin (EPO), platelet-derived growth factor (PDGF), and stromal derived factor-1 (SDF-1)[51,52] . Following the release of proangiogenic cytokines from tissue-resident cells due to hypoxia, factors bind to receptors on endothelial cells to stimulate angiogenesis[46,52]. Endothelial tip cells guide the development of the new capillary towards the angiogenic stimulus such as VEGF-A[52,53] (Figure 1.1A).

Sprouting angiogenesis relies on a delicate balance between numerous inhibitory and stimulatory angiogenic signals such as VEGF/VEGF-receptor (VEGFR) and angiopoietin-1(Ang1) /TIE2 receptor signalling pathways[54]. EC are maintained predominantly in a quiescent state, however, when a vessel senses a pro-angiogenic signal such as VEGF, Ang2, or fibroblast growth factor (FGF), a series of events occur to sprout a new blood vessel[46]. First, the permeability of the vessel is increased through VEGF activity[45], and a single EC becomes the tip cell to allow for coordinated migration towards a pro-angiogenic signal[46,55]. Lagging behind the tip cell are stalk cells, which divide to elongate the stock and will later form the lumen of the new vessel[51,55].

Thin cellular processes on the tip cells secrete proteolytic enzymes such as matrix metalloproteinases (MMPs), digesting a pathway through the ECM for the sprouting vessel[46,56]. Tip cells also possess filopodia to sense the surrounding environment and guide the elongating stalk[46,51]. The ECM provides critical structural and cell-instructive roles throughout the angiogenic process, and requires a balance between formation and degradation for physiological angiogenesis to occur[56]. To ensure matrix degradation is balanced, activated EC also secrete tissue inhibitors of matrix metalloproteinases (TIMPs) that inhibit MMPs[46]. An inner lumen forms through vacuole formation and coalescence within a series of stalk cells[51]. Maturation and stabilization of the new blood vessel are then achieved by the recruitment of pericytes to wrap around the blood vessel, as well as the deposition of ECM and resumed EC quiescent

state[46,51]. Notably, processes of this angiogenic cascade are also supported by cytokines and growth factors secreted by circulating myeloid progenitor cells and monocytes (collectively referred to as circulating angiogenic cells or CAC) and by matrix remodelling activities by polarized tissue macrophages.

1.3.2 Vasculogenesis

Vasculogenesis predominantly occurs in the developing fetus and is defined as the *de novo* synthesis of blood vessels from endothelial precursor / progenitor cells (EPC)[47,57]. In the embryonic yolk sac, vasculogenesis occurs in multiple blood islands in the mesodermal layer, mediated primarily by highly proliferative EPC. During embryonic development, EPC undergo coalescence to form major embryonic vessels from cords of adherent EC that become endothelial tubes through morphogenesis and form a vascular plexus[57,58].

It was first believed that vasculogenesis only occurred during embryonic development, however in 1997 Asahara isolated EPC from human bone marrow, using the hematopoietic marker CD34 and endothelial marker VEGFR2[59]. These markers are also expressed on hematopoietic stem and progenitor cells , as endothelial and hematopoietic precursors share a common progenitor during development[59]. Transplantation of $CD34^+/VEGFR2^+$ blood cells in immunodeficient mice with surgically-induced limb ischemia resulted in incorporation of the injected cells in new blood vessels, providing possible evidence of vasculogenesis[59]. Since then, a growing body of evidence has been investigating the occurrence of post-natal vasculogenesis in blood vessel maintenance (Figure 1.1B) which still remains controversial, and maybe stimulated by VEGF, granulocyte colony-stimulating factor (G-CSF), Ang-1, and SDF[57,60–63].

1.3.3 Arteriogenesis

Angiogenesis is primarily driven by hypoxia resulting from reduced blood supply or increased metabolic demand. In contrast, arteriogenesis is triggered by physical fluid and shear-stress forces[17,48]. Arteriogenesis is defined as the remodelling of pre-existing arterioles in fully developed blood vessels, or the growth of new collaterals in response to physical cues[48]. Redundancies in the vasculature exist, as collateral vessels with low blood flow supplying the same tissue can be activated to increase flow if

primary vessels become obstructed[48]. Blood is redirected through the collaterals from neighbouring vessels, and perfusion through the collateral arterioles induces a series of physiological changes to accommodate new blood supply.

As blood velocity increases through the vessel, it induces longitudinal shear stress sensed by EC[48,64]. This results in altered gene expression, primarily increasing the synthesis and release of NO, leading to vasodilation and subsequently increased blood flow[64]. Shear stress also induces the stimulation of VEGFR and further activates EC, leading to upregulation of monocyte chemoattractant protein-1 (MCP-1) and intracellular adhesion molecule-1 (ICAM-1), essential factors for the recruitment of monocytes[48,64]. Infiltrating monocytes release a variety of growth factors such as FGF, tumor necrosis factor alpha (TNF-α), and other chemokines that will induce matrix remodelling and the proliferation and migration of EC[48,64,65]. PDGF is also secreted by monocytes to promote SMC proliferation and pericyte stabilization of collateral vessels[64]. Collectively, this chain of events leads to the remodelling of the collateral vessel to become highly conductive and efficiently perfuse blood and nutrients to the ischemic area[64] (Figure 1.1C).

1.4 Cellular Therapies to Induce Vascular Regeneration

Due to limited treatment options for CLI, cellular-based therapies have been under intense investigation for the past few decades, focused on promoting angiogenesis and revascularization in patients with CVD[49,66]. To date, over 50 phase I/II clinical trials have investigated the therapeutic potential of a variety of cellular-based therapies to treat patients with PAD[49]. Most commonly, trials involved direct injection of bone marrow or peripheral blood-derived mononuclear cells (MNC), a heterogenous cell population of primarily mature cell types of the hematopoietic, endothelial, and mesenchymal lineages that support angiogenesis[49]. Although early clinical trials with autologous cells did not significantly reduce amputation rates, trials injecting unpurified autologous peripheral blood-MNC (PB-MNC) in CLI patients showed consistent improvements in ABI scores, pain-free walking time, wound healing, and ulcer healing compared to placebo[67–69].

Mesenchymal stromal/stem cells (MSC) are also under heavy investigation in cell therapies for CLI due to their pro-angiogenic, immunomodulatory, and differentiative potential into mural and perivascular cells[70]. Allogenic transplantation of BM-MSC increased ABI at 6 months compared to placebo[71], further

when injected into the ischemic hind limb of rats, BM-MSC induced greater perfusion and capillary density increase than BM-MNC[49,72]. A trial involving 41 CLI patients comparing BM-MSC and BM-MNC transplantation showed that the BM-MSC cohort had greater ulcer healing rates, limb perfusion, pain-free walking times, and ABI[73]. Thus, MSC represent a promising therapeutic cell source to treat patients with CLI. However, the field has yet to see a successful phase III trial. As such, further research is still being conducted to utilize the pro-angiogenic potential of BM-MSC and push the use of cellular based therapies a step closer to mainstream clinical use.

1.4.1 Mesenchymal Stromal/stem Cells

In 1974 Alexander Freidenstein isolated murine bone marrow cells that were distinct from hematopoietic stem cells (HSC)[74]. Freidenstein termed these cells colony forming units of fibroblasts (CFU-F), characterized as plastic adherent cells with clonogenic potential that were inherently osteogenic[75]. Subsequently, numerous contributions showed CFU-F also possessed adipogenic and chondrogenic differentiative capacities in culture and the population was subsequently termed multipotent stromal cells or MSC[76,77]. This supported Arnold Caplan's theory of the existence of a mesenchymal stem cell (also MSC) in the bone marrow[78], highlighting CFU-F's mesenchymal origin and their vast therapeutic potential[79]. However, the use of the term "stem cell" to describe these cells has long been debated as direct evidence of self-renewal remains controversial. As such, the nomenclature "mesenchymal stromal/stem cells" is now often used to describe this cell population[80].

MSC reside in the connective tissues of most organs, and many labs have isolated MSC or MSC-like cells from various tissues including skeletal muscle, adipose tissue, umbilical cord, pancreas, blood vessels, dental pulp, liver, and lung[81–86]. However, heterogeneity exists in cell surface marker expression and differentiative capacity between these MSC populations. Additionally, there has been great debate over the appropriate purifying techniques from different sources[79]. Hence, the International Society of Cell & Gene Therapy (ISCT) set the following three minimal defining criteria to characterize MSC: 1) tri-lineage differentiative abilities into fat, bone, and cartilage in culture; (2) plastic adherence, and (3) exhibit >95% cell surface expression of the stromal markers CD73, CD90, and CD105 while lacking the expression of the hematopoietic markers CD45, CD14, CD11b, CD19 and human leukocyte antigen (HLA) isotype DR in ≤ 2% of cells[79,87].

In addition to their phenotypic and differentiative traits, MSC also possess great regenerative potential to repair tissue damage in response to injury through the production and secretion of immunomodulatory and pro-angiogenic factors (Figure. 1.2)[70,79,88]. These therapeutic benefits have been translated in preclinical models for various diseases including osteogenesis imperfecta, lung injury, kidney disease, diabetes, graft-vs-host disease, myocardial infarction, and neurological disorders[79,89–91]. It is thought that MSC exert this therapeutic benefit primarily through paracrine means[79], noted because in clinical and pre-clinical trials a significant improvement was observed despite extremely low and transient engraftment[77].

1.4.2 Therapeutic Potential of MSC

MSC are regenerative cells that preferentially home to areas of injury and initiate regenerative processes through the secretion of a variety of growth factors and cytokines[70,79,90,91]. Nagaya *et al*., showed that intravenously administered MSC homed to infarcted myocardium in ischemic heart models in mice and improved cardiac function following acute myocardial infarction by enhancing angiogenesis and myogenesis[92]. This therapeutic benefit was not due to MSC differentiative potential, but rather their paracrine activity[92,93]. Several studies have shown that MSC secrete a variety of factors that are immunomodulatory, antiapoptotic, and pro-angiogenic[70,88,94,95]. MSC-conditioned media (CdM) promoted endothelial cell tubule formation, survival and proliferation *in vitro*, with proteomic analysis showing the presence of pro-angiogenic cytokines VEGF, hepatocyte growth factor (HGF), MCP-1, interleukin 6 (IL-6), TGF-β1, insulin-like growth factor-1 (IGF-1), epidermal growth factor (EGF-1), SDF-1, and Ang-1, that were secreted depending on the culture conditions[70,79,92,94–96]. Additionally, injected MSC CdM increased blood vessel formation and promoted blood flow in mice with surgically induced limb-ischemia[96]. MSC CdM also increased endothelial cell migration and survival[94,97], and improved EC growth and EPC recruitment to the ischemic limb in CLI-mouse models[95,96].

MSC also exert a therapeutic effect through the production of membrane-enveloped exosomes involved in the induction of tissue regeneration and angiogenesis[98]. Exosomes are extracellular vesicles, approximately 30-100 nm in diameter that contain genetic material and other bioactive factors including proteins, RNA and lipid molecules[99]. MicroRNA (miR), which regulate gene expression at the post-transcriptional level by binding to specific mRNA and inducing degradation or translational inhibition, are also found in exosomes. MiR are crucial to regulate various cellular physiologies such as cell cycle progression, hematopoiesis, cancer, and aging[100]. MSC have been found to secrete a wide array of pro-

angiogenic miRs, such as miR-30b, miR-30c, miR-424, and let-7f. Notably, MSC were able to transfer miR through exosomes to human umbilical vein endothelial cells (HUVEC), resulting in increased tubule formation, suggesting a role of miR secretion by MSC within exosomes to support angiogenesis[98,100–102].

In addition to pro-angiogenic properties, MSC also attenuate inflammation, a delicate process that must be regulated during wound healing and angiogenesis[103,104]. The addition of MSC to an inflammatory environment induces the secretion of various immunomodulatory cytokines such as prostaglandin E2 (PGE-2), indoleamine 2,3-dioxygenase (IDO), NO, IL-6, HGF and TGF-β[105–107]. These effectors are involved in a myriad of complex reciprocal signalling with various inflammatory cells, leading to the formation of immunoregulatory T cells[108], conversion of pro-inflammatory M1 macrophages to regenerative M2 macrophages[88], and downregulation of natural killer cell activity[105]. *In vitro,* MSC supress mixed lymphocyte reactions and are a key regulator of adaptive immune responses, modulating lymphocyte proliferation and apoptosis[108,109]. MSC also prevented graft rejection in a baboon skin allograft model and have mediated immunosuppression in several mouse models[109]. In 2012, Health Canada approved the use of MSC in the treatment of graft-vs-host disease, utilizing their potent immunomodulatory properties[110]. It is the immunosuppressive qualities of MSC that make them a promising therapeutic cell source to treat inflammatory diseases such as atherosclerosis, diabetes, critical limb ischemia, allergy, asthma, and hepatitis[103,104,109].

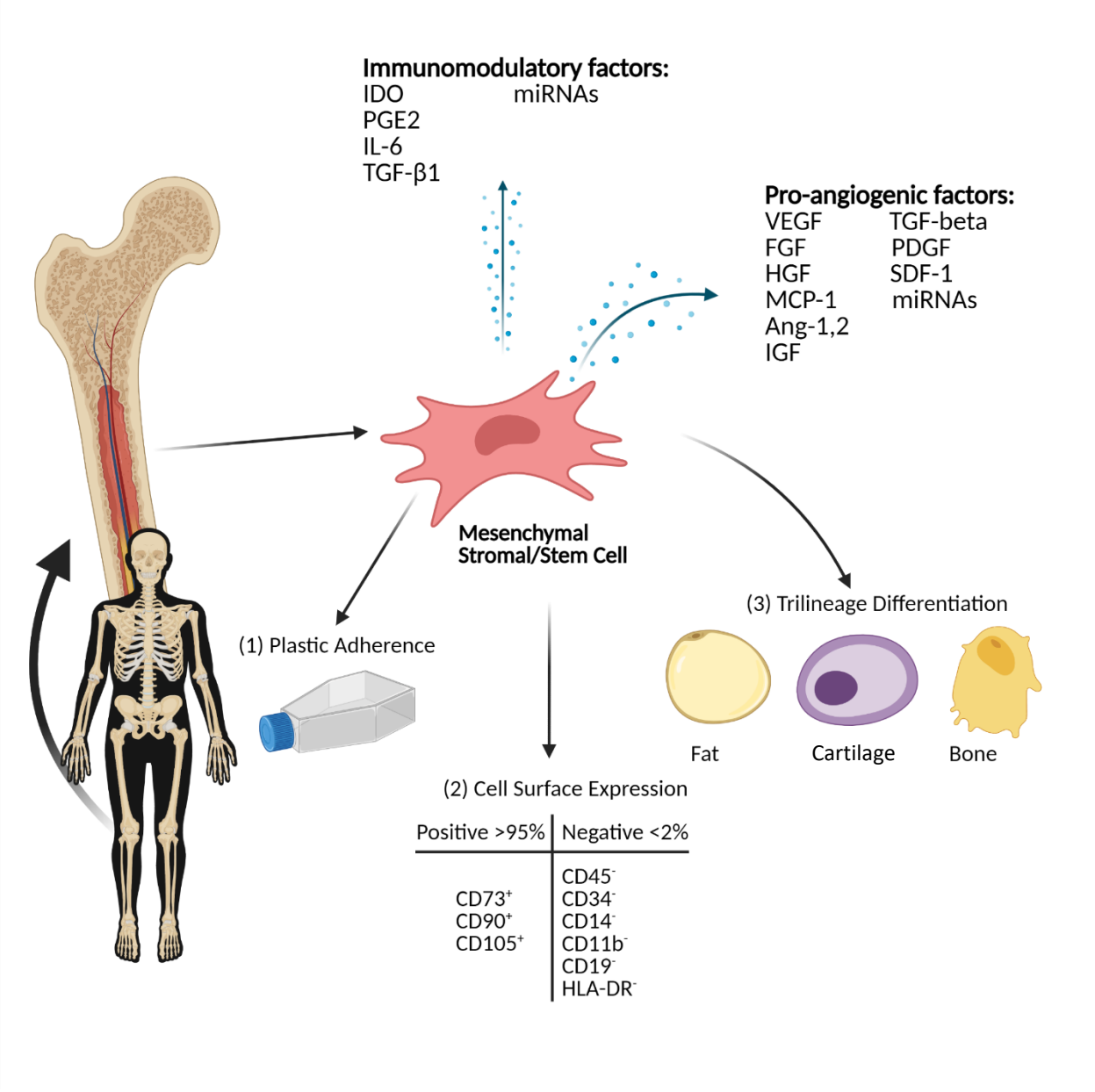

Figure. 1.2 Overview summary of bone marrow mesenchymal stromal/stem cell properties. MSC can be obtained from the bone marrow, and are characterized according to three minimal defining criteria; *(1)* plastic adherence, *(2)* cell surface marker expression, and *(3)* multipotent differentiative capacity into fat, bone, and cartilage[87]. In addition to these properties, MSC secrete a wide array of pro-angiogenic and immunomodulatory cytokines and miRNAs involved in blood vessel formation and the inhibition of excessive inflammation[79]. Figure generated using Biorender.

1.4.3 Current Limitations of Cellular-based Therapies for Ischemic CVD

Although preclinical progress has yielded promising results, challenges associated with MSC expansion and delivery have hindered clinical translation[49]. Notably, the survival of MSC after direct injection into the ischemic limb is transient[72], and cell delivery is complicated by detachment-induced apoptosis initiated upon detaching cells from plastic prior to transplantation[111]. Additionally, the requirement to generate many cells with preserved pro-angiogenic function has posed a challenge. It is estimated that billions of cells will be required for therapeutic purposes in humans, a critical challenge, as MSC lose desired characteristics such as pro-angiogenic secretory potential and differentiative properties through extensive proliferation[49,111,112]. After 4 passages (20-30 generations), more than half of the cells have been reported to stop proliferating and their differentiative capacity is diminished[113,114]. For clinical applications, expansion presents a critical challenge as generating enough cells leads to a significant frequency of cells that no longer possess the required proliferative and differentiative phenotype[115]. Furthermore, BM-MSC from different donors exhibit tissue-specific molecular and functional heterogeneity, leading to varying levels of immunomodulatory and pro-angiogenic affects[49,113].

Conventionally, BM-MSC are cultured on rigid tissue-culture plastics (TCP). Notably, this simplified 2-D culture of BM-MSC does not recapitulate the complex biochemical and biomechanical properties of the native ECM-rich environment, resulting in unwanted cell differentiation and loss of secretory function during expansion[49,113–116]. The presence of an ECM-rich environment exerts an effect on MSC through a variety of cell surface receptors. Thus, ECM-derived scaffolds can provide cell-instructive cues to modulate MSC proliferation, differentiation, and regenerative capacity[115,117,118]. Lastly, BM-MSC are typically cultured under static culturing conditions, which lack mechanical stimulation that can provide important cues that can direct cell phenotype and function through mechano-transduction[119]. Combining ECM scaffolds with three-dimensional (3D) dynamic culturing platforms, such as the use of spinner flask bioreactors, may provide an alternative platform to expand and deliver BM-MSC and harness their therapeutic potential[120].

1.5 The Extracellular Matrix

The ECM is composed of a wide variety of macromolecules that form organized structures to support cell homeostasis[115,121]. Beyond structural support as physical scaffolds, the ECM also provides crucial

biochemical and biomechanical cues that regulate cell growth, migration, differentiation, survival, and morphogenesis[121–123]. Fundamentally, the ECM consists of water, proteins, and polysaccharides, however the exact components are tissue-specific, as each niche has a unique composition and structural organization[124]. During tissue development, crosstalk exists between cellular and ECM components that guide the unique remodelling of a tissue-specific ECM[122–124]. Through physical and compositional characteristics, the ECM generates unique structural and biochemical properties in each organ, such as tensile and compressive strength, elasticity, and water retention[124]. Additionally, ECM composition is governed by dynamic processes that can vary greatly not only between different tissues, but between physiological and pathological states in response to cellular cues[124,125]. Lastly, the ECM acts as a reservoir for a variety of latent growth factors, cytokines, and chemokines that are sequestered through specific ECM binding, and are liberated at physiologically and pathologically relevant times[121,124,125].

Cells interact with the ECM through a series of cell surface receptors. More specifically, cell adhesion is mediated by integrins, discoidin domain receptors (DDRs) and syndecans[126]. Binding of integrins to the ECM initiates a bi-directional mechano-transduction signal that regulates gene expression and induces a variety of signalling molecules to reorganize the cell cytoskeleton and activate various intracellular pathways[127,128]. A myriad of signalling pathways can be initiated depending on the integrin heterodimer bound, and the exact ECM composition[126,128].

1.5.1 ECM Composition and Structure

The ECM is predominantly composed of collagen, elastin, glycoproteins, and proteoglycans/glycosaminoglycans, each serving unique structural and/or functional roles[122]. Broadly, ECM components can be divided into structural components consisting of collagen and elastin[124,129] and non-structural components consisting of fibronectin, laminins, and other glycoproteins[124,130]. The most abundant protein in the ECM is collagen, a family of fibrous proteins that provide structural support to tissues. To date, 28 different types of collagen have been characterized[123,124,131]. Fibrous collagens include collagen types I, II, III, V, and XI, while collagen type IV is classified as a network type or sheet-like forming collagen[123]. Fibrous collagens impart stiffness and tensile strength to connective tissues to withstand tension, shear, and pressure forces[123,132]. Collagen also possesses a functional role in the ECM and guides adhesion, proliferation, migration, and tissue development through integrin singalling[124,133].

Elastin can be combined with collagen to provide tissue elasticity and is predominantly composed of tropoelastin subunits cross-linked to an outer layer of microfibrils[124,134].

Fibronectin is another fibrous protein that is involved in directing cell attachment through pleotropic effects and functions as a mechano-regulator of cell behaviour and wound healing[124,135]. Laminins, are glycoproteins involved in mediating multiple cell functions including migration and differentiation through their target integrin receptor binding[122,136].

Proteoglycans are another crucial component of the ECM and consist of a core protein covalently attached to one or more glycosaminoglycan (GAG) chains, which play a major role in water retention [122,124]. GAGs and proteoglycans bind a variety of growth factors, which establishes cytokine gradients in the ECM that play vital roles during tissue development[121]. GAGs are also directly cell-instructive, playing a role in cell survival, proliferation, and migration[124,127]. The bioactivity of GAGs is achieved directly through intra-cellular signalling pathways, or indirectly by sequestered cytokines and growth factors that are released following ECM degradation[127,137].

Collectively, the complex composition of the ECM allows for a cell-instructive niche to support cell homeostasis and initiate appropriate responses to various pathologies and tissue injury[122–124,126]. Hence, the use of ECM to guide and support cell growth presents as an alternative expansion platform to direct cell behaviour using 3D engineered biomaterials[138].

1.5.2 The Effects of ECM on MSC

MSC possess a variety of cell surface receptors that allow for cell adhesion and interactions with the ECM, sensing structural and biochemical cues, which regulate proliferation and guide lineage-specific differentiation[115]. The composition, mechanical properties, and surface topography of the ECM elicit a variety of responses in MSC[115,139]. For example, MSC express tissue-specific transcription factors when cultured on substrates mimicking the elastic properties of different organs[139,140], and when cultured on soft substrates MSC better maintained multipotency compared to culture on stiff substrates[141]. Additionally, ECM stiffness can direct lineage-specific differentiation, where soft substrates promote cell rounding which favours adipogenic differentiation, and stiff substrates promote elongation, favouring osteogenic differentiation[140,142,143]. ECM stiffness and composition also affect MSC pro-angiogenic and

immunomodulatory properties, where culture on softer substrates enhanced the secretory potential of MSC in stimulating EC tubulogenesis[144,145].

MSC also secrete their own ECM, and recent interest has developed in obtaining ECM-derived from MSC for biomaterial applications[115]. Culture on ECM derived from MSC improved MSC proliferation, differentiative abilities, and reduced cellular senescence compared to culture on TCP or matrigel[115,146,147]. Compositional differences have also been observed between ECM produced by early and late passage MSC. Further, ECM produced by early MSC was able to rejuvenate properties of highly-expanded, late-passage MSC[115,119,148]. Finally, various components of the ECM when used alone can guide MSC behaviour. Tropoelastin, an ECM structural component, has been shown to improve human MSC expansion through integrin signalling and may reduce the need for serum requirements in culture[140,149,150]. Overall, these bioactive effects illuminate the complex role of the ECM in guiding and maintaining the growth, proliferation, and therapeutic potential of MSC, and warrants the investigation of utilizing ECM to enhance the pro-angiogenic potential of MSC in this thesis.

1.5.3 Decellularized Tissue as an ECM Source

To produce an ECM-like environment, decellularized materials that retain native chemical and mechanical composition have garnered tremendous attention in the past few decades[151]. To develop decellularized scaffolds for culture and delivery, tissues can be obtained and decellularized to remove cellular and immunogenic components, while the structural and functional proteins are minimally disrupted[152]. There are many methods for decellularization including physical, chemical, and enzymatic processes. Physical treatments use sonication, agitation, and/or freeze/thawing cycles to release cellular content[153]. Chemical treatments rely on detergents, organic solvents, chelating agents, and/or ionic solutions to disrupt cell membranes[152,153]. Finally, enzymatic treatments utilize proteolytic enzymes to degrade proteins and nucleases to digest nucleotide bonds[152]. Various methods are often combined to generate tissue-specific protocols to ensure efficient decellularization while conserving the native ECM structure and biochemical composition as much as possible[152,154]. Decellularized scaffolds have been fabricated from a variety of tissue sources including heart[155], blood vessels[156], lung[157], skin[158], nerve[159], cornea[160], liver[161], kidney[162], and fat[163], which have been investigated for various tissue engineering and regenerative medicine applications[154].

Decellularized scaffolds provide cell-ECM interactions that stimulate intracellular signalling pathways to regulate cell survival, proliferation, and differentiation[115,118,140]. Hence, decellularized scaffolds are promising biomaterials to enhance the survival and pro-angiogenic capacity of MSC. Further, decellularized scaffolds may be safe for clinical use since immunogenic components are removed, and ECM constituents are minimally immunogenic as they are generally conserved amongst species[152,164,165]. Although xenogeneic implants are well tolerated, it is not preferred due to various complications that can arise from xenogeneic rejections from residual cellular contamination[154]. As such, clinical applications should preferably use abundantly available human tissue sources that are rich in ECM and can be decellularized for tissue engineering applications.

1.5.4 Decellularized Adipose Tissue

Adipose tissue is abundantly found throughout the body and serves many essential roles in physiological homeostasis[166]. Beyond its energy storage roles, adipose tissue is a highly active metabolic and endocrine organ and serves an important role in providing body heat insulation and a protective cushioning for organs[166,167]. In addition to adipocytes that store energy in the form of triglycerides, many different cells exist in the complex niche of adipose tissue including stromal, nerve, vascular and immune cells[167,168]. These cells are anchored by an ECM-rich environment[169,170] and the porous cell-instructive nature of the ECM allows for adipose tissue to be highly vascularized to support complex metabolic and endocrine roles[171,172].

The ECM within adipose tissue is rich in collagen types I – VI, and also contains fibronectin, laminins, proteoglycans, and GAGs[163,170,172,173]. Further, it is readily available from routinely discarded waste during liporeduction surgeries, allowing sufficient quantities to be obtained with relative ease for research and clinical applications[163]. Hence, decellularized adipose tissue (DAT) represents a promising biomaterial to fabricate ECM-rich scaffolds to support cell expansion and delivery.

In 2010, the Flynn lab developed a protocol for fabricating DAT scaffolds as a biomaterial for soft tissue engineering strategies, which utilizes a detergent-free protocol of chemical, enzymatic, and physical processing to remove cellular components while retaining native ECM composition[163].The use of DAT for a variety of applications including soft tissue and vascular regeneration have since been investigated. For soft tissue regeneration, when seeded with adipose-derived stromal cells (ASC), DAT provided an

adipogenic-instructive microenvironment *in vitro* and induced pro-angiogenic responses *in vivo*[174]. Further, DAT implants stimulated an adipogenic and angiogenic response by inducing a more pro-regenerative macrophage phenotype[175]. Overall, DAT scaffolds were well tolerated and integrated well with the host tissues and provided a promising platform for accelerating wound healing[138,174,175].

Additionally, the Flynn lab has developed various protocols to fabricate many different DAT bioscaffold formats including coatings, foams, and microcarriers, each suited for unique tissue regeneration applications[163,175–177]. A recent collaboration with the Hess lab showed that DAT foams seeded with human hematopoietic progenitor cells (HPC) increased cell retention, recovery of limb perfusion, and improved functional limb use in the ischemic limb of CLI-mouse models in comparison to saline controls[178]. Microcarriers are also of specific interest as a cell expansion platform, as they can be utilized within stirred bioreactor systems to achieve dynamic culturing conditions, and could also potentially be applied as an injectable delivery vehicle[120].

1.5.5 Effects of Dynamic Culture on MSC Expansion and Differentiation

Cellular-based therapies have faced challenges in achieving scalable, robust, and cost-effective processes to generate clinically-applicable cell numbers without the loss of therapeutic potential[112,113,179]. Microcarrier technology presents an alternative culturing method involving spherical microcarriers that can be suspended in growth medium to enable cell adherence under dynamic conditions[180]. Since initial characterization in 1967 by Van Wezel[181], a variety of microcarriers have been fabricated with differing size, porosity, composition, and surface modifications tailored to unique *ex vivo* applications[180].

Dynamic culture can be achieved by suspending microcarriers in variety of reactors including rotating wall microgravity bioreactors[182], fluidized-bed bioreactors[183], and stirred-tank bioreactors[120,176]. The stirred bioreactor utilizes a spinning impeller to generate dynamic culture and allows for fine tuning of various parameters including pH, stirring rate, and oxygen tension[184]. Ultimately, microcarrier culturing strategies allow for efficient scale-up of cell production as they provide a high surface area : volume ratio, mechanical stimulation for cells, and can be fabricated out of various materials to provide a cell-instructive tissue engineering approach[180,181].

By electrospraying α-amylase digested DAT into liquid nitrogen, the Flynn lab generated DAT microcarriers comprised exclusively of ECM that were approximately 450 μm in diameter and are soft,

compliant, and highly porous[120,138,163]. When seeded on DAT microcarriers under dynamic conditions, ASC showed enhanced proliferation and tri-lineage differentiative capacity compared to cells cultured on commercially available Cultispher-S microcarriers[120]. Dynamic culture of MSC has been previously noted to enhance proliferation compared to conventional methods on TCP, and produced greater cell yields while reducing the need for enzymatic passaging[185,186]. Further effects on lineage-specific differentiation have been observed under different dynamic conditions, as varying shear stress may direct cell differentiation towards osteogenic or chondrogenic lineages[187–189]. Further, dynamic culture also affects MSC paracrine activity. More specifically, CdM generated by human ASC cultured under dynamic conditions contained higher concentrations of VEGF, bFGF, and HGF and promoted faster wound healing in athymic mice, compared to CdM generated from static culture on TCP[190]. Shear stress induced by dynamic conditions is thought to be one of the major factors stimulating MSC behaviour under dynamic culture, effectively altering MSC growth and differentiation, depending on the stirring rate used[189]. Overall, utilizing dynamic culture maybe a promising way to modulate the expansion, differentiation, and pro-angiogenic potential of MSC.

1.6 Project Overview

MSC serve as a promising therapeutic cell-based treatment for CLI as they secrete soluble factors that are immunomodulatory and pro-angiogenic. In preclinical studies, injection of BM-MSC into the ischemic limbs of mice with surgically induced CLI resulted in increased capillary density and improved limb perfusion. However, challenges associated with cell expansion, unwanted differentiation and sub-optimal delivery have hindered clinical translation. First, the requirement to generate many cells with preserved pro-angiogenic function has posed a challenge, as prolonged expansion can result in the loss of pro-angiogenic secretory function. Second, the survival of MSC after direct injection into the ischemic limb is transient, and cell delivery is complicated by detachment-induced apoptosis initiated upon preparing cells for transplantation. Utilizing the cell-instructive properties of ECM and the supportive properties of dynamic culture with microcarrier technology, the purpose of this project was to characterize the growth, cell phenotype, and pro-angiogenic secretory function of BM-MSC cultured on DAT substrates under dynamic and static conditions.

1.7 Hypothesis and Specific Aims

Based on the cell-supportive properties of DAT, it was hypothesized that BM-MSC cultured on DAT bioscaffolds would show enhanced growth, expression of MSC biomarkers, and pro-angiogenic secretory capacity compared to cells cultured on tissue culture plastic.

To address this hypothesis, the following specific aims were proposed:

> *AIM 1*. Characterize the viability and phenotype of BM-MSC cultured on DAT coatings and microcarriers in comparison to cells expanded on TCP.
>
> *AIM 2.* Assess the *in vitro* pro-angiogenic secretory function of BM-MSC cultured on DAT substrates in comparison to TCP cultured cells.

Chapter 2.0 Methods

2.1 DAT Scaffold Fabrication

2.1.1 Adipose Tissue Decellularization

Subcutaneous human adipose tissue was acquired with informed consent from patients undergoing elective breast reduction or abdominoplasty surgery from various clinics in the London area (University Hospital, Advanced Medical Group, St. Joseph Hospital, or Victoria Hospital, London, ON). Human Research Ethics Board approval was obtained from Western University (HREB #105426). Through a process previously optimized by the Flynn lab, adipose tissue was decellularized using a 5-day detergent-free protocol (Figure. 2.1)[163].

Briefly, tissue was excised into ~3 cm^3 blocks to maximize surface area and placed in a hypotonic solution containing 10 mM Tris base and 5 mM EDTA in dH_2O (pH 8.0) supplemented with 1% antibiotic-antimycotic solution (Gibco, Invitrogen, Carlsbad, CA, ABAM) and 0.07% phenyl-methanesulphonylfluoride (PMSF) (all steps included ABAM and PMSF supplementation, with exclusion of PMSF during enzymatic digestion). All agitation was performed at 37 ºC on an orbital shaker at 100 rpm. To initiate cell lysis, samples underwent 3 freeze-thaw cycles from - 80 ℃ to 37 ℃, with agitation during thawing and solution replacement after each thaw cycle. The tissue was then enzymatically digested with 0.25 % Trypsin-EDTA (Life Technologies, Carlsbad, CA) overnight under agitation. To remove lipid content, the tissue underwent polar solvent extraction in absolute isopropanol for 48 h, with solution changes twice daily. The samples were then rinsed in a rinsing buffer comprised of dH_2O with 137 mM NaCl, 2.68 mM KCl, 7 mM Na_2PO_4, and 1.47 mM KH_2PO_4. The tissue was then digested again for 6 h in 0.25 % Trypsin-EDTA and rinsed 3 times in rinsing buffer. To remove residual lipids and genetic material, the tissue was then incubated overnight in a digestion buffer comprised of 55 mM Na_2PO_4, 17 mM KH_2PO_4, 4.9 mM $MgSO_4 \cdot 7\ H_2O$, 15 000 U DNase Type II (from bovine pancreas), 12.5 mg RNase Type III A (from bovine pancreas), and 2000 U Lipase Type VI-S (from bovine pancreas). The tissue was rinsed 3 times in rinsing buffer and subjected to a final extraction in absolute isopropanol for 8 h.

At the end of processing, the DAT was rinsed 3 times in the rinsing buffer followed by dH_2O, transferred into 50 mL conical tubes, and frozen in -80℃. The DAT was lyophilized for 48 hours, and then minced with scissors into roughly 0.5 mm^2 fragments. Minced DAT was then placed in a milling chamber with

two 10-mm stainless steel milling balls and cryo-milled in a Retsch Mixer Mill 400 (Retsch, Haan, Germany). The chamber was submerged in liquid nitrogen for 3 minutes and milled for 3 minutes at 30 Hz. This was repeated for a total of three milling cycles until a fine powder was achieved. Cryomilled DAT (1 g) was collected in 50 mL conical tubes, weighed, and resuspended in 70% ethanol to decontaminate it prior to cell culture. Resuspended DAT was placed under agitation at room temperature (RT) overnight.

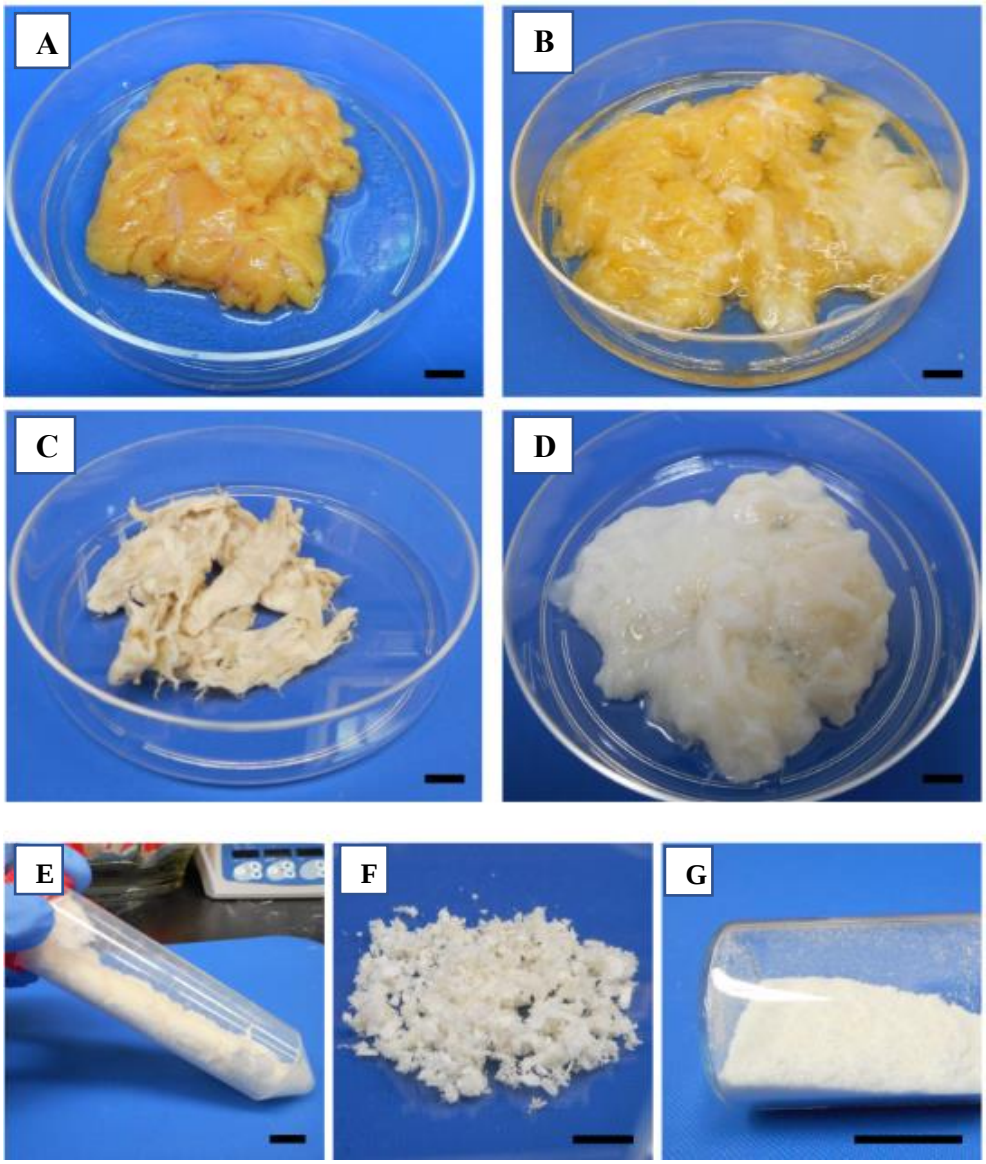

Figure 2.1 Overview of the decellularization and processing of fat tissue. (A) Excised human adipose tissue. **(B)** Tissue following freeze/thaw cycles, enzymatic digestion, and first polar extraction, and after **(C)** numerous polar extractions and mechanical pressing. **(D)** Decellularized adipose tissue (DAT) hydrated in PBS. **(E)** Lyophilized, and **(F)** minced lyophilized DAT. **(G)** Cryo-milled DAT. Scale bars represent 1 cm. Figure adopted with permission from[177].

2.1.2 DAT Suspension and Coating Fabrication

DAT suspension fabrication was performed following previously established methods in the Flynn lab[163]. The decontaminated DAT powder was centrifuged at 1500 x g for 10 minutes and the ethanol in the supernatant was removed and discarded. The samples were then resuspended in PBS to wash out residual ethanol and centrifuged at 1500 x g for 10 minutes, which was repeated for a total of three washes. The 1 g of milled DAT powder was digested in 40 mL of 0.22 mM NaH_2PO_4 solution (pH 5.4) containing 10 mg of α-amylase (1% w/w of DAT powder) for 72 hours under agitation at RT. The samples were then centrifuged at 1500 x g for 10 minutes, and the supernatant was discarded. The samples were washed by resuspending in 40 mL of 5% NaCl (w/v) under agitation for 10 minutes and centrifuged at 1500 x g for 10 minutes. The supernatant was discarded, and the samples were then washed in dH_2O to remove residual NaCl and centrifuged at 1500 x g for 10 minutes. Washing was repeated for a total of three washes. The digested DAT was resuspended in 0.2 M acetic acid to achieve a stock suspension concentration of 50 mg of DAT/mL and agitated overnight at 37 ºC. The DAT suspension was left to rest for 24 h at 4 ºC, and then homogenized with a Fisher Scientific Power Gen 125 (Fischer Scientific, Hampton, NH), and stored at 4 ºC until use.

To generate coatings, the DAT suspension was diluted to 25 mg/mL using 0.2 M acetic acid, and carefully layered over TCP at 125 µL/cm^2. DAT coatings were air dried for a minimum of 24 h. Coatings were washed 3 times by adding, gently swirling, and discarding PBS to remove residual acetic acid. Coatings were equilibrated overnight in Mesencult™ media + supplement (Stemcell Technologies, Vancouver, BC, Canada) at 37 ºC prior to cell seeding.

2.1.3 DAT Microcarrier Fabrication

To prepare the microcarriers, the DAT suspension was diluted with acetic acid to achieve a working concentration of 35 mg/mL, loaded in a 10 mL syringe, and attached to a 25G winged infusion set (BD medical, Mississauga, ON, Canada) secured on a syringe pump (PHD 22/2000 infusion, Harvard Apparatus, Holliston, MA) (Figure. 2.2). A Dewar flask containing liquid nitrogen was placed under the needle and positioned 5 cm above the liquid nitrogen. A voltage of 16 kV was applied to the needle tip and the DAT suspension was electrosprayed into liquid nitrogen at a rate of 30 mL/h. Microcarriers were collected in 50 mL conical tubes and lyophilized for a minimum of 48 h. Microcarriers were resuspended in 100% ethanol and stored at 4 ºC until use.

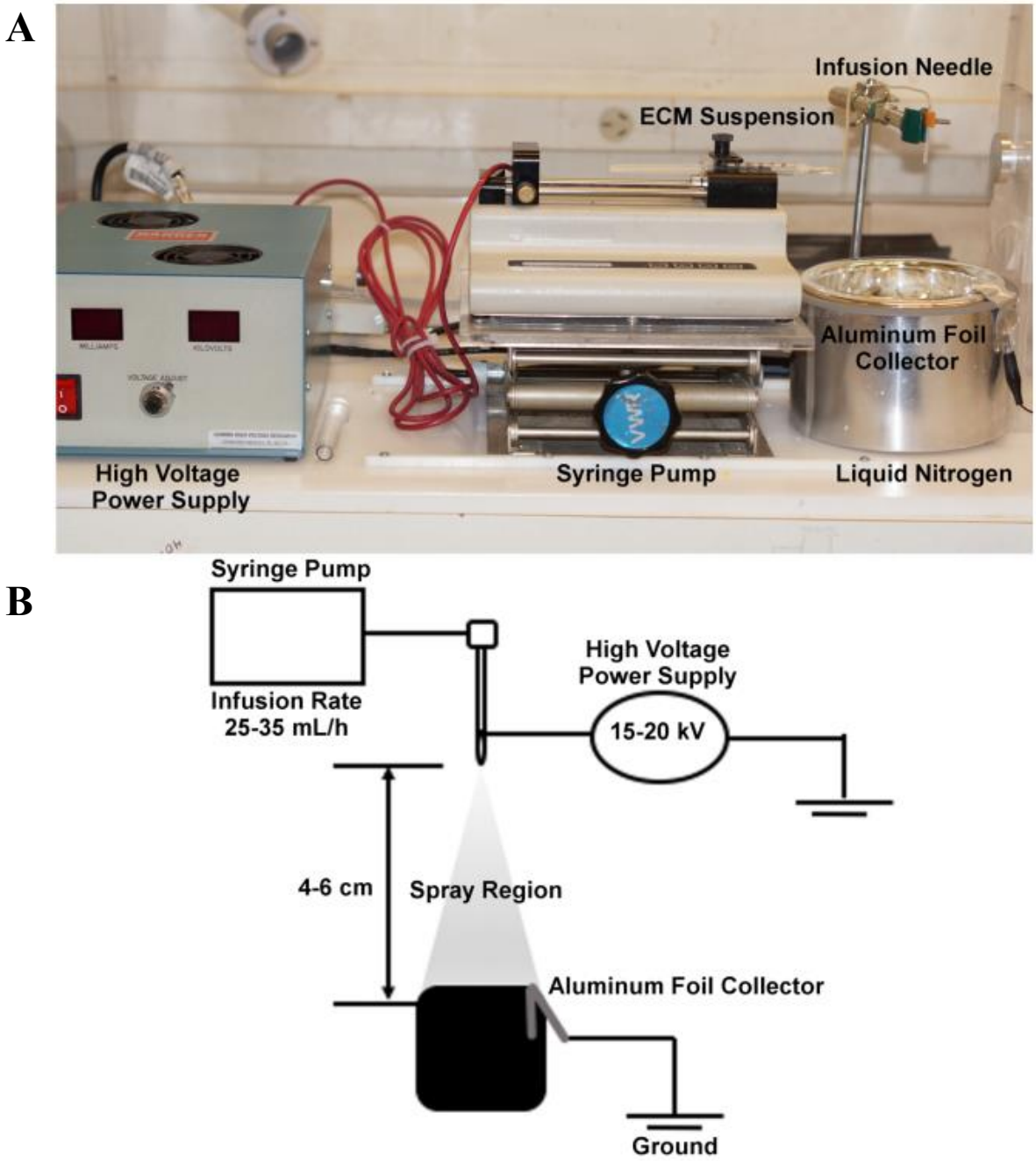

Figure 2.2 Overview of electrosparying used to generate DAT microcarriers. (A) Experimental set-up showing high voltage power supply, syringe pump, liquid nitrogen, infusion needle, DAT suspension, and aluminum foil collector in a Dewar flask. **(B)** Schematic showing experimental set up of voltage range, infusion rate, and distance between liquid nitrogen and needle tip. Figure obtained with permission from[191].

2.2 BM-MSC Isolation and Seeding on DAT Scaffolds

2.2.1 BM-MSC Isolation and Expansion

Human bone marrow aspirates were obtained from healthy donors with informed consent from the London Health Sciences Centre (University Hospital, London, Ontario). Hypaque-ficoll centrifugation was used to isolate mononuclear cells (MNC) and seeded on tissue-cultured plastic (TCP) at 270,000 cells/cm^2. Adherent colony forming unit-fibroblast (CFU-F) were established in Amniomax™ + supplement (Life Technologies, Calrsbad, CA). At passage 2, BM-MSC were cryopreserved. All experiments were performed using passage 4 cells when 80-85% confluency was reached in a T75 flask.

2.2.2 BM-MSC Seeding on DAT Coatings

The DAT suspension was coated on 6-well plates as previously described (2.1.2). Following 4 days expansion, BM-MSC in a T75 were detached using 2 mL of Trypsin-LE express (Gibco, Invitrogen, Carlsbad, CA) with 5 minutes incubation at 37 ºC. Enzymatic digestion was arrested using PBS + 5% FBS, and the cells were collected in a 50 mL conical tube. The sample was centrifuged at 350 x g for 7 minutes, counted using a Countess II automated cell counter (Thermofischer Scientific, Waltham, MA) and resuspended in 1 mL of supplemented Mesencult™ media. Next, 35,000 MSC were added per DAT coated well in 1 mL of Mesencult™ media. BM-MSC were also cultured on TCP alongside DAT coated wells as a control, and media was replaced every 3 days. MSC were cultured for a 1-week period to be assessed for viability and cell surface marker expression. Media was changed every 3 days.

2.2.3 BM-MSC Seeding on DAT Microcarriers

Prior to cell seeding, microcarriers were weighed to have 5 g/flask and rehydrated over a period of 3 days using an ethanol series diluted in PBS (100% - 0% in 5% increments). Microcarriers were equilibrated in a CELLSPIN flask (INTEGRA Biosciences AG, Switzerland) in 25 mL of complete Mesencult™ media overnight in a 37 ºC incubator. BM-MSC were trypsin-detached as previously described and 1.25 million cells (250,000 cells/g of microcarriers) were resuspended in 25 mL of complete Mesencult™ media and added to equilibrated microcarriers to achieve a total volume of 50 mL. A previously published 12 h seeding regimen was utilized to facilitate BM-MSC attachment[120]. Briefly, microcarriers were

intermittently stirred for 2 minutes at 25 rpm every 30 min for 3 h, followed by 6 h of static rest, and then another 3 h of intermittent stirring at 25 rpm. After seeding, the cells were cultured under continuous dynamic conditions at 25 rpm for a period of 1 week, and media was replaced every 3 days.

2.3 BM-MSC Survival Pilot Study

2.3.1 Extraction from DAT Coatings for Viability and Cell Counting

To confirm that the DAT coatings had a bioactive effect on BM-MSC, a pilot study was performed to evaluate their effects on cell viability and growth. At days 1, 3, and 7, media was collected, and wells were washed with 1 mL of PBS, the wash also collected to collect detached non-viable cells. The cells were trypsin-detached using 1 mL of TrypLE Express™/ well for 10 minutes at 37 ºC. Enzymatic activity was blocked using 3 mL of PBS + 5% FBS, then the wells were rinsed with 6 mL of PBS + 5% FBS. The mixture was then filtered using a 50 µm nylon mesh filter to remove large fragments of digested DAT. The cells were then centrifuged at 350 x g for 7 minutes and resuspended in PBS + 5% FBS.

2.3.2 Cell Viability Counts

Following extraction, cells were resuspended in 100 µL of Annexin V binding buffer (BioLegend, San Diego, CA) and counted using an automatic cell counter. Cells were then topped up to 300 µL of Annexin-V binding buffer and each tube received 1 µL of 1 mg/mL Calcein-AM (diluted 1:1000 in PBS+5% FBS) (Sigma Aldrich, St. Louis, MO), a marker for live cells, 4 µL of BV 421 Annexin-V 2.2 µg/mL (BioLegend, San Diego, CA), a marker for apoptotic cells, and 2 µL (diluted 1:10 in PBS) of 5mM DRAQ5 (Thermo Fisher, Waltham, MA), a marker for nucleated cells used to distinguish cellular events from scaffold debris. Cells were stained at RT for 20 minutes, washed with 1 mL of Annexin V binding buffer, and centrifuged at 350 x g for 7 minutes. Samples were resuspended in 300 µL of Annexin V binding buffer and analyzed by flow cytometry. All reagents used are defined in Table 2.1.

2.3.3 MSC Imaging on DAT substrates

BM-MSC were seeded as previously outlined on glass cover slips coated with DAT or uncoated as a control. At day 7, cells were washed with PBS, and a staining cocktail was prepared by adding 2 µL Calcein-AM and 4 µL DRAQ5 in 2 mL of PBS. Then 500 µL of cocktail was added to each well and stained for 30 minutes in 37 ºC incubator, rinsed 2x with PBS, and imaged using multiphoton microscopy (Nikon A1R MP+ Multiphoton Upright Scope). Imaging of BM-MSC on DAT microcarriers was performed at day 3. Microcarriers were resuspended in 1 mL of staining cocktail, incubated for 30 minutes at 37 ºC, rinsed twice with PBS, mounted on a cover slip and imaged using confocal microscopy (Olympus FluoView™ FV1000 confocal microscope).

2.4 BM-MSC Phenotypic Analyses

Following the pilot study, more advanced analyses involving dynamic culture were performed. To determine whether the DAT substrates influenced BM-MSC phenotype, ALDH-activity and cell surface marker expression was performed on BM-MSC at day 0 (prior to seeding) and at days 3 and 7. All reagents used are described in Table 2.1. Analyses were performed using flow cytometry (BD™ LSR II (BD Biosciences, San Jose, CA) at the London regional flow cytometry facility (LRFCF) and positive gating was achieved using fluorescence minus-one (FMO). Data was analyzed using FlowJo software (FlowJo LLC, Ashland, OR).

2.4.1 Extraction from DAT Coatings and Microcarriers for MSC Phenotype Analyses

ALDH-activity and cell surface marker analyses were performed on BM-MSC cultured on DAT microcarriers, DAT coatings, or TCP. To achieve complete enzymatic digestion of the scaffolds, samples of BM-MSC cultured on DAT coatings or TCP collected at days 1, 3 and 7 were digested using 1 mL of Liberase TL (Sigma-Aldrich, St. Louis, MO). DAT microcarriers were collected in a 15 mL falcon tube and resuspended in 1 mL of Liberase TL. The samples were digested for 1 h at 37 ºC and gently mixed every 10 minutes to ensure scaffold digestion. Enzymatic activity was arrested using PBS + 5% FBS, and

the samples were filtered using a 50 µm nylon mesh filter and centrifuged at 350 x g for 7 minutes and resuspended in PBS + 5% FBS.

2.4.2 Stromal Cell Surface Marker Analyses

The effects of culturing on the DAT substrates on the expression of the stromal surface markers CD73, CD90, and CD105 was assessed on samples that contained DRAQ5 to exclude scaffold debris from analyses. Following cell extraction, each tube contained 300 µL of PBS + 5% FBS and sequentially received 4 µL of the following antibodies: BV 421 100 µg/mL CD73 (BioLegend, San Diego, CA), FITC 200 µg/mL CD90 (BioLegend, San Diego, CA), and PE/Dazzle 100 µg/mL CD105 (BioLegend, San Diego, CA), and 2 µL of DRAQ5. Samples were incubated at 4 ºC for 30 minutes, washed with 4 mL of PBS + 5% FBS and centrifuged at 350 x g for 7 minutes. Samples were resuspended in 300 µL of PBS + 5 % FBS and analyzed by flow cytometry.

2.4.3 Cell Surface Marker Analyses

The effects of culture on DAT substrates CD146 and CD271 expression was assessed on samples that were stained with DRAQ5 to eliminate scaffold debris and Calcein-AM to select for viable cells. Following cell extraction, each tube contained 300 µL of PBS + 5% FBS and sequentially received 5 µL of FITC 300 µg/mL CD271 (BioLegend, San Diego, CA) and PE 200 µg/mL CD146 (BD Biosciences, San Jose, CA), 1 µL of Calcein-AM, and 2 µL of DRAQ5. Samples were incubated at RT for 30 minutes, washed with 4 mL of PBS + 5% FBS and centrifuged at 350 x g for 7 minutes. Samples were resuspended in 300 µL of PBS + 5 % FBS and analyzed by flow cytometry.

2.4.4 ALDH-activity analyses

Cells were resuspended in 300 µL of PBS + 5% FBS and sequentially stained with 1 µL of Calcein-AM and 2 µL of DRAQ5 at RT for 20 minutes, washed with 4 mL of PBS + 5% FBS and centrifuged at 350 x g for 7 minutes and resuspended in 300 µL of Aldefluor assay buffer (StemCell Technologies,

Vancouver, BC, Canada). Next, 1 µL of Aldefluor was added to each sample and incubated at 37 ºC for 30 minutes. Samples were centrifuged at 350 x g for 7 minutes and resuspended in 300 µL of Aldfeluor assay buffer. To establish positive ALDH gating, FMOs were generated using an ALDH-stained sample that also received DEAB (N-diethylaminobenzaldehyde, inhibitor of ALDH) as per the manufacturer's protocol, and analyzed by flow cytometry.

TABLE 2.1 FLUORESCENT ANTIBODY/MOLECULE PRODUCT SPECIFICATION FOR FLOW CYTOMETRY

Antibody/Molecule	Fluorophore	Clone	Catalog #	Company
Phosphatidyl Serine binding protein – Annexin-V	BV421	N/A	640924	Biolegend, San Diego, CA
Acetoxymethyl Ester-Calcein-AM	Calcein-AM	N/A	17783	Sigma Aldrich, St. Louise, MO
DNA Dye – DRAQ5	DRAQ5	N/A	62251	Thermo Fisher, Waltham, MA
Monoclonal mouse anti-human CD73	BV421	AD2	344008	Biolegend, San Diego, CA
Monoclonal mouse anti-human CD90	FITC	5E10	328108	Biolegend, San Diego, CA
Monoclonal mouse anti-human CD105	PE/Dazzle	43A3	3233224	Biolegend, San Diego, CA
Monoclonal mouse anti-human CD271	FITC	ME20.4	345104	Biolegend, San Diego, CA
Monoclonal mouse anti-human CD146	PE	P1H12	550315	BD Biosciences, San Jose, CA
Aldefluor	BODIPY-aminoacetaldehyde (BAAA)	N/A	01700	Stem Cell Technologies, Vancouver, BC
Dead cell dye – 7AAD	7AAD	N/A	420404	Biolegend, San Diego, CA
Azide fluorophore	Pacific Blue	N/A	C10418	Thermofisher, Waltham, CA

2.5 *In Vitro* Pro-angiogenic Secretory Assessment

To assess whether culture on the DAT substrates modulated the pro-angiogenic paracrine effects of BM-MSC, cells were cultured under the different conditions and conditioned media (CdM) was generated in basal Mesencult^{TM} media (i.e. without the supplements). Collected CdM was concentrated via centrifugation and supplemented onto human microvascular endothelial cells (HMVEC) cultured under growth factor-free conditions. The ability of CdM to affect HMVEC proliferation, survival, and tubule formation was assayed using the following protocols.

2.5.1 Generating Concentrated CdM

BM-MSC were seeded on DAT-coated or uncoated T25 flasks at 625,000 cells/flask with 4 mL of fully supplemented Mesencult™ media and placed in a 37 ºC incubator overnight to allow for cell attachment. A DAT-coated T25 flask not seeded with cells was included as a scaffold-only control. Similarly, 2.5 g of DAT microcarriers were weighed, and seeded with 625,000 cells in a total of 30 mL of supplemented Mesencult™ media. After equilibration, cells were washed 5 times with PBS, ensuring complete removal of growth factors, and Mesencult™ Basal media (without supplement) was added to each sample, 4 mL in each T25 and 30 mL in the CELLSPIN flask. Flasks were placed in the 37 ºC incubator and media was conditioned for 48 h. Collected CdM was filtered through a 40 μm nylon mesh filter, loaded into Amicon®Ultra-15 3 kDA centrifugal filters (Millipore Sigma, Burlington, MA), and centrifuged at 3220 x g at 4 ºC for 45 minutes for the 4 mL samples and 2 hours for the 30 mL DAT microcarrier samples, to achieve a final volume of 400 μL of concentrated CdM per group, and stored in -80 ºC. Before use, CdM samples were thawed at 4 ºC for 30 – 45 minutes.

2.5.2 HMVEC Culture with BM-MSC CdM

HMVEC were expanded in complete endothelial growth medium-2 media (EGM-2 = endothelial basal media-2 + 5% FBS, IGF, bFGF, EGF, and VEGF, Lonza, Morrisville, NC) and passaged in T75s until 80-85% confluency was reached. All experiments were performed using HMVEC at passage 7. At passage 6, HMVEC were detached with trypsin by adding 2 mL of TrypLE and incubating in 37 ºC for 5

minutes and inactivated using PBS + 5% FBS. Cells were centrifuged at 240 x g for 5 minutes, resuspended in 1 mL of EGM-2 media and counted. HMVEC were seeded at 60,000 cells per well in a 12-well plate containing 500 µL of EGM-2 media. The next day, EGM-2 media was removed, and wells were washed with 500 µL of PBS 3x, to ensure the removal of residual growth factors. Next, 450 µL of EBM-2 media was added to each well with 50 µL of CdM to achieve a 10% supplement. A no CdM control was supplemented with 50 µL of unconditioned Mesencult™ Basal media. HMVEC were harvested at days 1 and 3 for viability and proliferation assessment.

2.5.3 HMVEC Viability

At days 1 and 3, HMVEC were harvested and their viability was assessed. Wells were first rinsed with 500 µL of PBS, rinse was collected to obtain detached non-viable cells. Then 300 µL of TrypLE was added to each well and incubated at 37 ºC for 7 minutes. Next, digestion was blocked and rinsed with 1 mL of PBS + 5% FBS. The samples were then centrifuged at 240 x g for 5 minutes and resuspended in 300 µL of Annexin V binding buffer. The samples sequentially received 4 µL of BV 421 Annexin V and 5 µL of 50 µg/mL 7-AAD (dead cell marker, Biolegend, San Diego, CA) and were incubated for 20 minutes at RT. Finally, the samples were washed with 1 mL of Annexin V binding buffer, centrifuged at 240 x g for 5 minutes, and resuspended in 300 µL of Annexin V binding buffer and analyzed by flow cytometry.

2.5.4 HMVEC Proliferation

Proliferation was assessed using the EdU Assay (5-ethyl-2'-deoxyuridine). EdU is a thymidine analogue incorporated into the DNA of cells during S-phase and can be detected via conjugation to an Azide fluorophore. The Click-iT™ EdU Cell proliferation flow cytometry assay kit (Thermo Fisher, Waltham, MA) was used for this assessment. At 24 h prior to cell collection, 1 µM of EdU was added to each well. After 1 and 3 days of culture, cells were harvested as previously described, and resuspended in 500 µL of 10% buffered formalin fixation buffer for 5 minutes and blocked with 1 mL of PBS + 5% FBS. The samples were centrifuged at 400 x g for 7 minutes and resuspended in 100 µL of 1x saponin permeabilization buffer and incubated at RT for 15 minutes. The Click-it™ reaction utilizing copper (II)

sulfate ($CuSO_4$) was used to conjugate incorporated EdU to the Azide fluorophore Pacific Blue™ as per manufacturer's instructions. The frequency of EdU^+ cells was analyzed by flow cytometry. EdU positive cells were gated based on FMOs that did not receive CuSO4.

2.5.5 HMVEC Tubule Formation

Geltrex™ lactose dehydrogenase elevating virus (LDEV)-Free Reduced Growth Factor Basement Membrane Matrix (Thermo Fisher, Waltham, MA) was thawed overnight on ice at 4 ºC. Pipette tips and a 24-well plate were pre-chilled at -20 ºC for 20 minutes to keep the surfaces cold. While working on an ice block, 200 µL of Geltrex™ was added to each well, and the plate was gently swirled until an even layer coated the well. The plate was then incubated at 37 ºC for 2 h to allow the Matrigel™ to solidify. HMVEC obtained as previously described, were resuspended in EBM-2 Media, and each well of a 24-well plate received 30,000 HMVEC in 360 µL of EBM-2 media (positive control received 30,000 HMVEC in 400 µL of EGM-2 media) with 40 µL of CdM to achieve a 10% supplement. The plates were incubated at 37 ºC, and after 24 h, 5 photos were taken per well, and tubule formation was quantified by blinded manual counting of tubule branch points using ImageJ software.

2.6 Directed *In Vivo* Angiogenesis Assay (DIVAA™)

A DIVAA™ kit (R&D Systems, Minneapolis, MN) was used to assess endothelial cell (EC) recruitment into DIVAA inserts supplemented with CdM generated by BM-MSC cultured on DAT substrates compared to TCP. The DIVAA™ protocol was performed as per the manufacturer's instructions. Briefly, DIVAA™ inserts were loaded with 20 µL basement membrane extract supplemented at 10% with CdM. Inserts containing VEGF/FGF served as a positive control. DIVAA™ inserts were subcutaneously implanted into the flanks of NOD/SCID mice. Studies were approved by the Human Studies Research Ethics Board at Western University (see Appendix. 2). After 14 days, the mice were euthanized and EC infiltration into the DIVAA™ inserts was quantified by FITC-lectin uptake as per the manufacturer's instructions using a SpectraMax plate reader (Molecular Devices, Sunnyvale, CA). Results shown in Supplementary figure 1.

2.7 CdM Proteomic Analyses

2.7.1 CdM Protein Extraction and Digestion

To prepare CdM for proteomic analysis, ~100 µL of CdM were lyophilized and reconstituted in 8 M urea, 50 mM ammonium bicarbonate (AMBIC), 10 mM dithiothreitol (DTT), and 2% sodium dodecyl sulfate (SDS) lysis buffer. Proteins were sonicated with a probe sonicator (10 X 0.5 s pulses; Level 1) (Fisher Scientific, Waltham, MA), and reduced in 10 mM DTT for 30 minutes at RT. Samples were then alkylated in 100 mM iodoacetamide for 30 minutes at RT in the dark and precipitated in chloroform/methanol. On-pellet in-solution protein digestion was performed in 100 µL 50 mM AMBIC (pH 8) by adding Trypsin/LysC (Promega, Madison, WI) in a 1:50 ratio to precipitated proteins. Proteins were incubated at 37 °C overnight (~20 h) in a ThermoMixer C (Eppendorf, Hamburg, Germany) at 900 rpm before acidifying to pH 3 - 4 with 10% formic acid (FA). Salts and detergents were removed from peptide samples using C18 stagetips made in-house. Briefly, 10 layers were stacked into 200 µL pipette tips and rinsed with ice-cold methanol. Stagetips were conditioned with Solution A (80/20/0.1% acetonitrile(ACN)/Water/Trifluoic acid (TFA)), followed by Solution B (5/95/0.1% ACN/Water/TFA) prior to loading ~20 µg of peptides resuspended in solution B. Duplicate washes were performed with solution B prior to elution of peptides using solution C (80/20/0.1% ACN/Water/FA) and final elution using a 50/50 mixture of ACN/0.1%FA. Peptides were centrifuged at 45 °C under vacuum and resuspended in 0.1% FA prior to quantification by bicinchoninic acid assay (BCA).

2.7.2 Ultraperformance Liquid Chromatography (UPLC) Coupled to Tandem Mass Spectrometry (LC-MS/MS)

Following protein quantification by BCA, samples were injected into LC-MS/MS to analyze proteomic composition. Peptides were analyzed using a nanoAquity UHPLC M-class system (Waters, Wilfrod, MA) connected to a Q Exactive mass spectrometer (Thermo Scientific, Waltham, MA) using a nonlinear gradient. Buffer A consisted of water/0.1% FA and Buffer B consisted of ACN/0.1% FA. Peptides (~1 µg estimated by BCA) were initially loaded onto an ACQUITY UPLC M-Class Symmetry C18 Trap Column (Thermo Scientific, Waltham, MA), 5 µm, 180 µm x 20 mm and trapped for 5 minutes at a flow rate of 5

µL/min at 99% A/1% B. Peptides were separated on an ACQUITY UPLC M-Class Peptide BEH C18 Column (130Å, 1.7µm, 75µm X 250mm) operating at a flow rate of 300 nL/min at 35 °C using a non-linear gradient consisting of 1-10%B,10-20%B,20-30%B,30-40%B,40-50%B,60-70%B,80-90%B, for 10 minute intervals before cyclic washing between 5-95%B. Settings for data acquisition on the Q Exactive Plus are outlined in Table 2.2.

2.7.3 Proteomic Data Analysis

MS raw files were searched in MaxQuant (1.6.5.0) using the Human Uniprot database (reviewed only, updated November 2020). Cleavage was set to semi-specific and I=L. Cysteine carbamidomethylation was set as a fixed modification. Oxidation (M), N-terminal acetylation (protein), and deamidation (NQ) were set as variable modifications (max. number of modifications per peptide = 5) and all other setting were left as default. Precursor mass deviation was left at 20 ppm and 4.5 ppm for first and main search, respectively. Fragment mass deviation was left at 20 ppm. Protein and peptide false discovery rate (FDR) was set to 0.01 (1%) and the decoy database was set to revert. The match-between-runs feature was utilized across all sample types to maximize proteome coverage and quantitation. Datasets were loaded into Perseus (1.6.15) and proteins identified by site; reverse and potential contaminants were removed. Protein identifications with quantitative values in >50% samples across groups (DAT coatings, TCP, or DAT Microcarriers) were retained for downstream analysis unless specified elsewhere. Missing values were imputed using a width of 0.3 and down shift of 1.8 to enable statistical comparisons. Gene-ontology enrichment analyses were performed using open-source Metascape (Metascape.org).

TABLE 2.2 PARAMETERS FOR Q EXACTIVE PLUS DATA ACQUISITION.

Parameter	Parameter Setting
Orbitrap Resolution (MS1)	70K
Mass Range	300-1500
MS1 Injection Time	250ms
MS1 AGC Target	3E+06
Lock Mass	445.120025
MS2 Detection	FT
MS2 Resolution	17,500
MS2 AGC Target	1e5
MS2 Injection Time	25ms
Loop Count	15
Isolation Width	1.4 m/z
Isolation Offset	0.5 m/z
MS2 Activation	HCD
Normalized Collision Energy	27
Dynamic Exclusion	15
Minimum AGC Target	2.00E+03

MS2 Intensity Threshold	8.0E+04
Exclusion Duration	20s
Charge Exclusion	Unassigned,1,7,8
Polarity	Positive

2.8 Statistical Analyses

Statistical analyses were performed using a two-way ANOVA, unless otherwise stated, followed by Tukey's post hoc multiple comparisons test. For tubule formation and DIVAA™ experiments, a one-way ANOVA was performed. All calculations were performed using GraphPad Prism 7 software.

Chapter 3.0 Results

3.1 DAT Coatings Supported the Growth and Attachment of BM-MSC

Culture on tissue-culture plastic (TCP) does not provide complex extracellular matrix (ECM)-cell interactions that are known to influence cell survival, growth, and differentiation[49,189,192]. Thus, in this project, ECM-rich decellularized adipose tissue (DAT) scaffolds were used as an alternative culturing platform. A pilot study was first performed in which bone marrow-mesenchymal stromal/stem cells (BM-MSC) were cultured on DAT coatings under static conditions before advancing to more in depth studies involving dynamic culture. While DAT constructs have previously been shown to support the growth of adipose-derived stromal/stem cells (ASC)[120,138,175,193], this was the first time BM-MSC were investigated on the DAT platform. Thus, the purpose of this study was to determine if there were beneficial effects on BM-MSC following culture on DAT coatings.

BM-MSC were expanded on TCP and then seeded onto DAT coatings or TCP controls and cultured over 1-week *in vitro.* To label live versus apoptotic/dead cells, Calcein-AM and Annexin-V were used respectively, and flow cytometry was performed to quantify the frequency of viable ($Calcein^+/Annexin^-$) and non-viable cells ($Calcein^-/Annexin^+$) (Figure 3.1A,B). The mean frequency of non-viable BM-MSC was significantly decreased at day 7 when cultured on DAT coatings compared to TCP (19.2 ± 6.6 % vs 33.5 ± 9.9%, *$p<0.05$, Figure 3.1C). Applying cluster gating, the mean frequency of viable BM-MSC ($Calcein^+/Annexin^-$) was 73.4 ± 10.4% when cultured on DAT coatings, which was not significantly different compared to TCP at 62.0 ± 11.7% ($p=0.076$, Figure 3.1D).

Hemocytometer cell counting was combined with the viable cell frequency to obtain total live cell numbers. Total viable BM-MSC counts were significantly increased at day 7 when cultured on DAT coatings compared to TCP (396,445 ± 99,075 live cells vs 221,475 ± 42,586 live cells, ***$p<0.001$, Figure 3.1E). Thus, growth of BM-MSC on DAT coatings resulted in a reduced frequency of dead BM-MSC and increased the total yield of viable BM-MSC after 7 days of static culture.

3 3.2 Visualization of BM-MSC Attachment on TCP and DAT Bioscaffolds

Following the demonstration of increased BM-MSC expansion on DAT coatings, cells were seeded on TCP or DAT coatings under static culture, and on DAT microcarriers under dynamic culture conditions and cell attachment was visualized for all conditions. Representative multiphoton confocal images showed robust BM-MSC attachment across all conditions (Figure 3.2). Qualitative analyses compared at day 7 using multiphoton microscopy staining for DRAQ5 (cell nuclei) and Calcein-AM (live cells) showed an elongated and spindled-shaped appearance of BM-MSC on glass coverslips (Figure 3.2B). In contrast, a qualitatively less elongated appearance was observed on 3D DAT coatings (Figure 3.2A). Notably, DAT coatings demonstrated three-dimensional growth, and the coatings provided greater volume for the cells to occupy. Representative analysis at day 3 using confocal microscopy of BM-MSC on DAT microcarriers (Figure 3.2C), showed extensive cell attachment on the spherical microcarriers following dynamic culture conditions in a spinner flask.

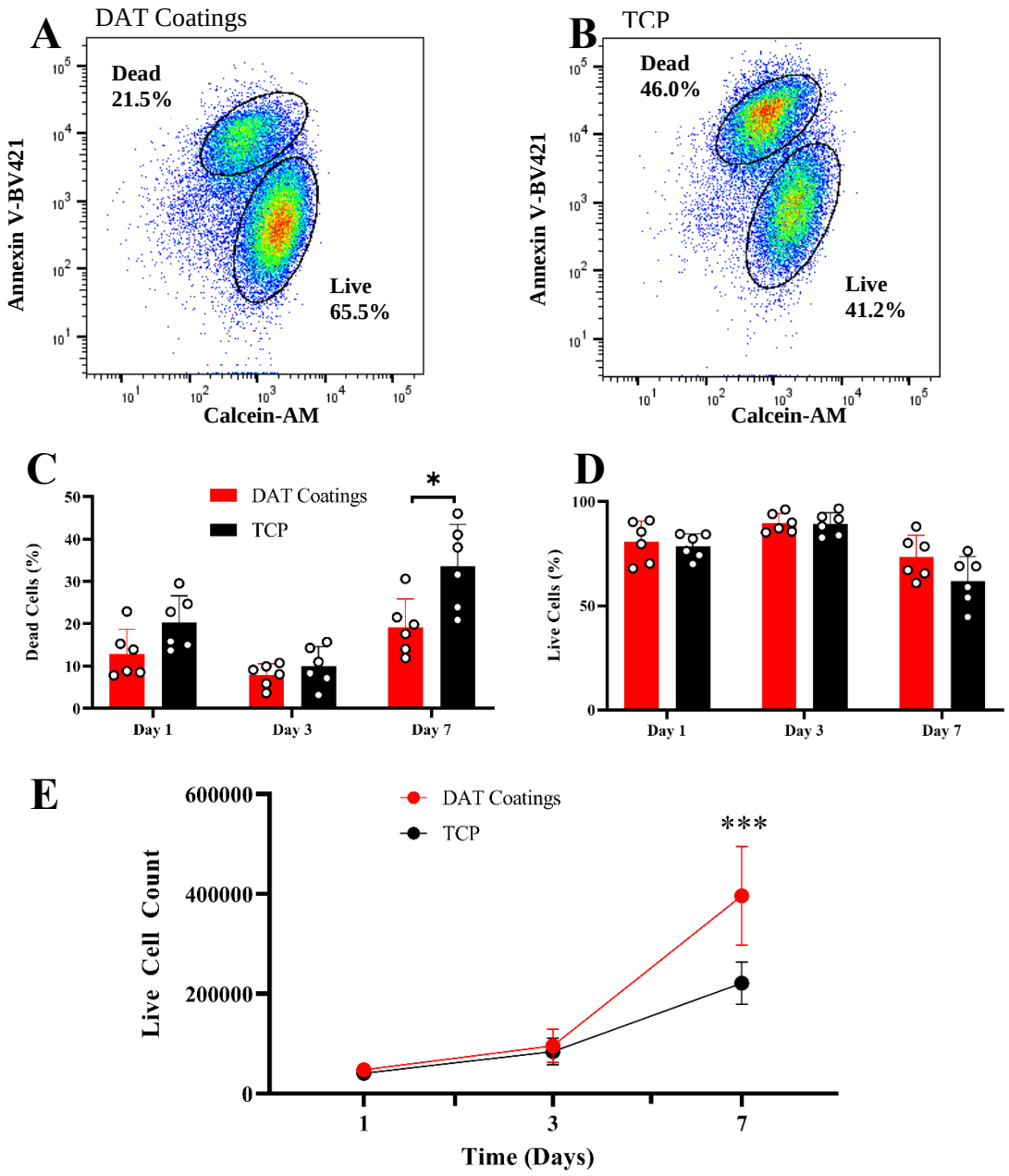

Figure 3.1 The yield of viable BM-MSC was increased after culture on DAT coatings compared to TCP. Representative flow cytometry plots of Calcein-AM$^+$ (live cells) and Annexin-V$^+$ (dead or apoptotic cells) at day 7 comparing BM-MSC cultured on **(A)** DAT coatings or **(B)** TCP. **(C)** The frequency of dead BM-MSC was significantly decreased after 7 days of culture on DAT coatings compared to TCP. **(D)** Frequency of live BM-MSC cultured on DAT coatings compared to TCP. **(E)** BM-MSC viable cell count was increased at day 7 when cultured on DAT coatings compared to TCP. Data represent Mean ± SD using BM-MSC purified from 6 different (N=6) human BM samples (*p<0.05, ***p<0.001). Analysis for statistical significance was performed using a two-way ANOVA followed by Tukey's post hoc multiple comparisons test.

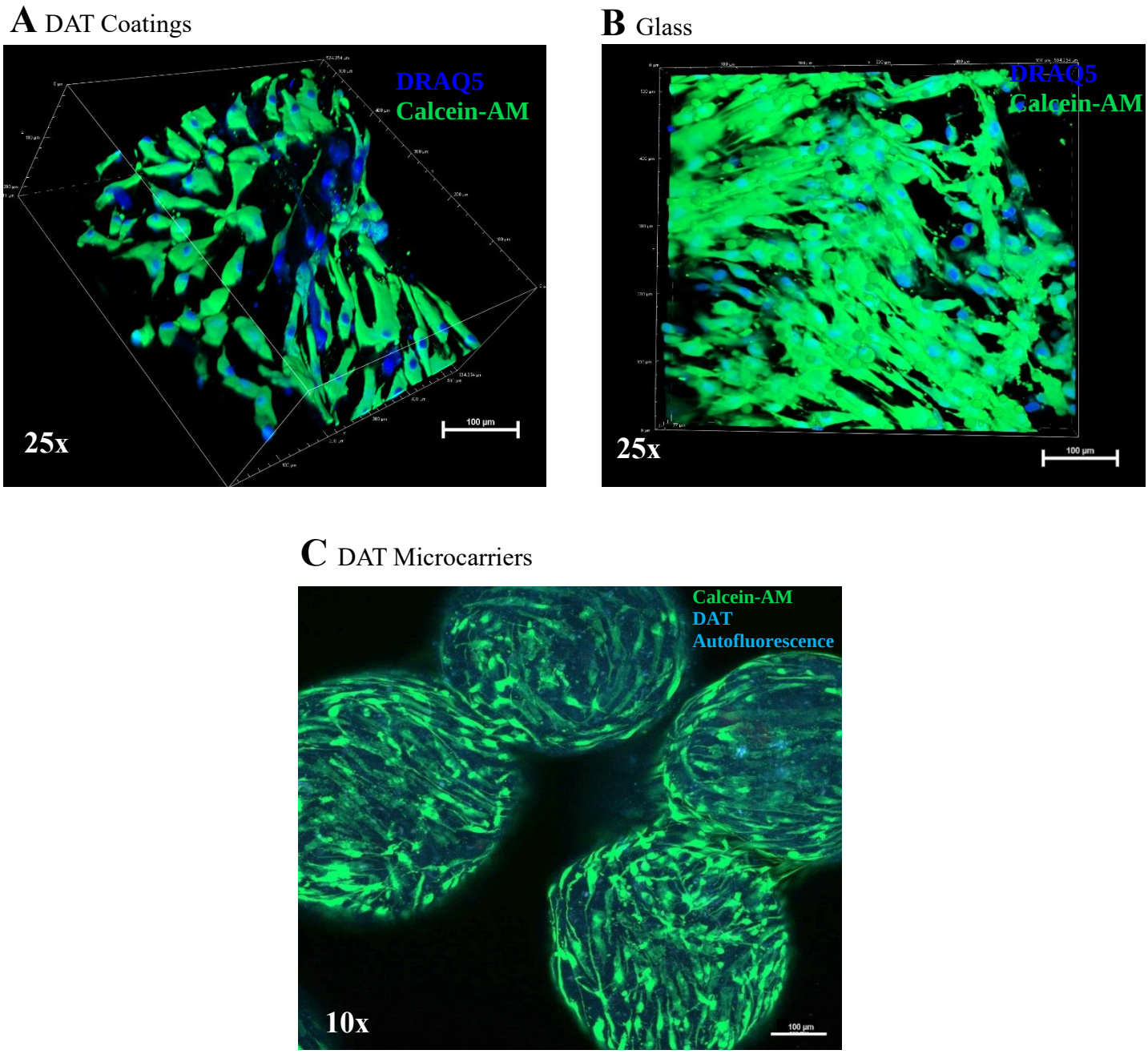

Figure 3.2 Representative photomicrographs showing BM-MSC grown on DAT coatings or uncoated glass coverslips under static conditions, and on DAT microcarriers under dynamic conditions. Multiphoton microscopy comparing live BM-MSC (Calcein-AM green) with cell nuclei labelled by DRAQ5 (blue) grown on **(A)** DAT coatings or **(B)** glass coverslip imaged at day 7 at 25x magnification. BM-MSC had a less spindle-shaped morphology when cultured on DAT compared to glass coverslip. **(C)** Confocal microscopy visualizing live BM-MSC (Calcein-AM green) on DAT microcarriers at day 3 imaged at 10x magnification. All scale bars = 100 µm.

3.3 The Fraction of BM-MSC Expressing Pericyte and Stromal Markers was not Significantly Altered when Cultured on DAT Constructs

The International Society of Cell Therapy (ISCT) specifies that one of the minimal criteria defining MSC is >95% cell surface expression of the stromal markers CD73 (ecto-5'-nucleotidase) , CD90 (Thy-1), and CD105 (Endoglin)[79,87]. Additionally, CD146 (MCAM) is associated with MSC vascular smooth muscle or pericyte commitment and ability to differentiate into supportive pericytes that wrap around and stabilize blood vessels[80,194]. BM-MSC seeded on DAT coatings, TCP, or DAT microcarriers were therefore assessed for the expression of these stromal markers (CD73, CD90, and CD105), as well as the pericyte marker (CD146), at the time of seeding (day 0 expression) and after 3 and 7 days of culture. Stromal marker expression was similar on BM-MSC cultured on the DAT substrates or TCP over a 1-week culturing period (>95%) and not significantly different compared to expression at day 0 just prior to seeding (Figure 3.3A-C). CD146 expression was not significantly different between groups and not significantly different compared to expression at day 0. At day 7, the mean frequency of $CD146^+$ BM-MSC were 77.7 ± 4.8%, 87.6 ± 3.6%, and 69.6 ± 14.9% when cultured on DAT coatings, TCP, and DAT microcarriers respectively (Figure 3.3D). Therefore, culturing on the DAT under either static or dynamic conditions did not alter the expression of the expected stromal or pericyte markers compared to traditional static culture on TCP.

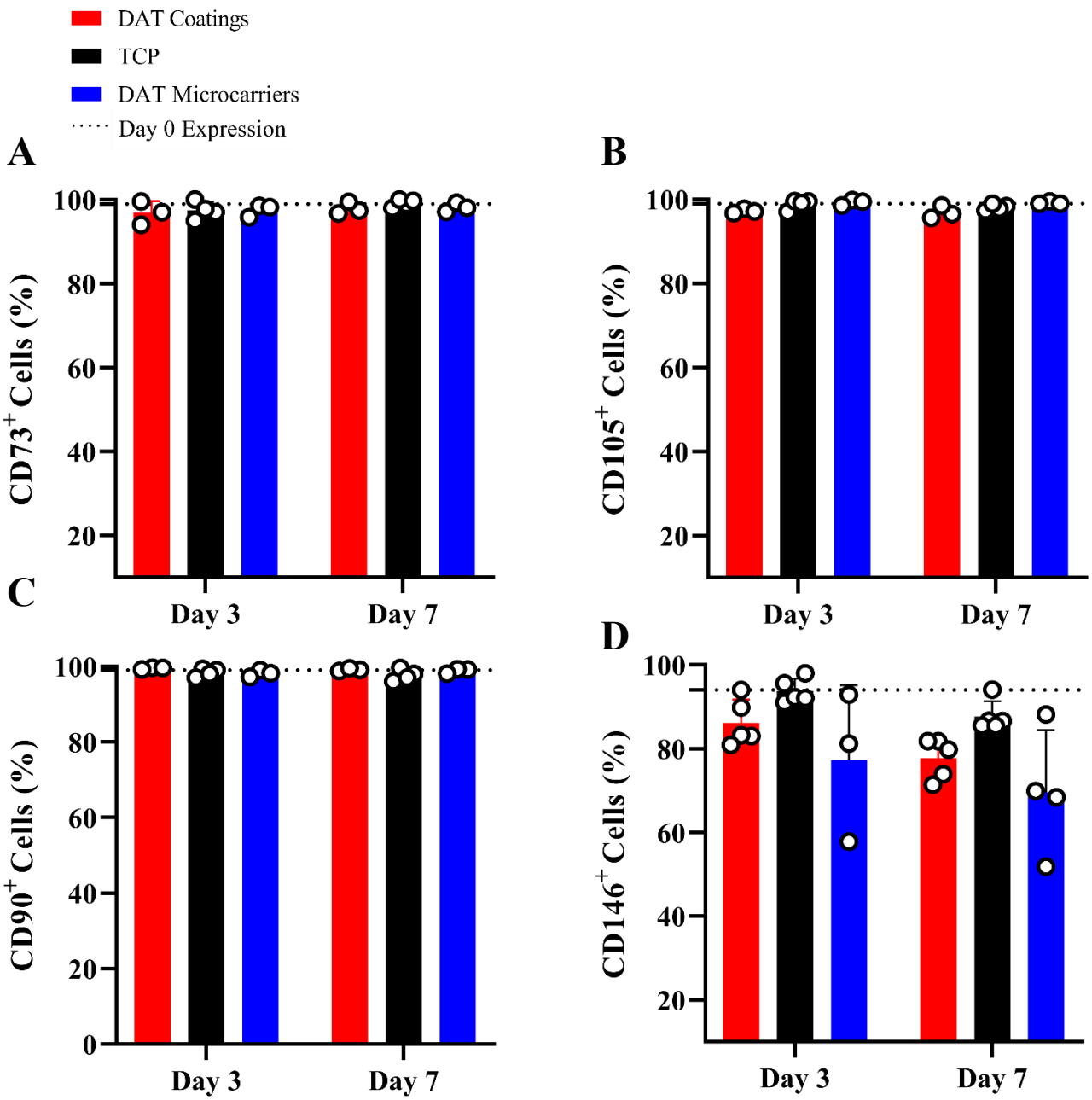

Figure 3.3 BM-MSC expression of stromal and pericyte markers was maintained throughout culture on DAT substrates. Analysis of cell surface markers showing BM-MSC expression of **(A)** CD73, **(B)** CD105, and **(C)** CD90 was not significantly altered by culture on DAT coatings or DAT microcarriers. **(D)** The pericyte marker CD146 was not significantly changed on BM-MSC when cultured on DAT coatings or DAT microcarriers. Data represent Mean ± SD using BM-MSC purified from 3-4 human BM samples. Analysis for statistical significance was performed using a two-way ANOVA followed by Tukey's post hoc multiple comparisons test.

3.4 The Frequency of BM-MSC with High Aldehyde Dehydrogenase Activity was better Maintained on DAT Coatings under Static Conditions

ALDH is an intracellular enzyme involved in the detoxification of reactive aldehydes into less reactive acetates and has been previously shown to be a conserved functional marker of primitive mesodermal progenitor cells of multiple lineages[72,195,196]. Thus, the purpose of these experiments was to assess the ability of DAT constructs to maintain ALDH-activity during culture, as a conserved functional progenitor cell characteristic. Representative flow cytometry plots for cytosolic ALDH-activity within BM-MSC cultured on DAT coatings, TCP or on DAT microcarriers after 7 days culture are shown in Figure 3.4A-C. At day 0 prior to seeding (Figure 3.4D), the frequency of $ALDH^{hi}$ BM-MSC was 23.7 ± 2.2 %, and similar to previous studies from our lab[195]. After 3 days of culture, the frequency of $ALDH^{hi}$ BM-MSC was not significantly different when cultured on DAT coatings (16.9 ± 7.5%) or DAT microcarriers (14.6 ± 1.9%) compared to TCP (16.2 ± 7.1%) (Figure 3.4E) compared to day 0. Further, no significant differences were observed between timepoints within groups. At day 7, the frequency of $ALDH^{hi}$ BM-MSC when cultured on DAT coatings (16.4 ± 6.4%) was not significantly different compared to day 0 levels, while culture on TCP (8.6 ± 3.9%, ***$p<0.001$) and DAT microcarriers (12.4 ± 3.3%, *$p<0.01$) resulted in significantly decreased frequencies of $ALDH^{hi}$ BM-MSC compared to day 0 levels (23.7 ± 2.2 %, Figure 3.4E). Therefore, culture of BM-MSC on DAT coatings under static conditions for 7 days best maintained the frequency of $ALDH^{hi}$ BM-MSC compared to day 0 levels prior to seeding on the various substrates.

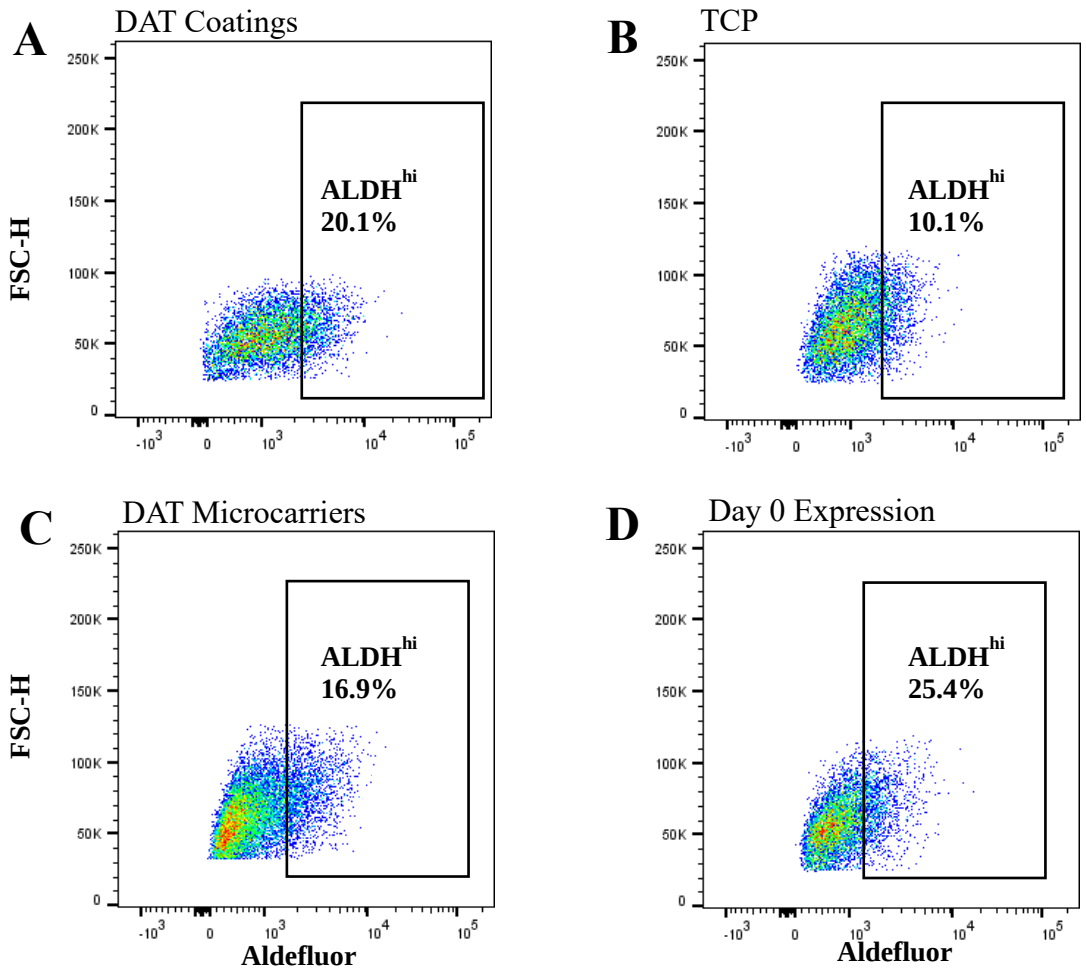
A
DAT Coatings
FSC-H
ALDH^hi
20.1%
B
TCP
ALDH^hi
10.1%
C
DAT Microcarriers
ALDH^hi
16.9%
Aldefluor
D
Day 0 Expression
ALDH^hi
25.4%
Aldefluor

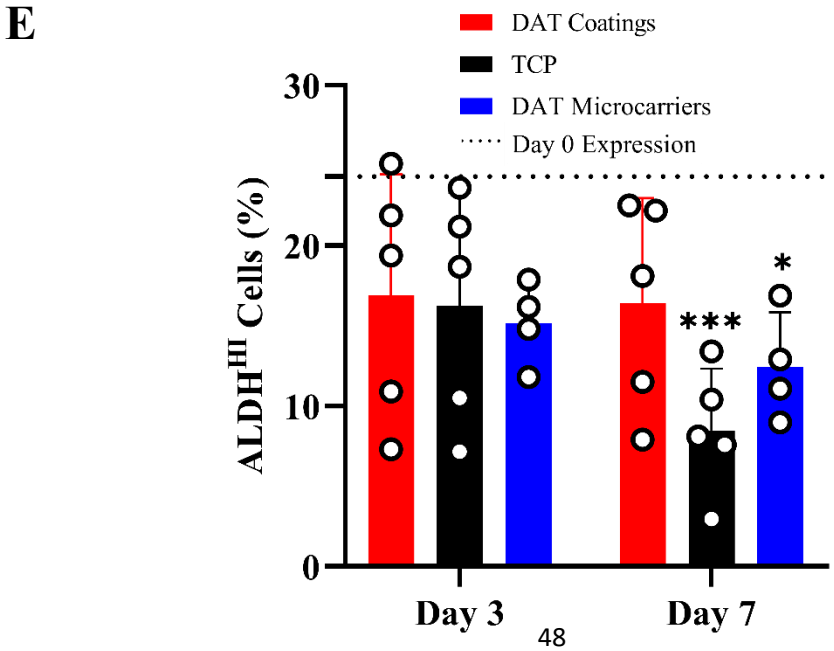
E
DAT Coatings
TCP
DAT Microcarriers
Day 0 Expression
ALDH^HI Cells (%)
***
*
Day 3
Day 7

Figure 3.4 BM-MSC cultured on DAT coatings preserved BM-MSC with high ALDH-activity for 7 days. Representative flow cytometry plots showing ALDH-activity in BM-MSC after 7 days of culture on **(A)** DAT coatings, **(B)** TCP, **(C)** DAT microcarriers, or at **(D)** day 0 prior to seeding. **(E)** Frequency of ALDH-high BM-MSC when cultured on various substrates at day 3 was not significantly different compared to Day 0. The frequency of BM-MSC that retained high ALDH-activity (a conserved progenitor cell function) was not significantly changed on DAT coatings after 7 days of culture, while a decline was observed TCP and DAT microcarriers compared to Day 0. Data represent Mean ± SD using BM-MSC purified from 4 – 5 human BM samples (**$p<0.01$, ***$p<0.001$). Analysis for statistical significance was performed using a two-way ANOVA followed by Tukey's post hoc multiple comparisons test.

3.5 BM-MSC Cultured on DAT Microcarriers Showed an Increased Fraction of Cells Expressing the Cell Surface Marker CD271

CD271/LNGFR (low-affinity nerve growth factor receptor) has been postulated as a primitive cell surface marker expressed on MSC early after isolation and is associated with increased clonogenic and immunogenic MSC functions[197,198]. Although the association of CD271 as a primitive marker remains controversial, analysis of CD271 expression was assessed on BM-MSC when cultured on DAT substrates or TCP. After 3 days of culture on DAT microcarriers under dynamic conditions, the frequency of $CD271^+$ BM-MSC was significantly increased from 6.5 ± 4.4% at day 0 to 27 ± 11.5% at day 3 (****$p<0.001$, Figure 3.5E). Interestingly, culture of BM-MSC under static conditions for 3 days on DAT coatings (5.4 ± 2.2%) or on TCP (0.77 ± 0.49%) showed that a significantly lower fraction of cells expressed CD271 expression compared to culture on the microcarriers (****$p<0.001$, Figure 3.5E). After 7 days of culture, the frequency of $CD271^+$ BM-MSC on DAT microcarriers was 11.6 ± 3.8% and was not significantly different from day 0 levels, but remained significantly increased compared to static culture on DAT coatings (2.5 ± 1.5% , *$p<0.05$) and TCP (0.44 ± 0.34%, **$p<0.01$). No significant differences were observed between timepoints within groups. Collectively, these data suggested that culture of BM-MSC on DAT microcarriers under dynamic conditions increased the fraction of cells that expressed CD271.

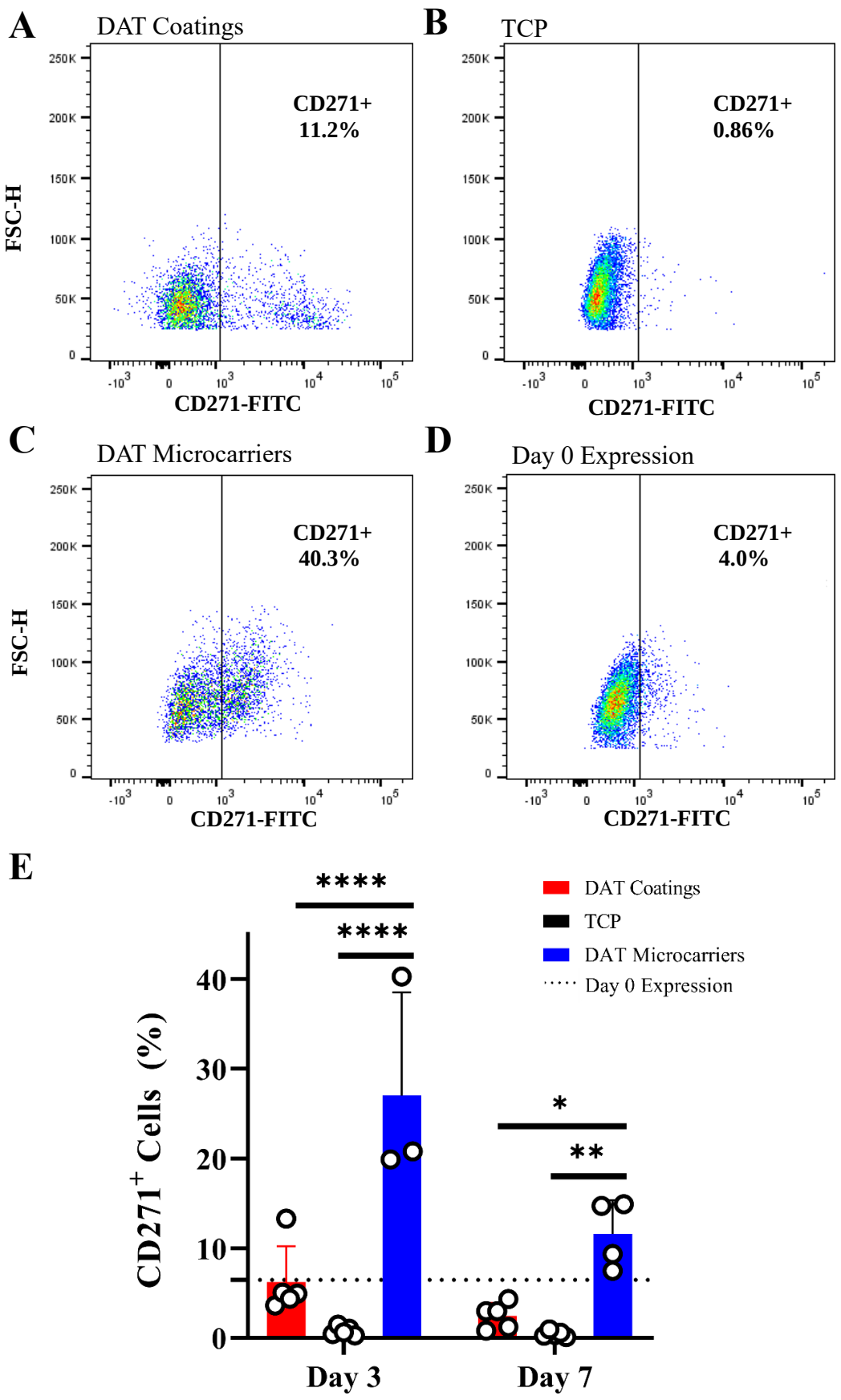
A
DAT Coatings
CD271+
11.2%
FSC-H
CD271-FITC
B
TCP
CD271+
0.86%
CD271-FITC
C
DAT Microcarriers
CD271+
40.3%
FSC-H
CD271-FITC
D
Day 0 Expression
CD271+
4.0%
CD271-FITC
E
DAT Coatings
TCP
DAT Microcarriers
Day 0 Expression
****
****
*
**
CD271+ Cells (%)
Day 3
Day 7

Figure 3.5 The fraction of BM-MSC that expressed CD271 was increased when the cells were cultured on DAT microcarriers under dynamic conditions. Representative flow cytometry plots showing CD271 expression (undifferentiated MSC marker) on BM-MSC at day 7 when cultured on **(A)** DAT coatings, **(B)** TCP, **(C)** DAT microcarriers, or at **(D)** day 0 prior to seeding**.** The frequency of $CD271^+$ BM-MSC was significantly increased on DAT microcarriers compared to DAT coatings and TCP across different time points **(E).** Data represent Mean ± SD using BM-MSC purified from 3 – 5 human BM samples (*$p<0.05$, **$p<0.01$, ***$p<0.001$, ****$p<0.0001$). Analysis for statistical significance was performed using a two-way ANOVA followed by Tukey's post hoc multiple comparisons test.

3.6 Conditioned Media Generated by BM-MSC on DAT Coatings Increased Endothelial Cell Survival

MSC are known to secrete a variety of growth factors *in vitro* that support endothelial cell homeostasis[96]. As such, the ability of the DAT to influence BM-MSC pro-angiogenic secretory potential *in vitro* was assessed. Conditioned media (CdM) was generated from BM-MSC cultured on the different substrates under serum-free conditions. Concentrated (10-fold) CdM was supplemented into human microvascular endothelial cell (HMVEC) cultures in endothelial basal media-2 (EBM-2) with no growth factors or serum, and the ability of CdM to influence HMVEC survival was determined by staining with 7-AAD (dead cell marker) and Annexin-V (apoptotic cell marker) after 1 and 3 days of culture. After 1 day of culture, the frequency of live HMVEC ($Annexin^-/7AAD^-$) was not changed between groups (Figure 3.6E). At day 3, the frequency of live HMVEC was significantly decreased as compared to day 1 for all groups. Additionally, at day 3, the frequency of HMVEC survival was significantly increased when HMVEC were supplemented with CdM from cells cultured on DAT coatings (47.6 ± 7.9%) compared to unconditioned EBM-2 (29.5 ± 10.1%, *$p<0.05$, Figure 3.6E). Interestingly, the frequency of HMVEC survival was also significantly increased when supplemented with DAT coating CdM compared to TCP CdM (31.4 ± 10.6%, *$p<0.05$) or unseeded DAT coating controls (28.1 ± 8.3%, **$p<0.01$, Figure 3.6E). Lastly, no significant differences were seen in HMVEC survival when supplemented with DAT microcarriers CdM (33.6 ± 19.8%, Figure 3.6E) compared to other groups.

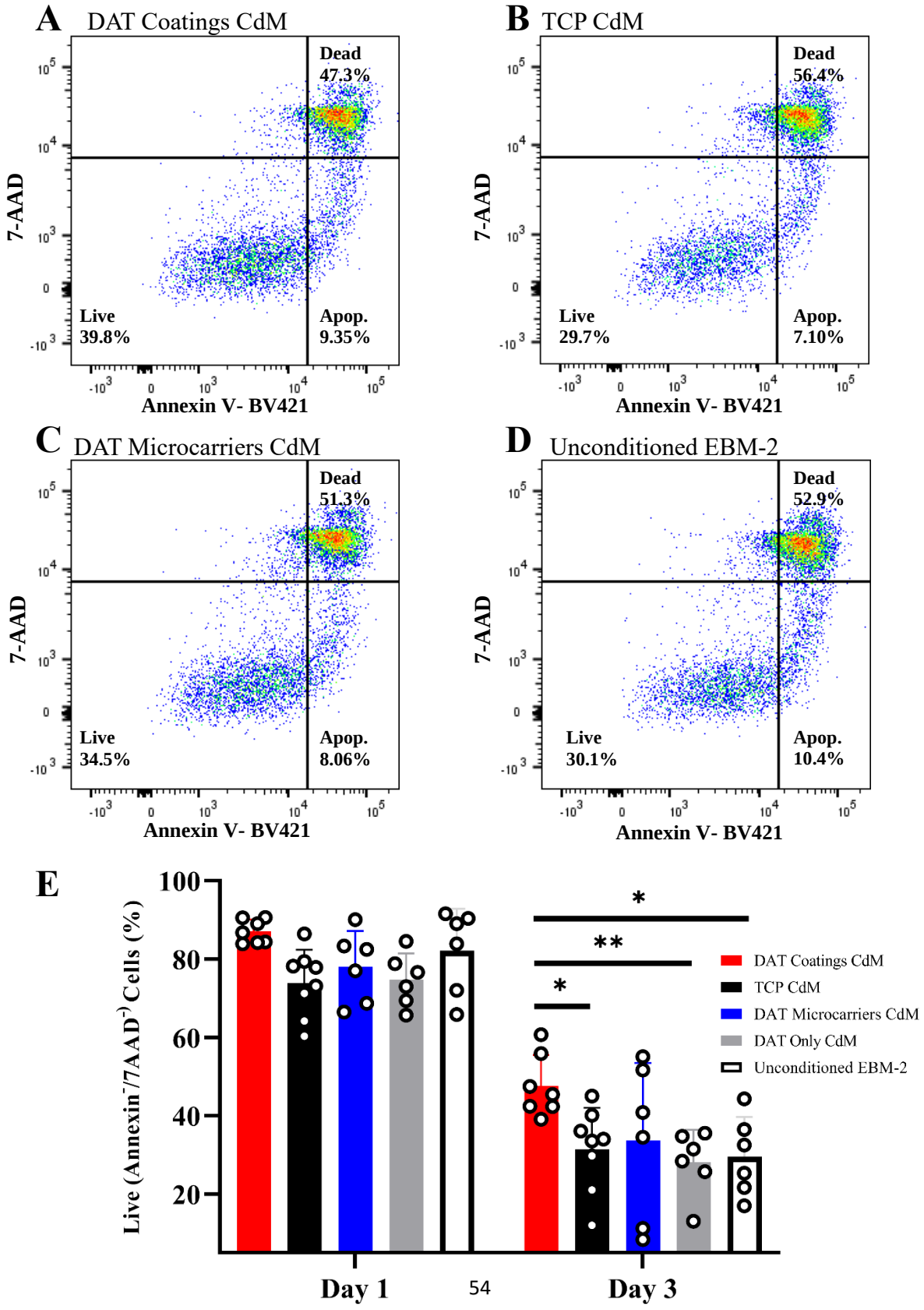
A
DAT Coatings CdM
Dead
47.3%
Live
39.8%
Apop.
9.35%
7-AAD
Annexin V- BV421
B
TCP CdM
Dead
56.4%
Live
29.7%
Apop.
7.10%
7-AAD
Annexin V- BV421
C
DAT Microcarriers CdM
Dead
51.3%
Live
34.5%
Apop.
8.06%
7-AAD
Annexin V- BV421
D
Unconditioned EBM-2
Dead
52.9%
Live
30.1%
Apop.
10.4%
7-AAD
Annexin V- BV421
E
Live (Annexin-7AAD-) Cells (%)
100
80
60
40
20
*
**
*
DAT Coatings CdM
TCP CdM
DAT Microcarriers CdM
DAT Only CdM
Unconditioned EBM-2
Day 1
Day 3

Figure 3.6 HMVEC survival was increased under serum-free conditions when cultures were supplemented with BM-MSC CdM. Representative flow cytometry plots showing 7AAD (dead) and Annexin-V (apoptotic) HMVEC after 3 days culture in EBM-2 media supplemented with CdM generated by BM MSC on **(A)** DAT coatings, **(B)** TCP, **(C)** DAT microcarriers, or **(D)** unconditioned EBM-2 media. **(E)** At Day 3, HMVEC survival was significantly increased when supplemented with CdM generated by BM-MSC on DAT coatings compared to CdM generated on TCP, DAT only, and unconditioned EBM-2. Data represent Mean ± SD using BM-MSC purified from 6 – 8 human BM samples. Abbreviations, CdM; conditioned media, EBM-2; endothelial basal media. Analysis for statistical significance was performed using a two-way ANOVA followed by Tukey's post hoc multiple comparisons test.

3.7 Conditioned Media Generated by BM-MSC Cultured on all Substrates had no Effect on Endothelial Cell Proliferation

Next, the ability of BM-MSC CdM to stimulate endothelial cell proliferation *in vitro* was assessed via the EdU uptake assay. HMVEC cultured under serum-free culture were supplemented with BM-MSC CdM generated on the various substrates. At 24 hours prior to HMVEC harvest at days 1 and 3, cultures were pulsed with EdU, and EdU uptake into proliferating HMVEC was quantified by EdU conjugation to the Azide fluorophore Pacific Blue™ to quantify the fraction of proliferating cells by flow cytometry. Representative flow cytometry detection of EdU^+ cells that underwent DNA-replication since the pulse period in HMVEC cultures supplemented with DAT coating CdM, TCP CdM, DAT microcarrier CdM, or unconditioned EBM-2 media are shown in Figure 3.7A-D. Within groups the frequency of EdU^+ HMVEC were significantly decreased across time points. However, no significant changes in HMVEC EdU uptake were observed between groups when supplemented with CdM generated by BM-MSC cultured under any of the conditions studied (Figure 3.7E). Thus, HMVEC proliferation under serum-free conditions *in vitro* was not augmented by supplementation with BM-MSC CdM generated under the various culture conditions tested.

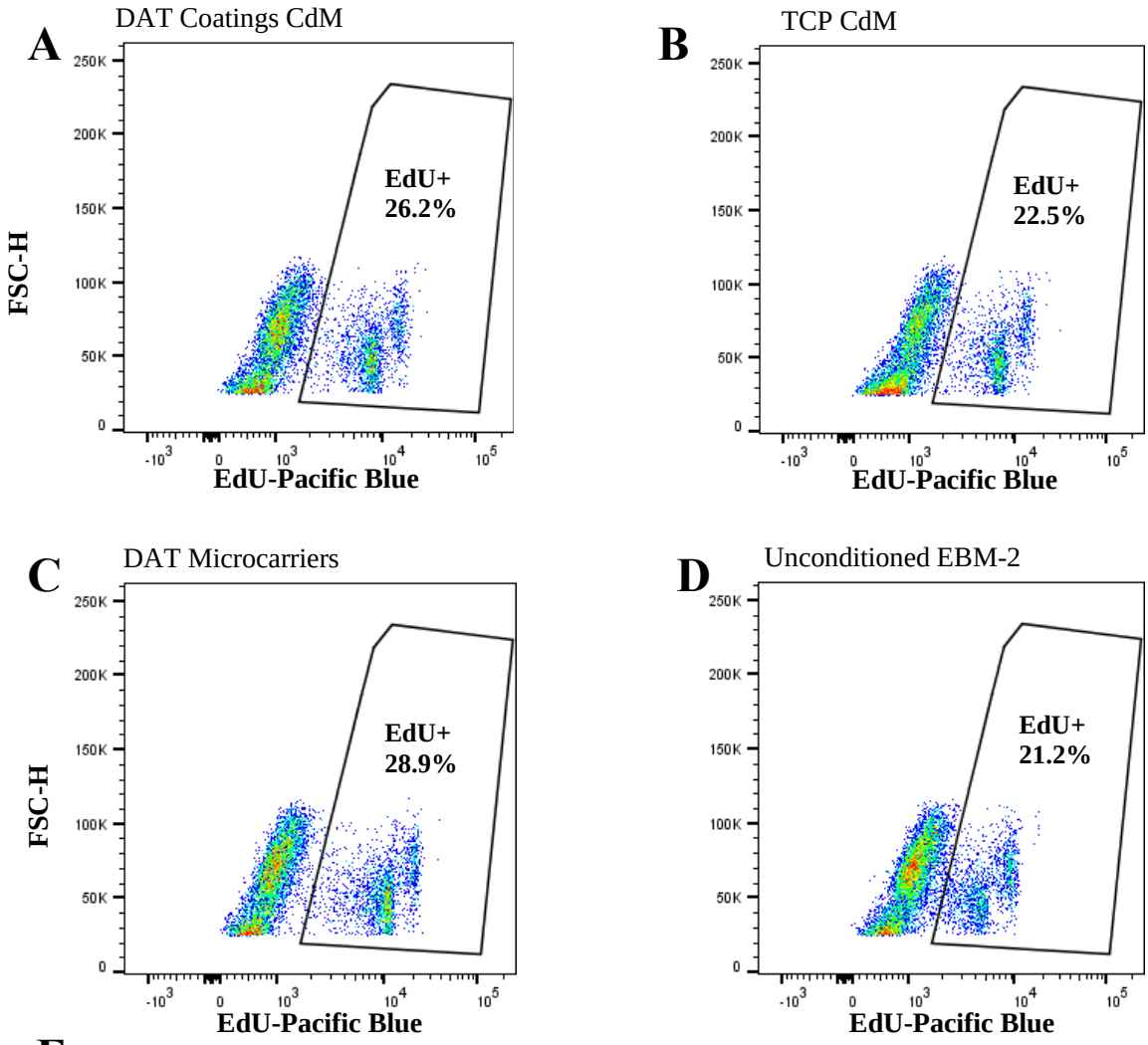
A
DAT Coatings CdM
EdU+
26.2%
FSC-H
EdU-Pacific Blue
B
TCP CdM
EdU+
22.5%
EdU-Pacific Blue
C
DAT Microcarriers
EdU+
28.9%
FSC-H
EdU-Pacific Blue
D
Unconditioned EBM-2
EdU+
21.2%
EdU-Pacific Blue

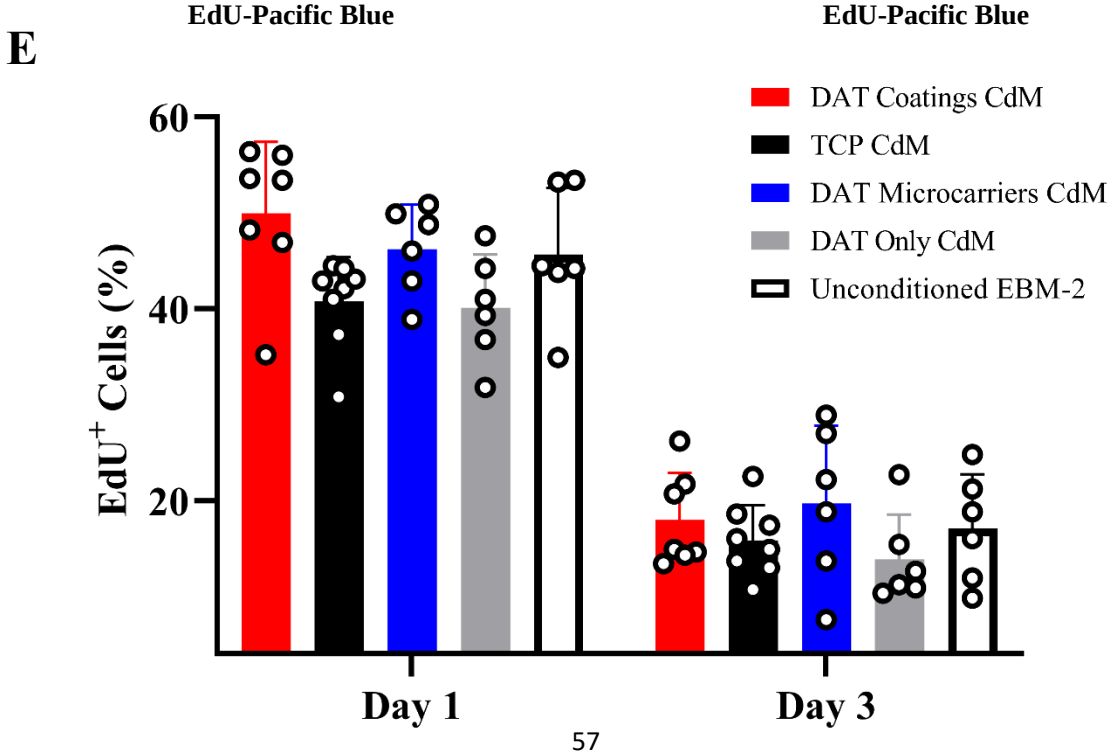
E
DAT Coatings CdM
TCP CdM
DAT Microcarriers CdM
DAT Only CdM
Unconditioned EBM-2
EdU+ Cells (%)
60
40
20
Day 1
Day 3

Figure 3.7 HMVEC proliferation under serum-free conditions was not changed when supplemented with BM-MSC CdM. Representative flow cytometry plots showing EdU uptake by HMVEC following a 24 hour EdU pulse when cultured in EBM-2 media supplemented with **(A)** DAT coatings CdM, **(B)** TCP CdM, **(C)** DAT Microcarriers CdM, or **(D)** Unconditioned EBM-2 media. (**E)** Frequency of EdU^+ HMVEC supplemented with CdM generated by BM-MSC on various substrates showed no significant differences between groups. Data represent Mean ± SD using BM-MSC purified from 6 – 8 human BM samples Analysis for statistical significance was performed using a two-way ANOVA followed by Tukey's post hoc multiple comparisons test.

3.8 Conditioned Media Generated by BM-MSC did not Influence Endothelial Cell Tubule Formation under all Culture Conditions Studied

To assay for the ability of collected CdM to induce tubule formation, HMVEC were cultured on growth factor reduced Geltrex™ and supplemented with CdM generated by BM-MSC under the conditions previously described. After 24 hours, HMVEC tubule formation was imaged (Figure 3.8A-D), and blinded counting of complete tubule branch points was performed. No significant differences in HMVEC tubule branch points/cm^2 were observed when supplemented with CdM generated by BM-MSC under any of the conditions (Figure 3.8E).

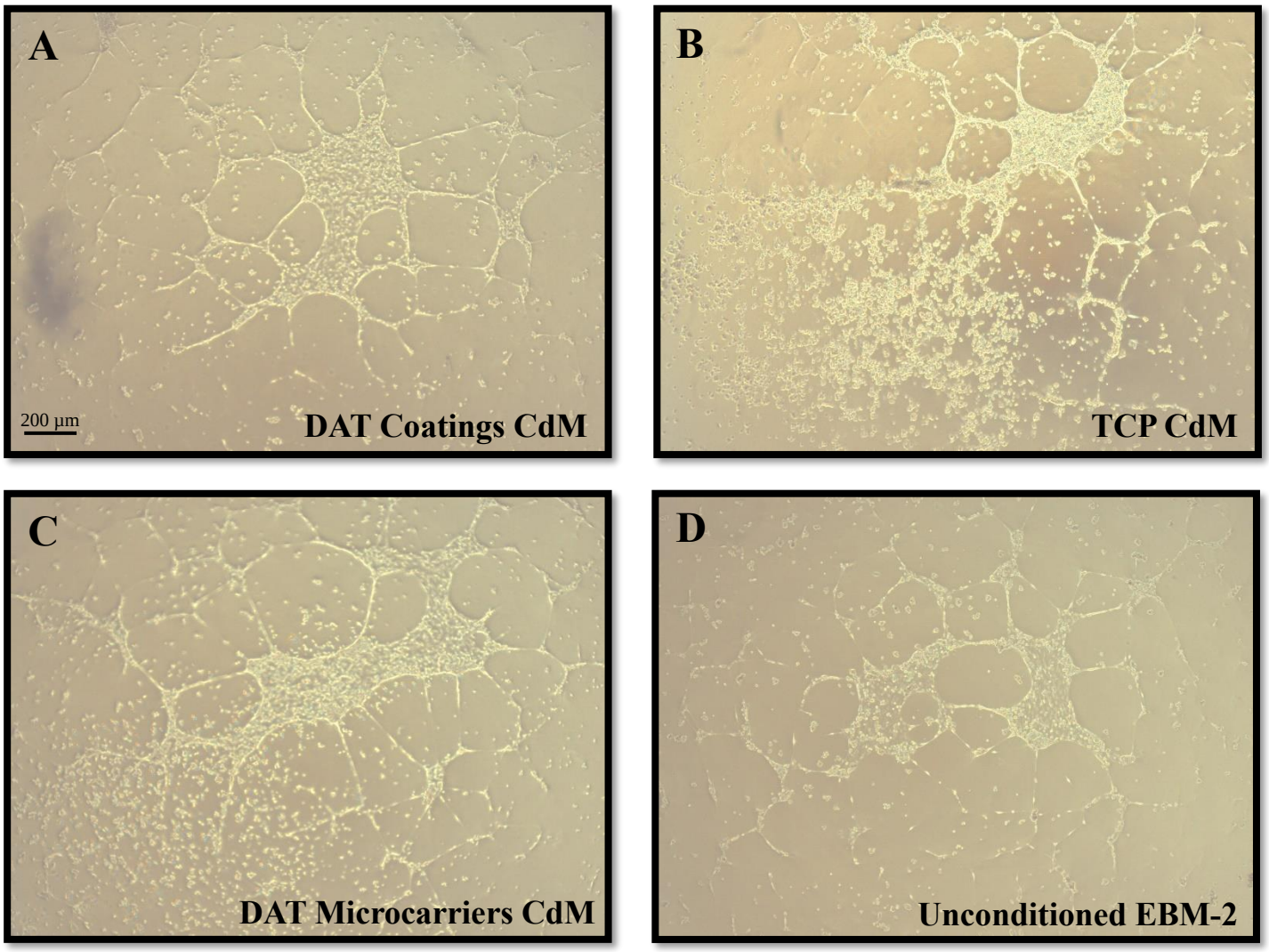
A
200 µm
DAT Coatings CdM
B
TCP CdM
C
DAT Microcarriers CdM
D
Unconditioned EBM-2

E

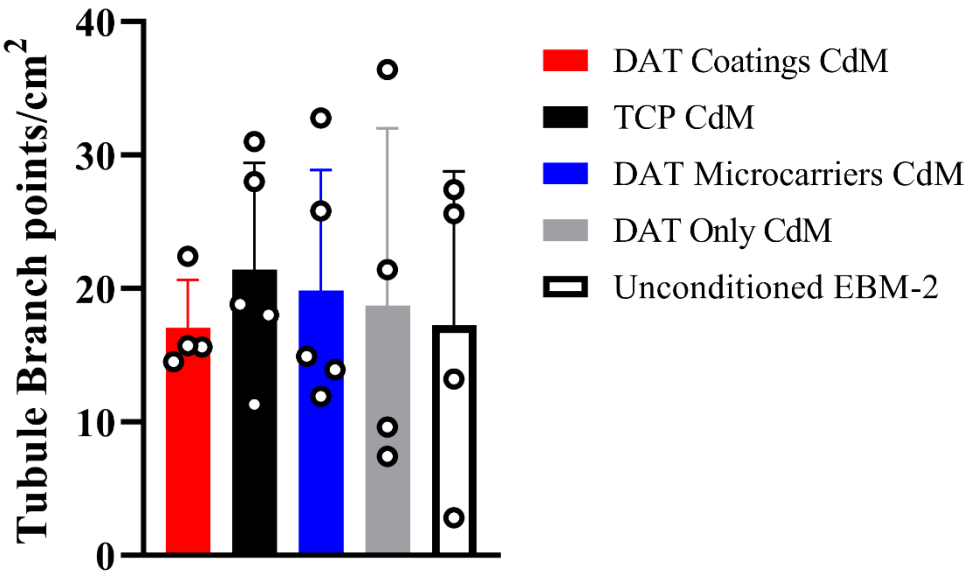
Tubule Branch points/cm^2
40
30
20
10
0
DAT Coatings CdM
TCP CdM
DAT Microcarriers CdM
DAT Only CdM
Unconditioned EBM-2

Figure 3.8 HMVEC tubule formation under serum-free conditions was not changed by supplementation with BM-MSC CdM. Representative images of HMVEC tubule formation after 24 hours culture in growth factor reduced Geltrex matrix supplemented with CdM generated by BM-MSC on **(A)** DAT coatings, **(B)** TCP, **(C)** DAT Microcarriers, or **(D)** Unconditioned EBM media. **(E)** CdM derived from BM-MSC did not change HMVEC tubule formation between groups. Data represent Mean ± SD using BM-MSC purified from 4 – 5 human BM samples. Analysis for statistical significance was performed using a one-way ANOVA followed by Tukey's post hoc multiple comparisons test.

3.9 BM-MSC Cultured on Various Substrates Secreted Unique Proteins

Following *in vitro* characterization of pro-angiogenic functions, CdM samples (N=3 / culture treatment) underwent global secretome analyses using label-free, quantitative mass spectrometry (Figure 3.9A). Total unique peptide and protein detection was statistically equivalent in CdM from DAT coatings (7449, 442) and TCP (8143, 585) showing excellent coverage, whereas a lower number of unique peptides and proteins were detected in CdM from the DAT microcarriers (3260, 139) (Figure 3.9B, C). A total of 834 unique proteins were identified, with 53 proteins unique to DAT coatings CdM, 279 proteins unique to TCP CdM, and 26 proteins unique to DAT microcarriers CdM (Figure 3.9D). Distinct secretory signatures were substrate and culture condition dependent, as revealed by principal component analysis (Figure 3.9E). BM-MSC cultured on DAT coatings or microcarriers showed unique secretory profiles that were very consistent between different donors. In contrast, greater variability was observed with one donor in the secretome of BM-MSC cultured on TCP. The PCA analysis showed a large difference in component 1 (69.8%), which separated the DAT microcarriers CdM from the other two groups. In contrast, the lower magnitude of component 2 (9.2%), which segregated the DAT coatings CdM from the TCP CdM, suggests that the secretome in these two groups was more similar.

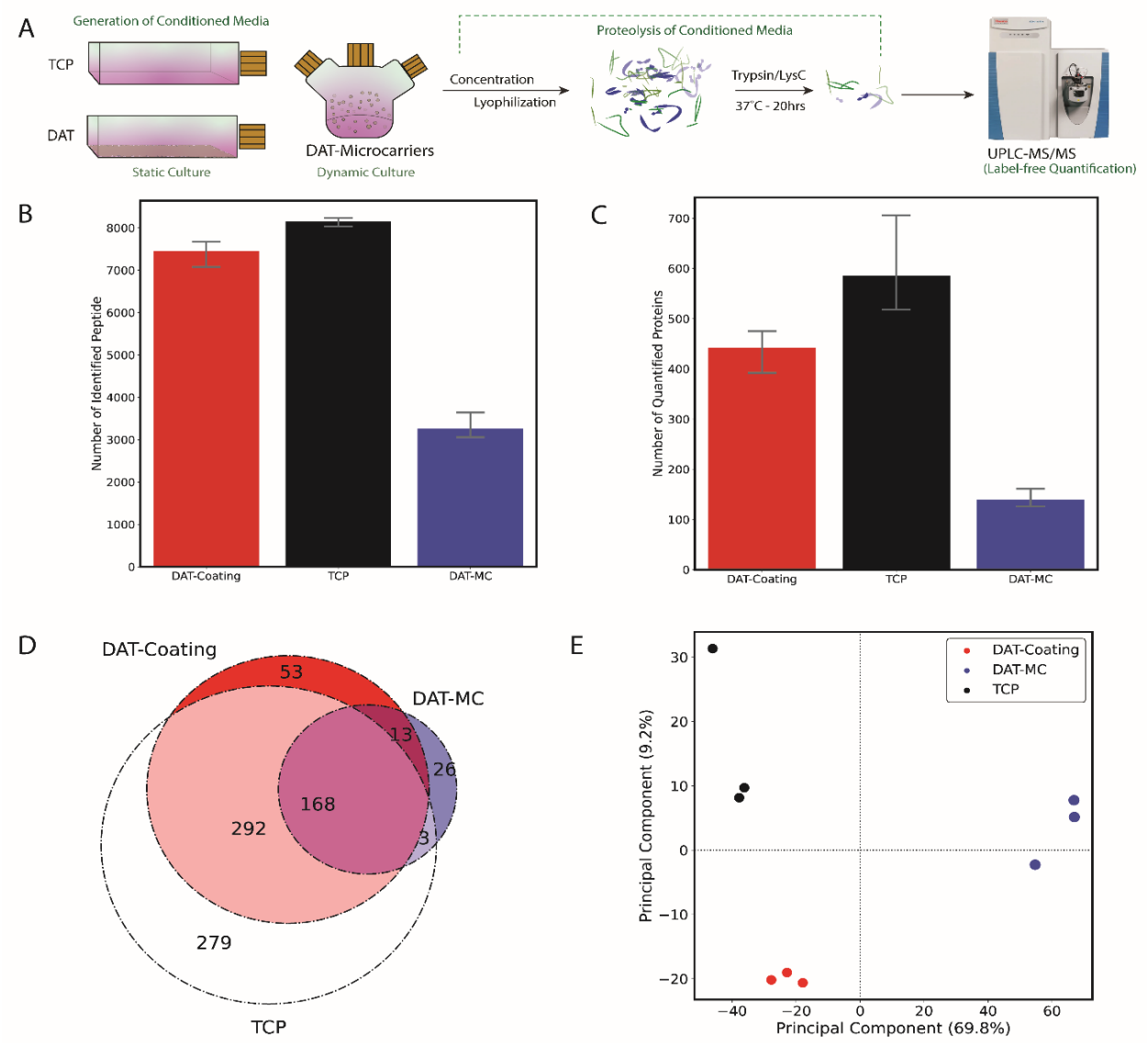

Figure 3.9 Global secretome of BM-MSC was distinct when cultured on DAT coatings, TCP, or DAT microcarriers. (A) Overview of experimental methodology showing collection, concentration, lyophilization, proteolysis, and subsequent label-free MS quantification of CdM. Number of peptides **(B)** and **(C)** proteins identified in CdM collected from BM-MSC cultured on different conditions. **(D)** A total of 834 unique proteins were identified, of which 53, 279, and 26 were unique to DAT coatings, TCP, and DAT microcarriers CdM respectively. **(E)** Principle component analysis revealed divergent proteomic signatures of BM-MSC cultured on DAT coatings, TCP, or DAT microcarriers. Data represent Mean ± SD using BM-MSC purified from 3 human BM samples.

3.10 BM-MSC Cultured on DAT Coatings Secreted Factors Associated with Wound Healing and ECM Remodelling Compared to BM-MSC Cultured on TCP.

Within the proteins that were co-expressed under all 3 conditions, volcano plots comparing DAT coatings CdM to TCP CdM further revealed 79 proteins were increased in TCP CdM, whereas only 18 proteins were increased in DAT coatings CdM and only 9 proteins were increased in DAT microcarriers CdM compared to TCP CdM (>2-fold, $p<0.05$, Figure 3.10A,B). Upregulated proteins in TCP CdM and DAT coatings CdM were also cross-referenced to Gene-ontology (GO) Biological Processes annotations[199]. In the DAT coatings CdM eight factors were associated with regulation of wound healing or ECM remodelling (Table 3.1). The other unique proteins included 4 ECM components (chondroadherin, tenascin, proteoglycan, epoxide hydrolase), 2 immunomodulatory factors (mast cell carboxypeptidase and neutrophil defensin), 2 enzymes (peptidyl isomerase and citrate synthase), and 2 proteins of unknown function (c-type mannose receptor and plexin-domain containing protein). Enrichment association of GO Biological Processes revealed upregulation of factors by BM-MSC on DAT coatings associated with wound healing, ECM organization, epithelial cell proliferation, and gland development (Figure 3.10C). Upregulated proteins in TCP CdM compared to DAT coatings CdM were associated with supramolecular fibre organization, ECM organization, blood vessel morphogenesis, and negative regulation of cell migration (Figure 3.10D). Upregulated peptides in TCP included D-dopachrome decarboxylase, SERPINF1, Dickopff-related protein-1, MMP2, follistatin-related protein, and myeloid derived growth factor. Analysis of peptides secreted by BM-MSC cultured on DAT coatings and DAT microcarriers revealed that out of the 9 unique proteins in DAT microcarrier CdM, 5 were also upregulated on DAT coatings CdM including, fibroblast activation protein (FAP), thrombospondin 4 (THBS4), fibromodulin (FMOD), antithrombin-III (SERPINC1), and contactin-1 (CNTN1) (Figure 3.10E).

TABLE 3.1 SELECT UPREGULATED PROTEINS SECRETED BY BM-MSC WHEN CULTURED ON DAT COATINGS COMPARED TO TCP.

Protein	Gene Name	Primary Function	Fold Change	P-value
Fibroblast Activation Protein	FAP	Cell surface glycoprotein that participates in wound healing, tissue remodelling, and inflammation.	3.56	2.00E-10
Alpha-1-Antitrypsin	SERPINA1	Modulating acute inflammation, tissue repair, and regeneration.	2.13	8.60E-10
Thrombospondin-4	THBS4	Cell-to-cell and cell-to-matrix interactions, involved in cell proliferation, migration, adhesion, and	3.49	1.35E-03
Extracellular Sulfatase-1	SULF1	Integral regulator of cell signalling pathways involving cell growth, proliferation, differentiation, and migration.	3.48	1.45E-03
Hepatocyte Growth Factor-like Protein	MST1	Monocyte regulation and wound healing.	5.57	8.81E-03
Fibromodulin	FMOD	Extracellular matrix remodelling.	3.99	3.10E-02
Antithrombin-III	SERPINC1	Anti-coagulant and anti-angiogenic.	2.63	4.80E-02
Contactin-1	CNTN1	Cell adhesion and neuronal development.	4.72	6.99E-03

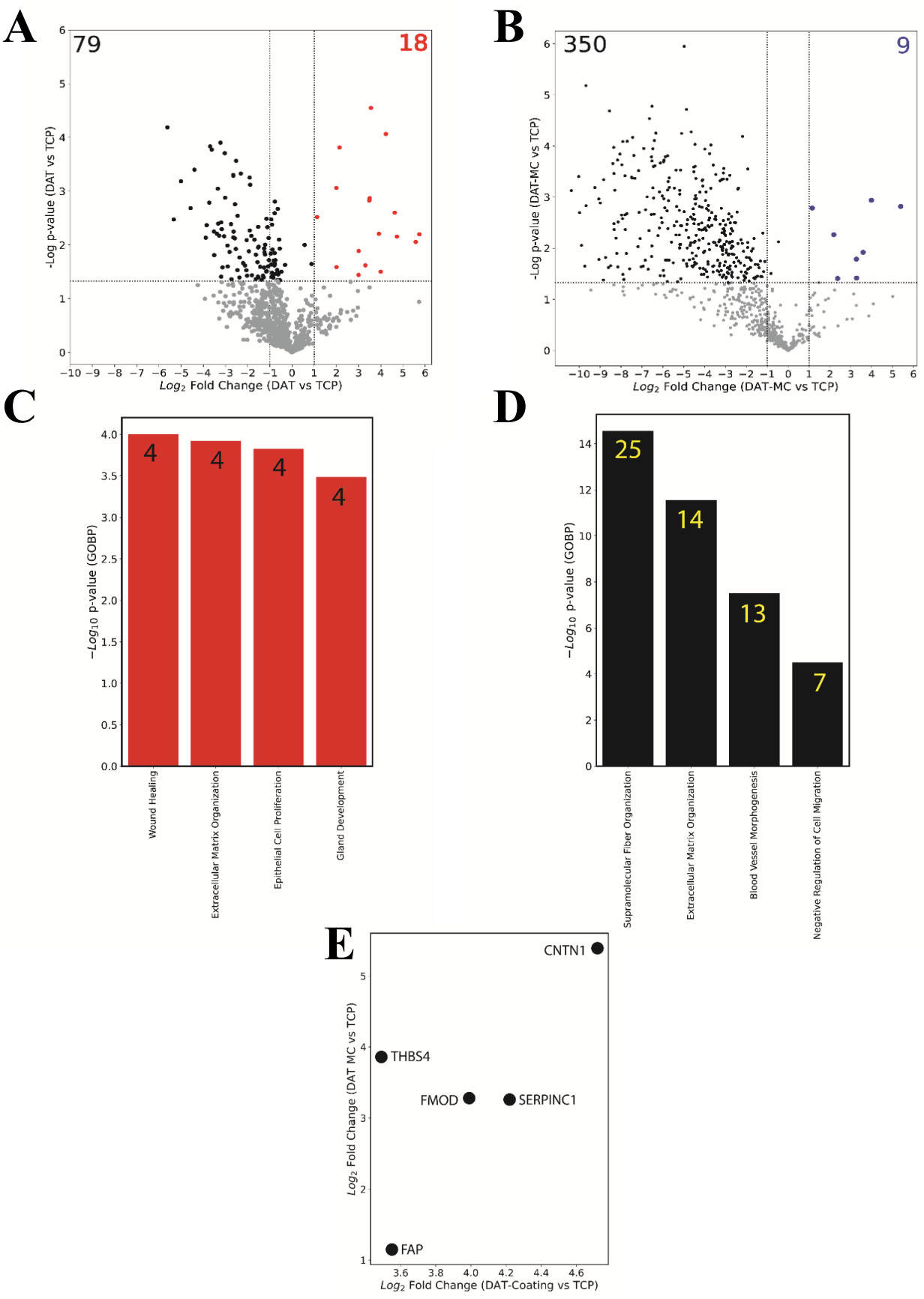
A
79
18
-Log p-value (DAT vs TCP)
Log2 Fold Change (DAT vs TCP)
B
350
9
-Log p-value (DAT-MC vs TCP)
Log2 Fold Change (DAT-MC vs TCP)
C
4
4
4
4
−Log10 p-value (GOBP)
Wound Healing
Extracellular Matrix Organization
Epithelial Cell Proliferation
Gland Development
D
25
14
13
7
−Log10 p-value (GOBP)
Supramolecular Fiber Organization
Extracellular Matrix Organization
Blood Vessel Morphogenesis
Negative Regulation of Cell Migration
E
CNTN1
THBS4
FMOD
SERPINC1
FAP
Log2 Fold Change (DAT MC vs TCP)
Log2 Fold Change (DAT-Coating vs TCP)

Figure 3.10 BM-MSC secreted factors associated with wound healing and ECM remodelling when cultured on DAT coatings compared to TCP. (A) Volcano plot comparing DAT coatings CdM to TCP CdM showing 18 and 79 unique proteins respectively that were significantly increased >2.0-fold. **(B)** Further comparison between DAT microcarriers CdM and TCP showing 9 and 350 unique proteins respectively, that were significantly increased >2.0-fold. **(C)** Enrichment association revealed that BM-MSC on DAT coatings secreted factors that were associated with wound healing, ECM organization, epithelial cell proliferation, and gland development. **(D)** Upregulated proteins in TCP CdM were associated with supramolecular fibre organization, ECM organization, blood vessel morphogenesis, and negative regulation of cell migration. **(E)** Similar hits were identified in DAT coatings and DAT microcarrier CdM compared to TCP, which included FAP, THBS4, FMOD, SERPINC1, and CNTN1. GO enrichment analyses were performed using open-source Metascape (Metascape.org)[199]. Data represent Mean ± SD using BM-MSC purified from 3 human BM samples ($p<0.05$).

Chapter 4.0 Discussion

4.1 Summary of Observations

The following novel observations were uncovered during the course of my thesis experiments:

1) DAT coatings supported the attachment and growth of BM-MSC.

2) The fraction of cells expressing the defining BM-MSC stromal markers CD73, CD90, and CD105, and the pericyte marker CD146, was not altered by culture on DAT substrates under static or dynamic conditions.

3) The frequency of BM-MSC with high ALDH-activity was reduced relative to baseline levels at the time of seeding with culture on TCP and better preserved with culture on DAT coatings.

4) The fraction of cells expressing low affinity nerve growth factor receptor (LNGFR or CD271) was increased relative to baseline levels at the time of seeding by culture on DAT microcarriers under dynamic culture conditions, but not by culture on DAT coatings under static conditions.

5) BM-MSC conditioned media (CdM) generated on DAT coatings under static conditions increased HMVEC survival under serum-free conditions but did not alter HMVEC proliferation or tubule formation *in vitro.*

6) BM-MSC cultured on DAT coatings had a secretome associated with enhanced wound healing, ECM remodelling, epithelial cell proliferation, and gland development.

4.2 Discussion of Observations

4.2.1 DAT Coatings Supported the Attachment and Growth of BM-MSC

While DAT constructs have previously been shown to support the growth of adipose-derived stromal/stem cells (ASC)[120,175,177,191], this was the first time that bone marrow-derived mesenchymal stromal/stem cells (BM-MSC) were investigated on DAT platforms. Thus, a pilot study was performed to confirm that the DAT coatings supported the attachment and growth of human BM-MSC under static conditions before advancing to more in-depth studies involving dynamic culture. Culture on DAT coatings reduced the frequency of non-viable BM-MSC and increased viable BM-MSC counts after a 7-day period compared to culture on tissue culture polystyrene (TCP). The enhanced yield may be attributed in part to favorable cell-ECM interactions associated with culturing on the DAT.

MSC possess a variety of cell surface receptors including integrins, which are critical in facilitating cell-ECM interactions[150]. Broadly, integrins are heterodimeric proteins consisting of α and β subunits, the latter are involved in various cell-ECM interactions. These heterodimers can bind laminins, fibronectins, GAG, and collagens[200], which are ECM components that have been identified in DAT[163,176,201]. Binding of integrins to ECM components has been shown to regulate survival, apoptosis, proliferation, and migration in various cell types including MSC[127,200]. It was observed that the frequency of non-viable BM-MSC was decreased and viable cell count was increased when cultured on DAT coatings compared to TCP which maybe due to cell-ECM interactions. However future studies should further explore whether culturing on the DAT coatings stimulated proliferation, prevented cell death, or resulted in both.

In addition to providing supportive biochemical cues, DAT coatings may have provided a greater surface area for BM-MSC growth as compared to TCP, with a 3-D topography evident by multiphoton microscopy. Cells cultured on TCP reached confluency by day 7, while it appeared that there was more available volume for BM-MSC proliferation on the DAT, which likely contributed to the higher viable BM-MSC yield. Multiphoton imaging also showed a qualitatively less elongated cell morphology in the BM-MSC cultured on the DAT coatings as compared to TCP, where a more elongated-spindle shape was observed. These differences may be attributed to differences in the cell densities due to greater surface area, which can affect cell morphology[202]..

4.2.2 Expression of BM-MSC Stromal Markers (CD73, CD90, and CD105) and the Pericyte Marker (CD146) was not Altered by Culture on DAT Substrates under Static or Dynamic Conditions.

The expression of defining MSC stromal markers, CD73, CD90, and CD105, was not altered by culturing the BM-MSC on DAT substrates under static or dynamic conditions, indicating that prolonged culture on DAT did not influence native MSC. Similarly, previous work in the Flynn lab observed no significant differences in CD73, CD90, and CD105 expression on ASC following a 3-week expansion on DAT microcarriers[120]. In addition, the pericyte marker CD146, found on MSC with vascular smooth muscle commitment[194] was not changed following culture on DAT constructs. Due to the ability of ECM to support MSC primitive and non-differentiated phenotypes, it was hypothesized that prolonged culture on TCP would result in decreased CD146 expression while a maintenance would be observed on DAT, however this was not observed in these findings.

4.2.3 The Frequency of BM-MSC with High ALDH-activity was Reduced with Culture on TCP and Preserved with Culture on DAT Coatings.

In addition to cell surface marker analyses, the effects of culturing on the DAT substrates on the function of the self-protective enzyme aldehyde dehydrogenase (ALDH) was assessed. ALDH includes a large family of enzymes which detoxify cellular aldehydes. The isoforms ALDH1A1 and ALDH1A3 are of specific importance in MSC, as they regulate the production of retinoic acid (RA)[203]. RA induces transcription of a variety of genes involved in cell differentiation, and hence regulating RA production is crucial in maintaining progenitor cell fate[204]. As primitive progenitor cells differentiate, ALDH-activity is gradually reduced, and as such ALDH has been used as a conserved progenitor cell functional marker to select for cells with enhanced regenerative properties[72]. The Hess lab has previously shown that human umbilical cord blood-derived $ALDH^{hi}$ cells restored limb perfusion in a femoral artery ligation (FAL)-induced unilateral hindlimb ischemia model adapted to immunodeficient NOD/SCID mice[72,196]. Further, MSC purified using high ALDH-activity mediated enhanced cell recruitment into implanted DIVAA™ inserts compared to $ALDH^{lo}$ MSC[195]. Thus, analysis of ALDH-activity in BM-MSC cultured on DAT was performed.

BM-MSC cultured on DAT coatings retained the frequency of cells with high ALDH-activity, as a significant decrease from day 0 levels was observed after 7 days of culture on TCP. In contrast, the frequency of ALDH^{hi} BM-MSC was not significantly changed from day 0 levels after 7 days of culture on DAT coatings. As previously described, MSC-based therapies face challenges during expansion, as cells lose regenerative secretory capacity during the extensive proliferation required for translation to clinical applications in humans[49,205]. This study suggests that DAT coatings may be a superior platform to expand BM-MSC while retaining the regenerative marker ALDH.

Consistent with these findings, recent work in our lab showed an increase in frequency of ALDH^{hi} cells when human hematopoietic progenitor cells were cultured on DAT foams, which was associated with differentiation towards the monocyte/macrophage lineage[178]. Additionally, Begum *et al*. previously reported an increase in ALDH^{hi} pancreatic ductal cells when cultured on type I collagen compared to TCP due to enhanced $\alpha_2\beta_1$ integrin signalling – a central integrin in the modulation of MSC fate[206,207]. However, it is difficult to pinpoint exact components of DAT that maintain high ALDH-activity in BM-MSC. Most likely, a complex interplay between various ECM components and MSC integrin interactions are involved. Interestingly, culture on DAT microcarriers under dynamic conditions did not elicit a similar response, as a decline in the frequency of ALDH^{hi} BM-MSC was observed from day 0 expression similar to TCP. This may be attributed to the impact of dynamic culture and additional exposure to shear stress forces rather than the DAT substrate itself, as high ALDH-activity was preserved in BM-MSC cultured on DAT coatings under static culture conditions. This may indicate that shear stress forces were not optimized for the maintenance of high ALDH-activity in BM-MSC, and the effects of different stirring rates on ALDH-activity should be investigated in future experiments.

4.2.4 The Fraction of BM-MSC Expressing LNGFR (CD271) was Increased by Culture on DAT Microcarriers under Dynamic Culture Conditions, but not Through Culture on DAT Coatings under Static Conditions

The fraction of cells expressing CD271, also known as low-affinity nerve growth factor receptor (LNGFR), was assessed on the BM-MSC under the various culture conditions studied. CD271 has been purported as a primitive MSC marker to enrich for undifferentiated cells that retain high proliferative capacity from bone marrow sources[197]. Although, it should be noted that the association of CD271

expression and primitive MSC function has yet to be proven. However, it has been shown that CD271 identifies a subset of MSC with enhanced immunomodulatory potential[198]. Smith *et al*. observed that ASC selected for CD271 expression showed enhanced pro-angiogenic gene expression, while demonstrating lower inflammatory gene expression than $CD271^-$ ASC[208]. In our analyses, a higher percentage of BM-MSC expressed CD271 when cultured on DAT microcarriers compared to day 0. The frequency of BM-MSC expressing this marker was also increased compared to DAT coatings and TCP throughout the 7-day culture period. The significant change seen following culture on the DAT microcarriers is likely attributed to dynamic culturing parameters, since an increase in CD271 expression from day 0 was not observed when BM-MSC were cultured on DAT coatings under static conditions. It is possible that increased shear stress from the spinner flask platform may increase CD271 expression on BM-MSC through putative mechano-transduction signalling. A synergistic effect between DAT-integrin signalling and MSC and shear forces may also account for these differences seen.

Additionally, CD271 is also a receptor for a variety of neutrotrophins including brain-derived neutrotrophin factor (BDNF), neutrotrophin 3 (N3), neutrotrophin 4 (N4), and nerve growth factor (NGF)[209]. Neutrotrophins are reported to play a major role in regulating survival, development, and function of neurons and many other cell types through receptor tyrosine kinase (RTK) signalling[210]. Criger *et al*., showed that subpopulations of MSC secrete BDNF and NGF, which promoted neuronal survival and function *in vitro*[211]. Later Milczarek *et al*. found that $CD271^+$ MSC express BDNF, NGF, and a variety of other neutrotrophins[212]. We hypothesize that secreted neutrotrophins may be acting on the MSC through an autocrine fashion. In this project, it was observed that the frequency of BM-MSC expressing CD271 increased when cultured on DAT microcarriers, which may permit increased autocrine signalling through CD271-mediated RTK signals that influence cell behaviour[213]. The importance of $CD271^+$ MSC in neuro-regeneration has been highlighted in clinical studies that showed intrathecal (IT) and intravenous (IV) transplantation of autologous $CD271^+$ MSC improved neural, cognitive, and motor symptoms in epileptic patients[212] and restored sensation and movement in a patient with spinal cord injury[214]. Collectively, the findings in this thesis with CD271 expression warrant further investigation for the use of DAT culturing platforms to generate BM-MSC for neuro-regeneration applications.

4.2.5 BM-MSC CdM Generated on DAT Coatings Increased HMVEC Survival under Serum-free Conditions but did not Alter HMVEC Proliferation or Tubule Formation *In Vitro*

MSC are well recognized to secrete factors that promote angiogenesis *in vivo* and *in vitro*[94]. In this project, the pro-angiogenic secretory functions of BM-MSC following culture on DAT constructs were assessed *in vitro*. Conditioned media (CdM) was collected from the BM-MSC cultured statically on the DAT coatings or TCP, or dynamically on the DAT microcarriers, under serum-free conditions. The effects of supplementation with this CdM on the survival, proliferation, and tubule formation of human microvascular endothelial cell (HMVEC) cultured under growth factor and serum-reduced conditions were explored. HMVEC cultured in fully supplemented EGM-2 media (positive control) showed excellent viability (about 85 – 90% live cells) and EdU uptake (roughly 40 - 60% EdU positive cells), data for EGM condition not shown. BM-MSC CdM generated on DAT coatings increased HMVEC survival compared to unconditioned media and BM-MSC CdM generated on TCP. Surprisingly, a significant difference was not observed when supplementing with BM-MSC CdM generated on DAT microcarriers. This may indicate that culture under static conditions was more instructive for BM-MSC pro-angiogenic secretory function. However, this effect could also be explained by loss of cells through shearing off the microcarriers during the conditioning process, as cells may be more sensitive to detachment under serum-free conditions[215]. Importantly, CdM collected from an unseeded DAT only control was significantly lower than BM-MSC-seeded wells, suggesting that residual growth factors or ECM constituents released from the DAT did not account for the differences seen in HMVEC survival. Collectively, these data suggest that culture on DAT coatings may alter the secretory function of BM-MSC to support endothelial cell survival *in vitro*.

Previously, MSC CdM has been reported to contain a mixture of pro-angiogenic growth factors including VEGF, FGF, IGF, HGF, MCP-1, and SDF-1, that supported HMVEC survival, proliferation, and tubule formation[94,97,216]. However, our study found no significant differences in HMVEC survival when supplemented with BM-MSC CdM generated on TCP as previously reported in the literature[96,97,216]. Further, no differences were observed in HMVEC proliferation and tubule formation when supplemented with BM-MSC CdM from the various groups. This lack of response is likely associated with the relatively low cell numbers used in this study to generate CdM. For comparison, previous groups generated CdM using 1.6 – 4 million MSC cultured on TCP[96,117,195,216,217]. In contrast, we generated CdM using 625K MSC per condition, likely resulting in reduced potency of CdM compared to the other studies. Further,

previous groups used 50 – 100% CdM supplemented into pro-angiogenic assays with varying concentrations, while our study used a 10% supplement.

Despite using 3 – 6 x fewer cell numbers and supplementing with smaller concentrations of CdM than previously reported, BM-MSC cultured on DAT coatings significantly increased HMVEC survival under serum-free conditions. There may be varying cytokines in the secreted CdM, which may explain why differences were observed in HMVEC survival while no differences were seen in HMVEC proliferation or tubule formation. However, it is difficult to predict which cytokines are present in the CdM, as many growth factors have ubiquitous roles in HMVEC homeostasis and are thus involved in a variety of interrelated pathways.

The observed pro-survival effects of the generated CdM may be attributed to the ECM composition and stiffness that can influence MSC behavior. Ogle *et al*. previously reported enhanced MSC CdM pro-angiogenic properties when cultured on soft hydrogels, with a Young's modulus of 30 kPa, containing integrin and cadherin engaging components[145]. DAT coatings are similarly soft (~36 kPa)[193] while DAT microcarriers are much softer (~0.73 kPa)[120], and DAT contains a wide array of bio-active ECM constituents that can interact with MSC[163,201]. The softer composition of DAT microcarriers may also explain effects seen on BM-MSC CdM, however it is difficult to attribute differences to material stiffness alone as BM-MSC were also exposed to shear stress on the DAT microcarriers. Overall, the increase in HMVEC survival following supplementation with CdM from BM-MSC cultured on DAT coatings is likely due to the biochemical and biomechanical properties of the DAT influencing the BM-MSC secretome. Similarly, previous work from the Flynn lab showed an angiogenic response from ASC seeded on DAT bioscaffolds, as $CD31^{+}/VEGF^{+}$ endothelial cell recruitment was observed into DAT scaffolds following *in vivo* implantation[175]. These findings suggest that DAT scaffolds may provide cell-instructive cues to increase ASC pro-angiogenic secretory abilities[175]. Collectively, these findings suggest that DAT coatings represent a promising culturing platform to generate CdM from BM-MSC that can increase HMVEC survival under serum-free conditions.

In vivo pro-angiogenic properties of BM-MSC generated under various conditions were also investigated in a pilot study utilizing the directed *in vivo* angiogenesis assay (DIVAA™). DIVAA™ inserts were loaded with basement membrane extract supplemented with CdM from various conditions and subcutaneously implanted into the flanks of NOD/SCID mice. Following a 14-day period *in vivo*, inserts containing CdM from BM-MSC cultured on DAT constructs qualitatively showed increased red blood cell recruitment compared to TCP culture (Supplementary Figure. 1). However, quantitative analysis did

not yield statistical significance in lectin uptake by recruited cells. The discrepancy in qualitative and quantitative data indicated that future optimization is needed to accurately quantify FITC-lectin uptake. As such, it is difficult to draw conclusions from these *in vivo* pilot studies. Additionally, angiogenesis is a complex process that relies on the recruitment of inflammatory cells to orchestrate new blood vessel formation *in vivo*[45]. This study was performed in NOD/SCID mice, with minimal immune cells to guide angiogenesis in response to pro-angiogenic factors. Future optimization of experiments should explore implanting CdM-supplemented DIVAA™ inserts in immunocompetent mice to assay for the presence of lectin uptake by infiltrating endothelial cells, monocytes, and macrophages by quantifying cell surface marker expression for each cell type using flow cytometry.

4.2.6 DAT Coatings Enriched the Secretome of BM-MSC with Factors Associated with Wound Healing and ECM remodelling.

To elucidate the composition of collected CdM, global proteomic analysis was performed using label-free mass spectrometry (MS) for CdM generated under each condition. Lower amounts of proteins were identified in the dynamic DAT microcarrier CdM group, compared to static culture on TCP or DAT coatings. Interestingly, this lower secretory breadth correlated with the *in vitro* studies that showed minimal effects of DAT Microcarrier CdM on HMVEC survival, proliferation and tubule formation. The lower number of proteins detected may be attributed to decreased protein secretion under dynamic culture conditions. However, why this occurred requires further investigation, as reduced protein secretion in dynamic culture on DAT microcarriers may also be explained by loss of cells though shearing off the microcarriers during the conditioning process under serum free conditions. Interestingly, principal component analysis (PCA) revealed tight sample clustering patterns that were culture condition dependent, indicating that culture of BM-MSC on DAT coatings, TCP, or DAT microcarriers yielded unique secretory proteomic fingerprints. It should also be noted that greater variability was observed between MSC from different bone marrow donors cultured on TCP, whereas more clustered analyses were observed on DAT coatings and DAT microcarriers.

Proteomic analysis identified 18 unique proteins that were upregulated on DAT coatings compared to TCP, which included fibroblast activation protein (FAP), alpha-1-antitrypsin (SERPINA1), thrombospondin 4 (THBS4), extracellular sulfatase-1 (SULF1), hepatocyte growth factor-like protein (MST-1), fibromodulin (FMOD), antithrombin-III (SERPINC1), and contactin-1 (CNTN1). Cross

referencing these proteins on gene-ontology (GO) Metascape data base revealed they were associated with wound healing, ECM organization, epithelial cell proliferation, and gland development annotations.

FAP, is a serine-protease that serves important roles that support tumor cell migration and proliferation[218,219]. Additionally, when supplemented onto human umbilical vein endothelial cells (HUVEC), FAP increased cell proliferation rates[220]. DAT coatings CdM also contained SERPINA1, an inhibitory enzyme involved in the modulation of acute inflammation by protecting tissues from inflammatory cell-mediated enzymatic digestion[221], further, recombinant SERPINA1 is currently used clinically for the treatment of lung emphysema[222]. Another SERPIN was also identified in DAT coating CdM, SERPINC1, a potent anti-coagulant[223] that is also described to possesses anti-angiogenic properties [223,224]. THBS4, is an ECM component that is known to be pro-angiogenic, primarily by inducing ECM remodelling and inflammatory cell recruitment[225,226]. Other factors associated with ECM remodelling were also detected that included FMOD[227], likely secreted by MSC in response to the ECM-rich DAT environment. SULF1, belongs to a family of sulfatases that readily modify the ECM by chemically altering heparan sulfate proteoglycans in the ECM, thus regulating proteoglycan-cell signalling and influencing cell survival, growth, and proliferation[228,229]. MST-1 plays a role in monocyte regulation and exhibits both pro- and anti-inflammatory effects on macrophages[230,231]. Additionally, MST-1 is involved in wound healing through the stimulation of keratinocyte migration *in vitro* and in mouse wound models[231]. Lastly, the cell adhesion molecule[232], CNTN1 was also increased in DAT coating CdM and microcarrier CdM. CNTN1 is expressed by a diversity of neurons and is known to play a role in axonal development, axon-glia communication, and myelination[232–234]. These secretome analyses observed an increase in CNTN1 levels in DAT coatings CdM and DAT microcarriers CdM, at 4.72- and 5.39-fold increases compare to TCP respectively. Collectively, these findings further warrant the investigation of BM-MSC on DAT culturing platforms for neuro-regeneration applications. It should further be noted, that while DAT microcarriers CdM only contained 9 unique proteins compared to TCP, 5 of those were also upregulated in DAT coatings CdM. Which included FMOD, FAP, SERPINC1, CNTN1, and THBS4. Indicating that increased release of these factors can be attributed to the DAT substrate independent of static versus dynamic conditions.

Chapter 4.3 Clinical Implications

Human DAT is a clinically relevant biomaterial that can be readily obtained from elective lipo-reduction surgeries, and thus an abundant supply of biomaterial exists for scaling up cell production using both static or dynamic culture with different DAT substrate formulations[163]. This study showed the potential of using DAT constructs to expand BM-MSC while retaining regenerative markers favorable for pro-vascular clinical applications. Our analyses showed that DAT coatings decreased the frequency of non-viable BM-MSC and increased total viable cell counts over time, indicating that culture on DAT coatings may yield increased BM-MSC numbers by permitting increased surface area, preventing apoptosis and/or enhancing BM-MSC proliferation. Additionally, prolonged culture on DAT coatings better preserved the activity of the regenerative and conserved progenitor cell marker, ALDH. Thus, DAT coatings provide an acceptable alternative to TCP to efficiently expand BM-MSC,

Our studies further observed increases in the frequency of BM-MSC expressing CD271 when the cells were cultured on DAT microcarriers under dynamic culture. CD271 represents a marker that has been previously associated with immunomodulatory, angiogenic, and neuroprotective MSC[197,198,208,212]. Thus, by retaining ALDH activity and increasing CD271 expression, DAT constructs may be used to expand MSC while retaining regenerative markers applicable for a variety of therapeutic applications, including neuro-regeneration applications. Additionally, for blood-vessel regeneration, DAT coatings may enhance the pro-angiogenic secretome of MSC. Proteomic analyses demonstrated that DAT coatings enhanced the secretome of BM-MSC with factors associated with wound healing, further supporting future use of DAT culturing platforms for blood-vessel regeneration applications.

Additionally, the utility of DAT as a potential MSC delivery platform still needs to be addressed. MSC delivered on DAT coatings or microcarriers may be used to increase MSC survival and retention after delivery and/or provide a supportive environment that may potentially direct cell function. MSC retention at the site of injury during clinical translation is predicted to improve the efficacy of MSC-based therapies by reducing detachment-induced apoptosis.

Chapter 4.4 Study Limitations and Future Directions

This study attempted to characterize the growth and phenotype of BM-MSC on DAT constructs, however, some limitations persist regarding how DAT directly influences BM-MSC behavior. Although the viable yield of BM-MSC was improved when cultured on DAT coatings, it is not clear if there were specific components within the DAT that contributed to this response. Previous proteomic analysis done by the Flynn lab identified 804 unique proteins in DAT, of which collagens 1A1, 1A2, and 3A1 were the most abundant[201]. As such, it is difficult to predict which component(s) were critical in the responses seen. Additionally, multiphoton confocal analyses data raised another question, as increased available surface area was observed between DAT and TCP. Therefore, the question remains whether the DAT is providing cell-instructive cues to prevent MSC apoptosis or simply provides more surface area available for cell growth. Further, an increase in total viable MSC counts was observed after culture on DAT coatings, however, whether this is due to increased proliferation or reduced apoptosis needs to be determined. Future work should explore the EdU incorporation assay to quantify the frequency of proliferating MSC on DAT substrates versus TCP.

This study also aimed to characterize cell surface marker expression and regenerative phenotype, comparing TCP to DAT coatings and DAT microcarriers. We observed no differences in the fraction of cells expressing the mature stromal markers (CD73, CD90, and CD105) or CD146. However, tri-lineage differentiation capacity following BM-MSC culture on DAT has yet to be investigated. While previous work by the Flynn lab showed increased tri-lineage differentiative abilities by ASC following prolonged culture on DAT microcarriers under dynamic conditions[120], this should also be assessed for BM-MSC. More specifically, future work should investigate differentiation capacity of BM-MSC into fat, bone, and cartilage following prolonged culture on DAT substrates.

In addition, we observed the retention of high ALDH activity on DAT coatings and an increase in the frequency of CD271 expression on BM-MSC cultured on DAT microcarriers. Indeed, imaging showed varying levels of confluency and cell contact between the TCP and DAT conditions, which is known to influence cell behaviour[205,235,236]. This is of special importance during DAT microcarrier cultures, as it is difficult to accurately quantify the surface area available for cell adhesion and growth. Whether the observed differences in the progenitor markers are due to the instructive properties of the DAT or can be explained by cell-cell contact mediated cell behaviour requires careful future investigation. Future work should explore a non-DAT substrate microcarrier/coating control (such as collagen beads/coatings) to

elucidate DAT-related effects that are independent of cell density. Overall, it is difficult to draw a direct comparison between DAT coatings and DAT microcarriers as many differences exist in the culture platforms such as stiffness, cell density, and shear stresses. As such it can be difficult to uncouple which parameter had the greatest effect on the observed responses.

In terms of the increase in the neutrotrophin receptor CD271 on BM-MSC following culture on DAT microcarriers. Future work should perform functional neural survival/proliferation assays to elucidate the presence of neutrotrophins in BM-MSC CdM. Furthermore, the use of DAT microcarriers with BM-MSC for neuro-regeneration should be further explored in mouse models.

In this study the pro-angiogenic signalling of BM-MSC was assessed by collecting CdM and assaying for HMVEC survival, proliferation, and tubule formation. Although differences in HMVEC survival were observed when the media was supplemented with DAT coatings CdM compared to other groups, we did not observe differences in cell proliferation or tubule formation as previously reported in the literature[96,97,216]. As discussed previously, this may be due to the lower cell numbers used in this study (625K), and future work should collect CdM from 2 – 4 million BM-MSC similar to the cell numbers used to generate CdM in previous studies[97,144,195]. In addition, supplementation of HMVEC cultures was limited to 10% CdM, and future experiments should supplement with previously reported concentrations that range from 50 – 100% CdM supplements[96,97,195].

Additionally, to obtain a more pro-angiogenic secretome from BM-MSC, future work should condition BM-MSC under hypoxia as a stressor to stimulate the release of pro-angiogenic factors. It was previously shown that MSC or ASC cultured under hypoxia (1 - 3% oxygen) exhibited a more pro-angiogenic secretory profile than those cultured under normoxic (20 - 21% oxygen) conditions[237–239]. Although BM-MSC in this study were exposed to serum- and growth factor-free cultures during conditioning, culture under atmospheric oxygen tension would not be expected to stimulate the secretion of potent pro-angiogenic effectors that are stimulated by the actions of the HIF-1α-hypoxia signalling axis[52].

It should also be noted that while CD271 and ALDH-activity have been associated with regenerative phenotypes in MSC[72,195–198,203], it is difficult to draw conclusions about cell behaviour without performing additional functional assays. This study lacked a complete *in vivo* characterization of pro-angiogenic stimulatory properties of BM-MSC on DAT constructs. This is crucial as proteomic analyses detected factors that are supportive of angiogenesis such as SERPINA1, THSB4, MST-1, and FAP, however many of these factors exhibit a pro-angiogenic response through inflammatory cell modulation, ECM-

remodelling, and/or modulating coagulation[220,222,226,231], all mechanism that could only be fully detected *in vivo*. This warrants future investigations to involve direct injections of BM-MSC CdM into immunocompetent mice. In this project, the DIVAA™ assay was performed to quantify endothelial cell infiltration following supplementation with CdM, however quantification of this experiment requires future optimization and further repeats. Future work could also assess alternative markers to quantify immune cell infiltration into inserts in immunocompetent mice, to detect potential activity by FAP, MST, and/or SERPINA1. Macrophage & monocyte infiltration maybe quantified by measuring lectin uptake alongside CD14, CD11b, or CD144 expression[240,241] by flow cytometry. Future work should also utilize an applicable *in vivo* model of ischemia such as the femoral artery ligation (FAL)-induced limb ischemia[72]. Subsequently, CdM generated by MSC could be injected into the ischemic limb of mice that have underwent FAL, and laser doppler imaging, the CatWalk™ assay, and immunohistochemistry (IHC) could be used to quantify limb perfusion, functional limb use, and new capillary formation, respectively.

Proteomic analyses also revealed an interesting observation regarding total quantified proteins in the DAT microcarriers CdM, as lower numbers of unique peptides were detected. This may be due to a decreased secretome when BM-MSC are cultured under dynamic conditions. However, as previously discussed, the lower protein amounts may be explained by loss of cells that could be more sensitive to the shear forces applied within the spinner flasks following conditioning in serum-free culture. Future work should include imaging of the seeded DAT microcarriers before and after conditioning to observe whether there are any issues with cell detachment.

Finally, the utility of DAT microcarriers as a delivery vector should be fully explored using the FAL-mouse model, where BM-MSC adherent on DAT microcarriers could be subcutaneously delivered into to the ischemic limb and human cell retention would be quantified using IHC. Collectively, these additional assessments with the work uncovered in this thesis will help elucidate MSC function within DAT constructs, and characterize the potential for blood-vessel regeneration applications.

Chapter 4.5 Conclusions

This novel multidisciplinary study aimed to improve the expansion and therapeutic potential of BM-MSC using an extracellular matrix-rich scaffold derived from DAT. DAT provided a robust cell-supportive environment that promoted BM-MSC attachment and growth while retaining regenerative markers. Culture on DAT coatings under static conditions maintained the fraction of BM-MSC expressing the conserved progenitor marker ALDH-activity, while culture on DAT microcarriers under dynamic conditions increased the frequency of cells expressing the potentially regenerative marker, CD271. These findings suggest that DAT constructs may be used to expand BM-MSC suitable for a variety of therapeutic applications. Further, BM-MSC cultured on DAT coatings generated CdM that increased the survival of endothelial cells under serum-free conditions. Lastly, culture of BM-MSC on DAT coatings resulted in a secretome that contained factors associated with wound healing. Overall, these studies support the further investigation of DAT constructs as a cell expansion platform for BM-MSC, which may have future potential for blood vessel regeneration applications.

References

1. Stefanovska, A. & Bračič, M. Physics of the human cardiovascular system. *Contemp. Phys.* **40**, 31–55 (1999).

2. Gordan, R., Gwathmey, J. K. & Xie, L.-H. Autonomic and endocrine control of cardiovascular function. *World J. Cardiol.* **7**, 204 (2015).

3. Lüscher, T. F. & Barton, M. Biology of the Endothelium. *Clin. Cardiol.* **20**, (1997).

4. Galley, H. F. & Webster, N. R. Physiology of the endothelium. *Br. J. Anaesth.* **93**, 105–113 (2004).

5. Gary, P. H. . J. B. M. . S. C. T. et al. The New England Journal of Medicine Downloaded from nejm.org on April 1, 2015. For personal use only. No other uses without permission. Copyright © 1990 Massachusetts Medical Society. All rights reserved. *New English J. Med.* **323**, 1120–1123 (1990).

6. Sugimoto, T. Cardiovascular disease. *Nippon rinsho. Japanese J. Clin. Med.* **58**, 2139–2148 (2000).

7. Herrmann, J. & Lerman, A. The endothelium: Dysfunction and beyond. *J. Nucl. Cardiol.* **8**, 197–206 (2001).

8. Gimbrone, M. A. & García-Cardeña, G. Endothelial Cell Dysfunction and the Pathobiology of Atherosclerosis. *Circ. Res.* **118**, 620–636 (2016).

9. Libby, P., Ridker, P. M. & Maseri, A. Inflammation and atherosclerosis. *Circulation* **105**, 1135–1143 (2002).

10. Jamwal, S. & Sharma, S. Vascular endothelium dysfunction: a conservative target in metabolic disorders. *Inflamm. Res.* **67**, 391–405 (2018).

11. Cook, C., Cole, G., Asaria, P., Jabbour, R. & Francis, D. P. The annual global economic burden of heart failure. *Int. J. Cardiol.* **171**, 368–376 (2014).

12. Allender, S., Peto, V., Scarborough, P., Kaur, A. & Rayner, M. Coronary heart disease statistics . *Br. Hear. Found.* 208 (2008).

13. Laslett, L. J. *et al.* The worldwide environment of cardiovascular disease: Prevalence, diagnosis, therapy, and policy issues: A report from the american college of cardiology. *J. Am. Coll. Cardiol.* **60**, (2012).

14. Wilkins, E. *et al.* European Cardiovascular Disease Statistics 2017, European Heart Network, Brussels. *Eur. Cardiovasc. Dis. Stat.* **34**, 3028–3034 (2017).

15. Pugsley, M. . & Tabrizchi, R. The vascular system: An overview of structure and function. *Pharmacol. Toxicol. Methods* **44**, 333–340 (2000).

16. Schwartz, S. M., Majesky, M. W. & Murry, C. E. The intima: development and monoclonal

responses to injury. *Atherosclerosis* **118**, (1995).

17. Semenza, G. L. Vasculogenesis, angiogenesis, and arteriogenesis: Mechanisms of blood vessel formation and remodeling. *J. Cell. Biochem.* **102**, 840–847 (2007).

18. Mitchell, R. N. & Schoen, F. J. Systemic Pathology : Diseases of Organ Systems Page 1 of 65 Chapter 11 – Blood Vessels The Structure and Function of Blood Vessels file://C:\Documents and Settings \ User \ Local Settings \ Temp \ ~ hh91D1 . htm Systemic Pathology : Diseases of Organ Syst. 1–65.

19. Von Tell, D., Armulik, A. & Betsholtz, C. Pericytes and vascular stability. *Exp. Cell Res.* **312**, 623–629 (2006).

20. Furchgott, R. & Zawadski, J. V. The obligatory role of endothelial cells in the relaxation of atrial smooth muscle. *Nature* **288**, 373–376 (1980).

21. Yau, J. W., Teoh, H. & Verma, S. Endothelial cell control of thrombosis. *BMC Cardiovasc. Disord.* **15**, 1–11 (2015).

22. Dora, K. A., Xia, J. & Duling, B. R. Endothelial cell signaling during conducted vasomotor responses. *Am. J. Physiol. - Hear. Circ. Physiol.* **285**, 119–126 (2003).

23. Spieker, L. E., Flammer, A. J. & Lüscher, T. F. *The vascular endothelium in hypertension*. *Handbook of Experimental Pharmacology* vol. 176 (2006).

24. Matheny, H. E., Deem, T. L. & Cook-Mills, J. M. Lymphocyte Migration Through Monolayers of Endothelial Cell Lines Involves VCAM-1 Signaling Via Endothelial Cell NADPH Oxidase. *J. Immunol.* **164**, 6550–6559 (2000).

25. Vestweber, D. Regulation of endothelial cell contacts during leukocyte extravasation. *Curr. Opin. Cell Biol.* **14**, 587–593 (2002).

26. Dubois, C., Panicot-Dubois, L., Gainor, J. F., Furie, B. C. & Furie, B. Thrombin-initiated platelet activation in vivo is vWF independent during thrombus formation in a laser injury model. *J. Clin. Invest.* **117**, 953–960 (2007).

27. Li, J., Chen, J. & Kirsner, R. Pathophysiology of acute wound healing. *Clin. Dermatol.* **25**, 9–18 (2007).

28. Falk, E. Pathogenesis of Atherosclerosis. *J. Am. Coll. Cardiol.* **47**, 0–5 (2006).

29. Naghavi, M. *et al.* From vulnerable plaque to vulnerable patient: A call for new definitions and risk assessment strategies: Part I. *Circulation* **108**, 1664–1672 (2003).

30. Cunningham, K. S. & Gotlieb, A. I. The role of shear stress in the pathogenesis of atherosclerosis. *Lab. Investig.* **85**, 9–23 (2005).

31. Yoshida, H. & Kisugi, R. Mechanisms of LDL oxidation. *Clin. Chim. Acta* **411**, 1875–1882 (2010).

32. Stocker, R. & Keaney, J. F. Role of oxidative modifications in atherosclerosis. *Physiol. Rev.* **84**, 1381–1478 (2004).

33. Parthasarathy, S., Wieland, E. & Steinberg, D. A role for endothelial cell lipoxygenase in the oxidative modification of low density lipoprotein. *Proc. Natl. Acad. Sci. U. S. A.* **86**, 1046–1050 (1989).

34. Newby, A. C. & Zaltsman, A. B. Fibrous cap formation or destruction - The critical importance of vascular smooth muscle cell proliferation, migration and matrix formation. *Cardiovasc. Res.* **41**, 345–360 (1999).

35. Chistiakov, D. A., Melnichenko, A. A., Myasoedova, V. A., Grechko, A. V. & Orekhov, A. N. Mechanisms of foam cell formation in atherosclerosis. *J. Mol. Med.* **95**, 1153–1165 (2017).

36. Caplice, N. M. *et al.* Smooth muscle cells in human coronary atherosclerosis can originate from cells administered at marrow transplantation. *Proc. Natl. Acad. Sci. U. S. A.* **100**, 4754–4759 (2003).

37. Kullo J, I. & Rooke W, T. Peripheral Artery Disease. *N. Engl. J. Med.* 2159-2167.e2 (2016) doi:10.1016/B978-0-323-35762-3.00148-7.

38. Lawrence A, G. Epidemiology and Pathophysiology of Lower Extremity Peripheral Arterial Disease. *J. Endovasc. Ther.* **13**, (2006).

39. Varu, V. N., Hogg, M. E. & Kibbe, M. R. Critical limb ischemia. *J. Vasc. Surg.* **51**, 230–241 (2010).

40. Tang, G., Chang, D., Sarkar, R., Wang, R. & Messina, L. The effect of gradual or acute arterial occlusion on skeletal muscle blood flow, arteriogenesis, and inflammation in rat hindlimb ischemia. *J Vasc Surg* **41**, 312–20 (2005).

41. Coats, P. & Wadsworth, R. Marriage of resistance and conduit arteries breeds critical limb ischemia. *Am J Physiol Hear. Circ Physiol* **288**, H1044-50 (2005).

42. Albers, M., Romiti, M., Brochado-Neto, F., De Luccia, N. & Pereira, C. Meta-analysis of popliteal-to-distal vein bypass grafts for critical isch- emia. *J Vasc Surg* **43**, (2006).

43. Duff, S., Mafilios, M. S., Bhounsule, P. & Hasegawa, J. T. The burden of critical limb ischemia: A review of recent literature. *Vasc. Health Risk Manag.* **15**, 187–208 (2019).

44. Folkman, J. Angiogenesis. *Biol. Endothel. Cells* 412–428 (1984).

45. Karamysheva, A. F. Mechanisms of angiogenesis. *Biochem.* **73**, 751–762 (2008).

46. Carmeliet, P. & Jain, R. K. Molecular mechanisms and clinical applications of angiogenesis. *Nature* **473**, 298–307 (2011).

47. Vailhé, B., Vittet, D. & Feige, J. J. In vitro models of vasculogenesis and angiogenesis. *Lab. Investig.* **81**, 439–452 (2001).

48. Heil, M., Eitenmüller, I., Schmitz-Rixen, T. & Schaper, W. Arteriogenesis versus angiogenesis: Similarities and differences. *J. Cell. Mol. Med.* **10**, 45–55 (2006).

49. Qadura, M., Terenzi, D. C., Verma, S., Al-Omran, M. & Hess, D. A. Concise Review: Cell Therapy for Critical Limb Ischemia: An Integrated Review of Preclinical and Clinical Studies.

Stem Cells **36**, 161–171 (2018).

50. Styp-Rekowska, B., Hlushchuk, R., Djonov, A. R. & Pries, V. Intussusceptive angiogenesis: pillars against the blood flow. *Acta Physiol.* **202.3**, 213–223 (2011).

51. Adair, T. H. & Jean-PierreMontani. Angiogenesis. in (2010).

52. Lee, J. W., Ko, J., Ju, C. & Eltzschig, H. K. Hypoxia signaling in human diseases and therapeutic targets. *Exp. Mol. Med.* **51**, 1–13 (2019).

53. Tvorogov, D. *et al.* Effective Suppression of Vascular Network Formation by Combination of Antibodies Blocking VEGFR Ligand Binding and Receptor Dimerization. *Cancer Cell* **18**, 630–640 (2010).

54. Saharinen, P., Eklund, L., Pulkki, K., Bono, P. & Alitalo, K. VEGF and angiopoietin signaling in tumor angiogenesis and metastasis. *Trends Mol. Med.* **17**, 347–362 (2011).

55. Jakobsson, L. *et al.* Endothelial cells dynamically compete for the tip cell position during angiogenic sprouting. *Nat Cell Biol* **10**, (2010).

56. Deryugina, E. I. & Quigley, J. P. Pleiotropic roles of matrix metalloproteinases in tumor angiogenesis: contrasting, overlapping and compensatory functions. *Biochim. Biophys. Acta* **1803**, 102 (2010).

57. Asahara, T. & Atsuhiko, K. Endothelial progenitor cells for postnatal vasculogenesis. *Am. J. Physiol. - Cell Physioloy* **287.3**, (2004).

58. Ferguson, J., Kelley, R. W. & Patterson, C. Mechanisms of Endothelial Differentiation in Embryonic Vasculogenesis. *Arterioscler. Thromb. Vasc. Biol.* **25**, 2246–2254 (2005).

59. Asahara, T., Murohara, T., Sullivan, A., Silver, M. & van der Zee, R. Isolation of putative progenitor endothelial cells for angiogenesis. *Science (80-.).* **275**, 964–7 (1997).

60. Asahara, T., Takahashi, T., Masuda, H. & Kalka, C. VEGF contributes to postnatal neovascularization by mobilizing bone marrow-derived endothelial progenitor cells. *EMBO* **14**, (1999).

61. Masamichi, E., Haruchika, M. & Asahara, T. Endothelial progenitor cells for postnatal vasculogenesis. *Clin. Exp. Nephrol.* **11**, 18–25 (2007).

62. Wang, Y. *et al.* M2 macrophages promote vasculogenesis during retinal neovascularization by regulating bone marrow-derived cells via SDF-1/VEGF. *Cell Tissue Res.* **380**, 496–486 (2020).

63. Urbich, C. & Dimmeler, S. Endothelial progenitor cells: characterization and role in vascular biology. *Circ. Res.* **95.4**, 343–353 (2004).

64. Schaper, W. & Scholz, D. Factors regulating arteriogenesis. *Arterioscler. Thromb. Vasc. Biol.* **23**, 1143–1151 (2003).

65. Heil, M. *et al.* Blood monocytes concentration is critical for enhancement of collateral artery growth. *Am J Physiol Hear. Circ Physiol* **283**, H2411–H2419. (2002).

66. Davies, M. Cell and molecular therapies for limb salvage. *Cardiovasc. Res.* **8**, 20–27 (2012).

67. Walter, D. H. *et al.* Intraarterial administration of bone marrow mononuclear cells in patients with critical limb ischemia a randomized-start, placebo-controlled pilot trial (PROVASA). *Circ. Cardiovasc. Interv.* **4**, 26–37 (2011).

68. Matoba, S. *et al.* Long-term clinical outcome after intramuscular implantation of bone marrow mononuclear cells (Therapeutic Angiogenesis by Cell Transplantation [TACT] trial) in patients with chronic limb ischemia. *Am. Heart J.* **156**, 1010–1018 (2008).

69. Li, M. *et al.* Autologous bone marrow mononuclear cells transplant in patients with critical leg ischemia: Preliminary clinical results. *Exp. Clin. Transplant.* **11**, 435–439 (2013).

70. Hung, S.-C., Pochampally, R. R., Chen, S.-C., Hsu, S.-C. & Prockop, D. J. Angiogenic Effects of Human Multipotent Stromal Cell Conditioned Medium Activate the PI3K-Akt Pathway in Hypoxic Endothelial Cells to Inhibit Apoptosis, Increase Survival, and Stimulate Angiogenesis. *Stem Cells* **25**, 2363–2370 (2007).

71. Gupta, P. K. *et al.* A double blind randomized placebo controlled phase I/II study assessing the safety and efficacy of allogeneic bone marrow derived mesenchymal stem cell in critical limb ischemia. *J. Transl. Med.* **11**, 1–11 (2013).

72. Capoccia, B. J. *et al.* Revascularization of ischemic limbs after transplantation of human bone marrow cells with high aldehyde dehydrogenase activity. *Blood* **113**, 5340–5351 (2009).

73. Lu, D. *et al.* Comparison of bone marrow mesenchymal stem cells with bone marrow-derived mononuclear cells for treatment of diabetic critical limb ischemia and foot ulcer: A double-blind, randomized, controlled trial. *Diabetes Res. Clin. Pract.* **92**, 26–36 (2011).

74. Friedenstein, A. J. & Panasuk, A. Precursors for fibroblasts in different populations of hematopoietic cells as detected by the in vitro colony assay method. *Exp Hematol* **2**, 83–92 (1974).

75. Friedenstein, A. J., Gorskaja, J. & Kulagina, N. Fibroblast precursors in normal and irradiated mouse hematopoietic organs. *Exp. Hematol.* **4**, 267–274 (1976).

76. Dennis, J. *et al.* A quadri-potential mesen- chymal progenitor cell isolated from the marrow of an adult mouse. *J Bone Min. Res* **14**, 700–9 (1999).

77. Pittenger, M. *et al.* Multilineage potential of adult human mesenchymal stem cells. *Science (80-.).* **284**, 143–7 (1999).

78. Caplan, A. The mesengenic process. *Clin. Plast. Surg.* **21**, 429–35 (1994).

79. Phinney, D. G. & Prockop, D. J. Concise Review: Mesenchymal Stem/Multipotent Stromal Cells: The State of Transdifferentiation and Modes of Tissue Repair-Current Views. *Stem Cells* **25**, 2896–2902 (2007).

80. Keating, A. Mesenchymal stromal cells. *Curr. Opin. Hematol.* **13**, 419–425 (2006).

81. Williams, J., Southerland, S., Souza, J., Calcutt, A. & Cartledge, R. Cells isolated from adult human skeletal muscle capable of differentiating into multiple mesodermal phenotypes. *Am Surg* **65**, 22–6 (1999).

82. Zuk, P. *et al.* Multilineage cells from human adipose tissue: implications for cell-based therapies. *Tissue Eng.* **7**, 211–28 (2001).

83. Erices, A., Conget, P. & Minguell, J. Mesenchymal progenitor cells in human umbilical cord blood. *Br. J. Hematol.* **109**, 235–42 (2000).

84. Gronthos, S., Mankani, M., Brahim, J., Robey, P. G. & Shi, S. Postnatal human dental pulp stem cells (DPSCs) in vitro and in vivo. *Proc. Natl. Acad. Sci. U. S. A.* **97**, 13625–13630 (2000).

85. Fan, C. G. *et al.* Characterization and neural differentiation of fetal lung mesenchymal stem cells. *Cell Transplant.* **14**, 311–321 (2005).

86. Young, H. E. *et al.* Mesenchymal stem cells reside within the connective tissues of many organs. *Dev. Dyn.* **202**, 137–144 (1995).

87. Dominici, M. *et al.* Minimal criteria for defining multipotent mesenchymal stromal cells. The International Society for Cellular Therapy position statement. *Cytotherapy* **8**, 315–317 (2006).

88. Abumaree, M. H. *et al.* Human Placental Mesenchymal Stem Cells (pMSCs) Play a Role as Immune Suppressive Cells by Shifting Macrophage Differentiation from Inflammatory M1 to Anti-inflammatory M2 Macrophages. *Stem Cell Rev. Reports* **9**, 620–641 (2013).

89. Ortiz, L. A. *et al.* Mesenchymal stem cell engraftment in lung is enhanced in response to bleomycin exposure and ameliorates its fibrotic effects. *Proc. Natl. Acad. Sci. U. S. A.* **100**, 8407–8411 (2003).

90. Ringdén, O. *et al.* Mesenchymal stem cells for treatment of therapy-resistant graft-versus-host disease. *Transplantation* **81**, 1390–1397 (2006).

91. Horwitz, E. M. *et al.* Isolated allogeneic bone marrow-derived mesenchymal cells engraft and stimulate growth in children with osteogenesis imperfecta: Implications for cell therapy of bone. *Proc. Natl. Acad. Sci. U. S. A.* **99**, 8932–8937 (2002).

92. Nagaya, N. *et al.* Transplantation of mesenchymal stem cells improves cardiac function in a rat model of dilated cardiomyopathy. *Circulation* **112**, 1128–1135 (2005).

93. Iso, Y. *et al.* Multipotent human stromal cells improve cardiac function after myocardial infarction in mice without long-term engraftment. *Biochem. Biophys. Res. Commun.* **354**, 700–706 (2007).

94. Chen, L., Tredget, E. E., Wu, P. Y. G., Wu, Y. & Wu, Y. Paracrine factors of mesenchymal stem cells recruit macrophages and endothelial lineage cells and enhance wound healing. *PLoS One* **3**, (2008).

95. Bhang, S. H. *et al.* Efficacious and clinically relevant conditioned medium of human adipose-derived stem cells for therapeutic angiogenesis. *Mol. Ther.* **22**, 862–872 (2014).

96. Kwon, H. M. *et al.* Multiple paracrine factors secreted by mesenchymal stem cells contribute to angiogenesis. *Vascul. Pharmacol.* **63**, 19–28 (2014).

97. Boomsma, R. A. & Geenen, D. L. Mesenchymal stem cells secrete multiple cytokines that promote angiogenesis and have contrasting effects on chemotaxis and apoptosis. *PLoS One* **7**, 2–9 (2012).

98. Qiu, G. *et al.* Mesenchymal stem cell-derived extracellular vesicles affect disease outcomes via transfer of microRNAs. *Stem Cell Res. Ther.* **9**, 1–9 (2018).

99. Wang, W. *et al.* Exosomes secreted from mesenchymal stem cells mediate the regeneration of endothelial cells treated with rapamycin by delivering pro-angiogenic microRNAs. *Exp. Cell Res.* **399**, 112449 (2021).

100. Gong, M. *et al.* Mesenchymal stem cells release exosomes that transfer miRNAs to endothelial cells and promote angiogenesis. *Oncotarget* **8**, 45200–45212 (2017).

101. DUFF, S. E., LI, C., GARLAND, J. M. & KUMAR, S. CD105 is important for angiogenesis: evidence and potential applications. *FASEB J.* (2003) doi:10.1096/fj.02-0634rev.

102. Das, S. & Halushka, M. K. Extracellular vesicle microRNA transfer in cardiovascular disease. *Cardiovasc. Pathol.* **24**, 199–206 (2015).

103. Sudhir, R. H. Harnessing the MSC Secretome for the Treatment of Cardiovascular Disease. *Cell Stem Cell* **10**, 244–258 (2013).

104. Wang, Y., Chen, X., Cao, W. & Shi, Y. Plasticity of mesenchymal stem cells in immunomodulation: Pathological and therapeutic implications. *Nat. Immunol.* **15**, 1009–1016 (2014).

105. Spaggiari, G. M. *et al.* Mesenchymal stem cells inhibit natural killer-cell proliferation, cytotoxicity, and cytokine production: Role of indoleamine 2,3-dioxygenase and prostaglandin E2. *Blood* **111**, 1327–1333 (2008).

106. Spaggiari, G. M., Capobianco, A., Becchetti, S., Mingari, M. C. & Moretta, L. Mesenchymal stem cell-natural killer cell interactions: Evidence that activated NK cells are capable of killing MSCs, whereas MSCs can inhibit IL-2-induced NK-cell proliferation. *Blood* **107**, 1484–1490 (2006).

107. Nemeth, K. *et al.* Bone marrow stromal cells use TGF-β to suppress allergic responses in a mouse model of ragweed-induced asthma. *Proc. Natl. Acad. Sci. U. S. A.* **107**, 5652–5657 (2010).

108. Chen, Q. H. *et al.* Mesenchymal stem cells regulate the Th17/Treg cell balance partly through hepatocyte growth factor in vitro. *Stem Cell Res. Ther.* **11**, 1–11 (2020).

109. Bartholomew, A. *et al.* Mesenchymal stem cells suppress lymphocyte proliferation in vitro and prolong skin graft survival in vivo. *Exp. Hematol.* **30**, 42–48 (2002).

110. Cyranoski, D. Canada approves stem cell product. *Nat. Biotechnol.* **30**, 571–571 (2012).

111. Subbhanna, P. Mesenchymal stem cells for treating GVHD: in-vivo fate and optimal dose. *Med. Hypotheses* 469 (2007).

112. Lukomska, B. *et al.* Challenges and Controversies in Human Mesenchymal Stem Cell Therapy. *Stem Cells Int.* **2019**, (2019).

113. Whitfield, M. J., Lee, W. C. J. & Van Vliet, K. J. Onset of heterogeneity in culture-expanded bone marrow stromal cells. *Stem Cell Res.* **11**, 1365–1377 (2013).

114. Binato, R. *et al.* Stability of human mesenchymal stem cells during in vitro culture: Considerations

for cell therapy. *Cell Prolif.* **46**, 10–22 (2013).

115. Shakouri-Motlagh, A., O'Connor, A. J., Brennecke, S. P., Kalionis, B. & Heath, D. E. Native and solubilized decellularized extracellular matrix: A critical assessment of their potential for improving the expansion of mesenchymal stem cells. *Acta Biomater.* **55**, 1–12 (2017).

116. Zhao, Y., Waldman, S. D. & Flynn, L. E. The effect of serial passaging on the proliferation and differentiation of bovine adipose-derived stem cells. *Cells Tissues Organs* **195**, 414–427 (2012).

117. Lu, H. *et al.* Cultured cell-derived extracellular matrix scaffolds for tissue engineering. *Biomaterials* **32**, 9658–9666 (2011).

118. rao Pattabhi, S., Martinez, J. S. & Keller, T. C. S. Decellularized ECM effects on human mesenchymal stem cell stemness and differentiation. *Differentiation* **88**, 131–143 (2014).

119. Ng, C. P. *et al.* Enhanced exvivo expansion of adult mesenchymal stem cells by fetal mesenchymal stem cell ECM. *Biomaterials* **35**, 4046–4057 (2014).

120. Yu, C., Kornmuller, A., Brown, C., Hoare, T. & Flynn, L. E. Decellularized adipose tissue microcarriers as a dynamic culture platform for human adipose-derived stem/stromal cell expansion. *Biomaterials* (2017) doi:10.1016/j.biomaterials.2016.12.017.

121. Hynes, R. O. The extracellular matrix: not just pretty fibrils. *Science (80-.).* **326**, 1216–1219 (2009).

122. Kular, J. K., Basu, S. & Sharma, R. I. The extracellular matrix: Structure, composition, age-related differences, tools for analysis and applications for tissue engineering. *J. Tissue Eng.* **5**, (2014).

123. Bosman, F. T. & Stamenkovic, I. Functional structure and composition of the extracellular matrix. *J. Pathol.* **200**, 423–428 (2003).

124. Frantz, C., Stewart, K. M. & Weaver, V. M. The extracellular matrix at a glance. *J. Cell Sci.* **123**, 4195–4200 (2010).

125. Bonnans, C., Chou, J. & Werb, Z. Remodelling the extracellular matrix in development and disease. *Nat. Rev. Mol. Cell Biol.* **15**, 786–801 (2014).

126. Harbuger, D. & Calderwood, D. Integrin signalling at a glance. *Cell Sci.* **122**, 159–163 (2009).

127. Kim, S. H., Turnbull, J. & Guimond, S. Extracellular matrix and cell signalling: The dynamic cooperation of integrin, proteoglycan and growth factor receptor. *J. Endocrinol.* **209**, 139–151 (2011).

128. Larsen, M., Artym, V. V., Green, J. A. & Yamada, K. M. The matrix reorganized: extracellular matrix remodeling and integrin signaling. *Curr. Opin. Cell Biol.* **18**, 463–471 (2006).

129. Labat-Robert, J., Robert, A. & Robert, L. Aging of the extracellular matrix. *Med Longev* 3–32 (2012).

130. Singh, P., Carraher, C. & Schwarzbauer, J. Assembly of fibronectin extracellular matrix. *Annu Rev Cell Dev Biol* **26**, (2010).

131. Theocharis, A. D., Skandalis, S. S., Gialeli, C. & Karamanos, N. K. Extracellular matrix structure. *Adv. Drug Deliv. Rev.* **97**, 4–27 (2016).

132. Goh, K. L. *et al.* Ageing changes in the tensile properties of tendons: Influence of collagen fibril volume fraction. *J. Biomech. Eng.* **130**, (2008).

133. Rozario, T. & DeSimone, D. The extracellular matrix in development and morphogenesis: a dynamic view. *Dev. Biol.* **341**, 126–140 (2010).

134. Wise, S. & Weiss, A. Tropoelastin. *Biochem. Cell Biol* **41**, 494–497 (2009).

135. Smith, M. *et al.* Force-induced unfolding of fibronectin in the extracellular matrix of living cells. *PloS Biol* **5**, (2007).

136. Eckes, B., Nischt, R. & Kriet, T. Cell-matrix interactions in dermal repair and scarring. *Fibrogenes. Tissue Repair* **3**, 4 (2010).

137. Lee, D. H., Oh, J. H. & Chung, J. H. Glycosaminoglycan and proteoglycan in skin aging. *J. Dermatol. Sci.* **83**, 174–181 (2016).

138. Turner, A. E. B., Yu, C., Bianco, J., Watkins, J. F. & Flynn, L. E. The performance of decellularized adipose tissue microcarriers as an inductive substrate for human adipose-derived stem cells. *Biomaterials* (2012) doi:10.1016/j.biomaterials.2012.03.026.

139. Gattazzo, F., Urciuolo, A. & Bonaldo, P. Extracellular matrix: A dynamic microenvironment for stem cell niche. *Biochim. Biophys. Acta - Gen. Subj.* **1840**, 2506–2519 (2014).

140. Engler, A. J., Sen, S., Sweeney, H. L. & Discher, D. E. Matrix Elasticity Directs Stem Cell Lineage Specification. *Cell* **126**, 677–689 (2006).

141. Winer, J. P., Janmey, P. A., McCormick, M. E. & Funaki, M. Bone marrow-derived human mesenchymal stem cells become quiescent on soft substrates but remain responsive to chemical or mechanical stimuli. *Tissue Eng. - Part A* **15**, 147–154 (2009).

142. Watt, F. M. & Huck, W. T. S. Role of the extracellular matrix in regulating stem cell fate. *Nat. Rev. Mol. Cell Biol.* **14**, 467–473 (2013).

143. Freeman, F. E. & Kelly, D. J. Tuning alginate bioink stiffness and composition for controlled growth factor delivery and to spatially direct MSC Fate within bioprinted tissues. *Sci. Rep.* **7**, 1–12 (2017).

144. Abdeen, A. A., Weiss, J. B., Lee, J. & Kilian, K. A. Matrix composition and mechanics direct proangiogenic signaling from mesenchymal stem cells. *Tissue Eng. - Part A* **20**, 2737–2745 (2014).

145. Ogle, M., Doron, G., Leyy, M. & Temenoff, J. Hydrogel Culture Surface Stiffness Modulates Mesenchymal Stromal Cell Secretome and Alters Senescence. *Tissue Eng. - Part A* **26**, 1259–1271 (2020).

146. Prewitz, M. C. *et al.* Tightly anchored tissue-mimetic matrices as instructive stem cell microenvironments. *Nat. Methods* **10**, 788–794 (2013).

147. Chen, X. D., Dusevich, V., Feng, J. Q., Manolagas, S. C. & Jilka, R. L. Extracellular matrix made by bone marrow cells facilitates expansion of marrow-derived mesenchymal progenitor cells and prevents their differentiation into osteoblasts. *J. Bone Miner. Res.* **22**, 1943–1956 (2007).

148. Pei, M., He, F. & Kish, V. L. Expansion on extracellular matrix deposited by human bone marrow stromal cells facilitates stem cell proliferation and tissue-specific lineage potential. *Tissue Eng. - Part A* **17**, 3067–3076 (2011).

149. Holst, J. *et al.* Substrate elasticity provides mechanical signals for the expansion of hemopoietic stem and progenitor cells. *Nat. Biotechnol.* **28**, 1123–1128 (2010).

150. Yeo, G. C. & Weiss, A. S. Soluble matrix protein is a potent modulator of mesenchymal stem cell performance. *Proc. Natl. Acad. Sci. U. S. A.* **116**, 2042–2051 (2019).

151. Fuchs, J. R., Nasseri, B. A. & Vacanti, J. P. Tissue engineering: A 21st century solution to surgical reconstruction. *Ann. Thorac. Surg.* **72**, 577–591 (2001).

152. Gilbert, T. W., Sellaro, T. L. & Badylak, S. F. Decellularization of tissues and organs. *Biomaterials* **27**, 3675–3683 (2006).

153. Woods, T. & Gratzer, P. F. Effectiveness of three extraction techniques in the development of a decellularized bone-anterior cruciate ligament-bone graft. *Biomaterials* **26**, 7339–7349 (2005).

154. Hoshiba, T., Hongxu, L., Naoki, K. & Guoping, C. Decellularized matrices for tissue engineering. *Am. J. Stem Cells* **3**, 1–20 (2010).

155. Ott, H. C. *et al.* Perfusion-decellularized matrix: Using nature's platform to engineer a bioartificial heart. *Nat. Med.* **14**, 213–221 (2008).

156. Funamoto, S. *et al.* The use of high-hydrostatic pressure treatment to decellularize blood vessels. *Biomaterials* **31**, 3590–3595 (2010).

157. Petersen, T. H. *et al.* Tissue-engineered lungs for in vivo implantation. *Science (80-.).* **329**, 538–541 (2010).

158. Zhang, Q. *et al.* Decellularized skin/adipose tissue flap matrix for engineering vascularized composite soft tissue flaps. *Acta Biomater.* **35**, 166–184 (2016).

159. Gao, S. *et al.* Comparison of morphology and biocompatibility of acellular nerve scaffolds processed by different chemical methods. *J. Mater. Sci. Mater. Med.* **25**, 1283–1291 (2014).

160. Sasaki, S. *et al.* In vivo evaluation of a novel scaffold for artificial corneas prepared by using ultrahigh hydrostatic pressure to decellularize porcine corneas. *Mol. Vis.* **15**, 2022–2028 (2009).

161. Uygun, B. E. *et al.* Organ reengineering through development of a transplantable recellularized liver graft using decellularized liver matrix. *Nat. Med.* **16**, 814–820 (2010).

162. Nakayama, K. H., Batchelder, C. A., Lee, C. I. & Tarantal, A. F. Decellularized rhesus monkey kidney as a three-dimensional scaffold for renal tissue engineering. *Tissue Eng. - Part A* **16**, 2207–2216 (2010).

163. Flynn, L. E. The use of decellularized adipose tissue to provide an inductive microenvironment for

the adipogenic differentiation of human adipose-derived stem cells. *Biomaterials* (2010) doi:10.1016/j.biomaterials.2010.02.046.

164. Zbek, S. O. ¨, Balasubramanian, P. G., Chiquet-Ehrismann, R., Tucker, R. P. & Adams, J. C. The Evolution of Extracellular Matrix. *Mol. Biol. Cell* **21**, 4300–4305 (2010).

165. Bernard, M. *et al.* Nucleotide sequences of complementary deoxyribonucleic acids for the pro alpha 1 chain of human type I procollagen. Statistical evaluation of structures that are conserved during evolution. *Biochemistry* **22**, 5213–23 (1983).

166. Kershaw, E. E. & Flier, J. S. Adipose tissue as an endocrine organ. *J. Clin. Endocrinol. Metab.* **89**, 2548–2556 (2004).

167. Fantuzzi, G. Adipose tissue, adipokines, and inflammation. *J. Allergy Clin. Immunol.* **115**, 911–919 (2005).

168. Ferrante, A. W. The immune cells in adipose tissue. *Diabetes, Obes. Metab.* **15**, 34–38 (2013).

169. Ruiz-Ojeda, F. J., Méndez-Gutiérrez, A., Aguilera, C. M. & Plaza-Díaz, J. Extracellular matrix remodeling of adipose tissue in obesity and metabolic diseases. *Int. J. Mol. Sci.* **20**, (2019).

170. Nakajima, I., Yamaguchi, T., Ozutsumi, K. & Aso, H. Adipose tissue extracellular matrix: newly organized by adipocytes during differentiation. *Differentiation* **63**, 193–200 (1998).

171. Divoux, A. & Clément, K. Architecture and the extracellular matrix: The still unappreciated components of the adipose tissue. *Obes. Rev.* **12**, 494–503 (2011).

172. Mariman, E. C. M. & Wang, P. Adipocyte extracellular matrix composition, dynamics and role in obesity. *Cell. Mol. Life Sci.* **67**, 1277–1292 (2010).

173. Gregoire, F., Smas, C. & Sul, H. Understanding adipocyte differentiation. *Physiol. Rev.* **78**, 783–809 (1998).

174. Yu, C. *et al.* Porous decellularized adipose tissue foams for soft tissue regeneration. *Biomaterials* (2013) doi:10.1016/j.biomaterials.2013.01.056.

175. Han, T. T. Y., Toutounji, S., Amsden, B. G. & Flynn, L. E. Adipose-derived stromal cells mediate in vivo adipogenesis, angiogenesis and inflammation in decellularized adipose tissue bioscaffolds. *Biomaterials* **72**, 125–137 (2015).

176. Turner, A. E. B. & Flynn, L. E. Design and Characterization of Tissue-Specific Extracellular Matrix-Derived Microcarriers. *Tissue Eng. Part C Methods* (2012) doi:10.1089/ten.tec.2011.0246.

177. Morisette Martin, P., Shridar, A., Yu, C., Brown, C. & Flynn, L. . Decellularized Adipose Tissue Scaffolds for Soft Tissue Regeneration and Adipose-Derived Stem/Stromal Cell Delivery. in *Bunnell B.A., Gimble J.M. (eds) Adipose-Derived Stem Cells. Methods in Molecular Biology* (2018).

178. Lecler, C. J. *et al.* Decellularized adipose tissue scaffolds guide hematopoietic differentiation and stimulate vascular regeneration in a hindlimb ischemia model. *Biomaterials* (2021).

179. Simaria, A. S. *et al.* Allogeneic cell therapy bioprocess economics and optimization: Single-use

cell expansion technologies. *Biotechnol. Bioeng.* **111**, 69–83 (2014).

180. Chen, X. Y. *et al.* Recent advances in the use of microcarriers for cell cultures and their ex vivo and in vivo applications. *Biotechnol. Lett.* **42**, 1–10 (2020).

181. AL Wezel, V. Growth of cell-strains and primary cells on micro-carriers in homogenous culture. *Nature* **216**, 64–65 (1967).

182. Radtke, A. L. & Herbst-Kralovetz, M. M. Culturing and applications of rotating wall vessel bioreactor derived 3D epithelial cell models. *J. Vis. Exp.* 1–10 (2012) doi:10.3791/3868.

183. Kong, D., Cardak, S., Chen, M., Gentz, R. & Zhang, J. High cell density and productivity culture of Chinese hamster ovary cells in a fluidized bed bioreactor. *Cytotechnology* **29**, 215–220 (1999).

184. Ismadi, M. Z. *et al.* Flow characterization of a spinner flask for induced pluripotent stem cell culture application. *PLoS One* **9**, (2014).

185. Majd, H. *et al.* A Novel Method of Dynamic Culture Surface Expansion Improves Mesenchymal Stem Cell Proliferation and Phenotype. *Stem Cells* **27**, 200–209 (2009).

186. Chen, A. K. L., Reuveny, S. & Oh, S. K. W. Application of human mesenchymal and pluripotent stem cell microcarrier cultures in cellular therapy: Achievements and future direction. *Biotechnology Advances* (2013) doi:10.1016/j.biotechadv.2013.03.006.

187. Holtorf, H. F., Janses, J. A. & Mikos, A. . Flow perfusion culture induces the osteoblastic differentiation of marrow stromal cell–scaffold constructs in the absence of dexamethasone. *J. Biomed. Mater. Res.* 326–334 (2006).

188. Gemmiti, C. V. & Guldberg, R. E. Fluid flow increases type II collagen deposition and tensile mechanical properties in bioreactor-grown tissue-engineered cartilage. *Tissue Eng.* 496–479 (2006).

189. Yeatts, A. B., Choquette, D. T. & Fisher, J. P. Bioreactors to influence stem cell fate: Augmentation of mesenchymal stem cell signaling pathways via dynamic culture systems. *Biochim. Biophys. Acta - Gen. Subj.* **1830**, 2470–2480 (2013).

190. Kwon, S. H., Bhang, S. H., Jang, H. K., Rhim, T. & Kim, B. S. Conditioned medium of adipose-derived stromal cell culture in three-dimensional bioreactors for enhanced wound healing. *J. Surg. Res.* **194**, 8–17 (2015).

191. Kornmuller, A., Brown, C. F. C., Yu, C. & Flynn, L. E. Fabrication of extracellular matrix-derived foams and microcarriers as tissue-specific cell culture and delivery platforms. *J. Vis. Exp.* **2017**, 1–11 (2017).

192. Tavassoli, H. *et al.* Large-scale production of stem cells utilizing microcarriers: A biomaterials engineering perspective from academic research to commercialized products. *Biomaterials* (2018) doi:10.1016/j.biomaterials.2018.07.016.

193. Shridhar, A. *et al.* Culture on Tissue-Specific Coatings Derived from α-Amylase-Digested Decellularized Adipose Tissue Enhances the Proliferation and Adipogenic Differentiation of Human Adipose-Derived Stromal Cells. *Biotechnol. J.* **15**, 1–10 (2020).

194. Espagnolle, N. *et al.* CD146 expression on mesenchymal stem cells is associated with their vascular smooth muscle commitment. *J. Cell. Mol. Med.* **18**, 104–114 (2014).

195. Sherman, S. E. *et al.* High Aldehyde Dehydrogenase Activity Identifies a Subset of Human Mesenchymal Stromal Cells with Vascular Regenerative Potential. *Stem Cells* (2017) doi:10.1002/stem.2612.

196. Putman, D. M. *et al.* Expansion of Umbilical Cord Blood Aldehyde Dehydrogenase Expressing Cells Generates Myeloid Progenitor Cells that Stimulate Limb Revascularization. *Stem Cells Transl. Med.* (2017) doi:10.1002/sctm.16-0472.

197. Álvarez-Viejo, M. CD271 as a marker to identify mesenchymal stem cells from diverse sources before culture. *World J. Stem Cells* **7**, 470 (2015).

198. Kuçi, S. *et al.* CD271 antigen defines a subset of multipotent stromal cells with immunosuppressive and lymphohematopoietic engraftment-promoting properties. *Haematologica* **95**, 651–659 (2010).

199. Zhou, Y. *et al.* Metascape provides a biologist-oriented resource for the analysis of systems-level datasets. *Nat. Commun.* **10**, (2019).

200. Vachon, P. H. Integrin Signaling, Cell Survival, and Anoikis: Distinctions, Differences, and Differentiation. *J. Signal Transduct.* **2011**, 1–18 (2011).

201. Kuljanin, M., Brown, C. F. C., Raleigh, M. J., Lajoie, G. A. & Flynn, L. E. Collagenase treatment enhances proteomic coverage of low-abundance proteins in decellularized matrix bioscaffolds. *Biomaterials* **144**, 130–143 (2017).

202. Uynuk-Ool, T. *et al.* The geometrical shape of mesenchymal stromal cells measured by quantitative shape descriptors is determined by the stiffness of the biomaterial and by cyclic tensile forces. *J. Tissue Eng. Regen. Med.* **11**, 3508–3522 (2017).

203. Vassalli, G. Aldehyde dehydrogenases: Not just markers, but functional regulators of stem cells. *Stem Cells Int.* **2019**, (2019).

204. Gudas, L. J. & Wagner, J. A. Retinoids regulate stem cell differentiation. *J. Cell. Physiol.* **226**, 322–330 (2011).

205. Fossett, E. & Khan, W. S. Optimising human mesenchymal stem cell numbers for clinical application: A literature review. *Stem Cells Int.* **2012**, (2012).

206. Begum, A. *et al.* The extracellular matrix and focal adhesion kinase signaling regulate cancer stem cell function in pancreatic ductal adenocarcinoma. A70–A70 (2015) doi:10.1158/1538-7445.panca2014-a70.

207. Murphy, K., Hoch, A., Haervestine, J., Zhou, D. & Leach, J. Mesenchymal Stem Cell Spheroids Retain Osteogenic Phenotype Through a2b1 Signaling. *Stem Cells Transl. Med.* 1229–1237 (2015).

208. Smith, R. J. P., Faroni, A., Barrow, J. R., Soul, J. & Reid, A. J. The angiogenic potential of CD271+ human adipose tissue-derived mesenchymal stem cells. *Stem Cell Res. Ther.* **12**, 1–14

(2021).

209. Yamamoto, M. *et al.* Nerve growth factor (NGF), brain-derived neurotrophic factor (BDNF) and low-affinity nerve growth factor receptor (LNGFR) mRNA levels in cultured rat Schwann cells; differential time- and dose-dependent regulation by cAMP. *Neurosci. Lett.* **152**, 37–40 (1993).

210. Barbacid, M. Neurotrophic factors and their receptors. *Curr. Opin. Cell Biol.* **7**, 148–155 (1995).

211. Crigler, L., Robey, R. C., Asawachaicharn, A., Gaupp, D. & Phinney, D. G. Human mesenchymal stem cell subpopulations express a variety of neuro-regulatory molecules and promote neuronal cell survival and neuritogenesis. *Exp. Neurol.* **198**, 54–64 (2006).

212. Milczarek, O. *et al.* Multiple Autologous Bone Marrow-Derived CD271+ Mesenchymal Stem Cell Transplantation Overcomes Drug-Resistant Epilepsy in Children. *Stem Cells Transl. Med.* **7**, 20–33 (2018).

213. Knight, C. *et al.* Epidermal growth factor can signal via β-catenin to control proliferation of mesenchymal stem cells independently of canonical Wnt signalling. *Cell. Signal.* **53**, 256–268 (2019).

214. Jarocha, D., Milczarek, O., Wedrychowicz, A., Kwiatkowski, S. & Majka, M. Continuous improvement after multiple mesenchymal stem cell transplantations in a patient with complete spinal cord injury. *Cell Transplant.* **24**, 661–672 (2015).

215. Merten, O. W. Advances in cell culture: Anchorage dependence. *Philos. Trans. R. Soc. B Biol. Sci.* **370**, (2015).

216. Potapova, I. A. *et al.* Mesenchymal Stem Cells Support Migration, Extracellular Matrix Invasion, Proliferation, and Survival of Endothelial Cells In Vitro. *Stem Cells* **25**, 1761–1768 (2007).

217. Chen, T. S. *et al.* Mesenchymal stem cell secretes microparticles enriched in pre-microRNAs. *Nucleic Acids Res.* **38**, 215–224 (2009).

218. Cheng, J. D. *et al.* Promotion of tumor growth by murine fibroblast activation protein, a serine protease, in an animal model. *Cancer Res.* **62**, 4767–4772 (2002).

219. Gao, L. M. *et al.* Roles of Fibroblast Activation Protein and Hepatocyte Growth Factor Expressions in Angiogenesis and Metastasis of Gastric Cancer. *Pathol. Oncol. Res.* **25**, 369–376 (2019).

220. Cao, F., Wang, S., Wang, H. & Tang, W. Fibroblast activation protein-α in tumor cells promotes colorectal cancer angiogenesis via the Akt and ERK signaling pathways. *Mol. Med. Rep.* **17**, 2593–2599 (2018).

221. Karnaukhova, E., Ophir, Y. & Golding, B. Recombinant human alpha-1 proteinase inhibitor: Towards therapeutic use. *Amino Acids* **30**, 317–332 (2006).

222. Rahaghi, F. F. & Miravitlles, M. Long-term clinical outcomes following treatment with alpha 1-proteinase inhibitor for COPD associated with alpha-1 antitrypsin deficiency: A look at the evidence. *Respir. Res.* **18**, 1–9 (2017).

223. Kerbel, R. S. Tumor angiogenesis: Past, present and the near future. *Carcinogenesis* **21**, 505–515

(2000).

224. Ribatti, D. Endogenous inhibitors of angiogenesis. A historical review. *Leuk. Res.* **33**, 638–644 (2009).

225. Muppala, S. *et al.* Proangiogenic properties of thrombospondin-4. *Arterioscler. Thromb. Vasc. Biol.* **35**, 1975–1986 (2015).

226. Stenina, O. I. *et al.* Thrombospondin-4 and its variants: Expression and differential effects on endothelial cells. *Circulation* **108**, 1514–1519 (2003).

227. Hedlund, H., Mengarelli-Widholm, S., Heinegård, D., Reinholt, F. P. & Svensson, O. Fibromodulin distribution and association with collagen. *Matrix Biol.* **14**, 227–232 (1994).

228. Holst, C. R. *et al.* Secreted sulfatases Sulf1 and Sulf2 have overlapping yet essential roles in mouse neonatal survival. *PLoS One* **2**, (2007).

229. Dhoot, G. K. *et al.* Regulation of Wnt signaling and embryo patterning by an extracellular sulfatase. *Science (80-.).* **293**, 1663–1666 (2001).

230. Bezerra, J. A., Carrick, T. L., Degen, J. L., Witte, D. & Degen, S. J. F. Biological effects of targeted inactivation of hepatocyte growth factor- like protein in mice. *J. Clin. Invest.* **101**, 1175–1183 (1998).

231. Kretschmann, K. L., Eyob, H., Buys, S. S. & Welm, A. L. The Macrophage Stimulating Protein/Ron Pathway as a Potential Therapeutic Target to Impede Multiple Mechanisms Involved in Breast Cancer Progression. *Curr. Drug Targets* **999**, 1–12 (2010).

232. Lamprianou, S., Chatzopoulou, E., Thomas, J. L., Bouyain, S. & Harroch, S. A complex between contactin-1 and the protein tyrosine phosphatase PTPRZ controls the development of oligodendrocyte precursor cells (Proceeding of the National Academy of Sciences of the United States of America (2011) 108, 42 (17498-17503)). *Proc. Natl. Acad. Sci. U. S. A.* **109**, 4708 (2012).

233. Çolakoğlu, G., Bergstrom-Tyrberg, U., Berglund, E. O. & Ranscht, B. Contactin-1 regulates myelination and nodal/paranodal domain organization in the central nervous system. *Proc. Natl. Acad. Sci. U. S. A.* **111**, (2014).

234. Chen, Y. A., Lu, I. L. & Tsai, J. W. Contactin-1/F3 regulates neuronal migration and morphogenesis through modulating rhoa activity. *Front. Mol. Neurosci.* **11**, 1–13 (2018).

235. Kim, D. *et al.* Cell culture density affects the stemness gene expression of adipose tissue-derived mesenchymal stem cells. *Biomed. Reports* **6**, 300–306 (2017).

236. Patel, D. B. *et al.* Impact of cell culture parameters on production and vascularization bioactivity of mesenchymal stem cell-derived extracellular vesicles. *Bioeng. Transl. Med.* **2**, 170–179 (2017).

237. Rasmussen, J. G. *et al.* Prolonged hypoxic culture and trypsinization increase the pro-angiogenic potential of human adipose tissue-derived stem cells. *Cytotherapy* **13**, 318–328 (2011).

238. Bader, A. M. *et al.* Hypoxic preconditioning increases survival and pro-Angiogenic capacity of human cord blood mesenchymal stromal cells in vitro. *PLoS One* **10**, (2015).

239. Efimenko, A., Starostina, E., Kalinina, N. & Stolzing, A. Angiogenic properties of aged adipose derived mesenchymal stem cells after hypoxic conditioning. *J. Transl. Med.* **9**, 1–13 (2011).

240. Pilling, D., Fan, T., Huang, D., Kaul, B. & Gomer, R. H. Identification of markers that distinguish monocyte-derived fibrocytes from monocytes, macrophages, and fibroblasts. *PLoS One* **4**, 31–33 (2009).

241. Hu, Z., Van Rooijen, N. & Yang, Y. G. Macrophages prevent human red blood cell reconstitution in immunodeficient mice. *Blood* **118**, 5938–5946 (2011).

Appendices

Appendix. 1 Supplementary Figures

Directed *In Vivo* Angiogenesis Assay™:

The ability of BM-MSC CdM to induce an angiogenic response *in vivo* was assessed in a preliminary study using the directed *in vivo* angiogenesis assay (DIVAA™). DIVAA™ inserts were loaded with basement membrane extract supplemented with BM-MSC CdM generated under the various culture conditions and subcutaneously implanted into the flanks of NOD/SCID mice. After 14 days *in vivo* inserts were retrieved and imaged. Inserts containing CdM from BM-MSC cultured on DAT constructs qualitatively showed higher infiltration of red blood cells compared to TCP CdM (Figure 3.9A). To quantify endothelial cell infiltration into DIVAA™ angioreactors, DIVAA™ inserts were digested and infiltrating endothelial cells were stained with FITC-Lectin and quantified using a fluorescent plate reader. Surprisingly, there were no significant differences in FITC-Lectin uptake in DIVAA™ inserts when supplemented with CdM from BM-MSC cultured on the various substrates (Figure 3.9B).

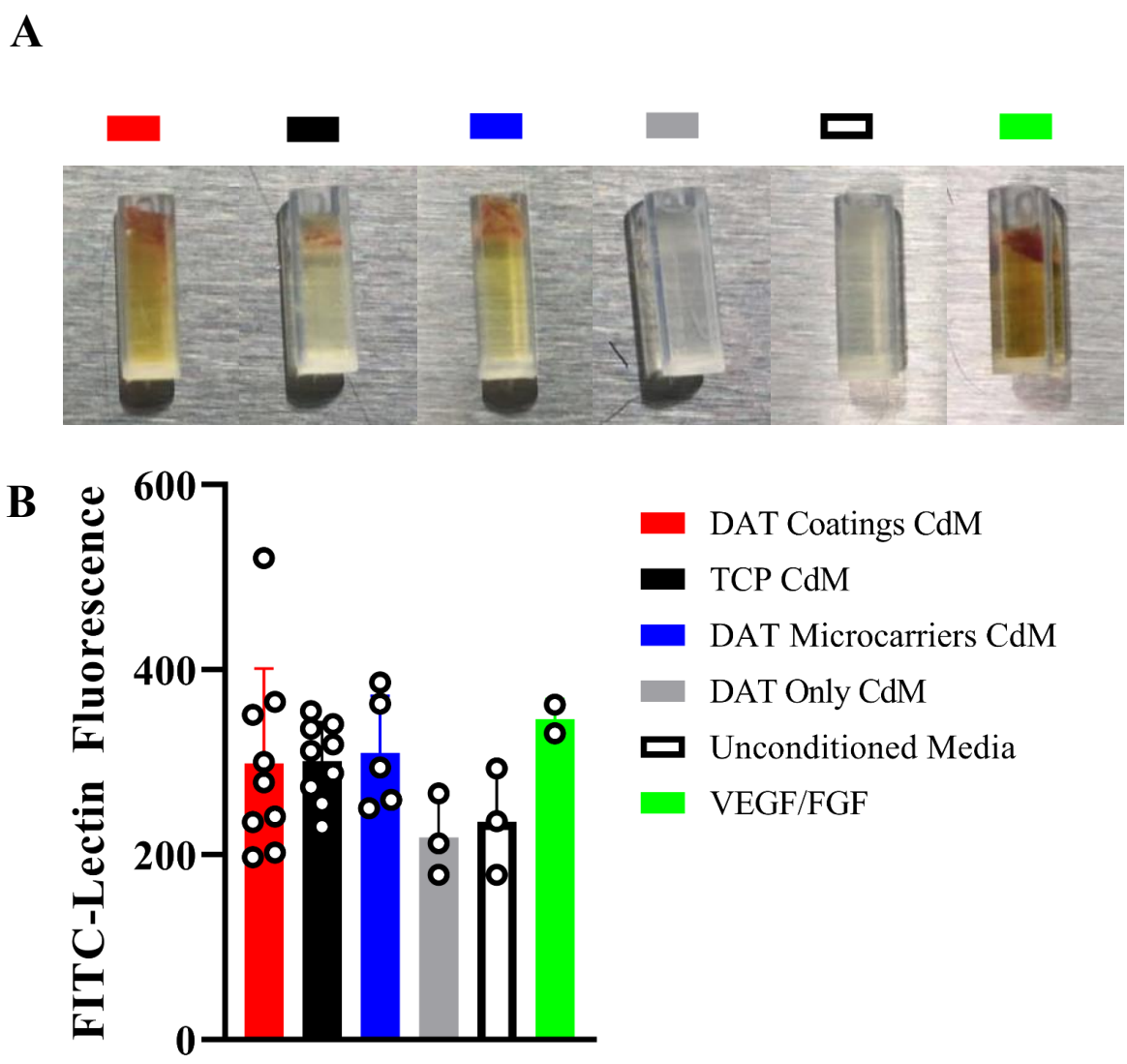

Supplementary figure 1. Preliminary analyses of cell infiltration into DIVAA™ inserts containing BM-MSC CdM. DIVAA™ inserts loaded with BM-MSC CdM generated under the various culture conditions were retrieved 14 days after subcutaneous implantation in NOD/SCID mice. Endothelial cell infiltration was quantified using lectin-FITC uptake. **(A)** Representative images of retrieved DIVAA™ inserts at 14 days post-implantation, with apparent red blood cell infiltration observed in the BM-MSC CdM groups and growth factor-supplemented positive controls. **(B)** Surprisingly, no significant differences in EC infiltration into DIVAA^{TM} inserts were detected when supplemented with BM-MSC CdM generated under the various culture conditions. Data represents Mean ± SD, showing CdM from three different BM donors (N=3, n=3-9). Analysis for statistical significance was performed using a one-way ANOVA followed by Tukey's post hoc multiple comparisons test. Quantitative analysis requires future optimizations.

Appendix. 2 Animal Use Protocol Approval

Western

2019-024:2:

AUP Number: 2019-024
AUP Title: Characterization of the Angiogenic Potential of Stem cells derived from Human Bone Marrow, Umbilical Cord Blood or adipose tissue.
Yearly Renewal Date: 06/01/2021

The YEARLY RENEWAL to Animal Use Protocol (AUP) 2019-024 has been approved by the Animal Care Committee (ACC), and will be approved through to the above review date.

Please at this time review your AUP with your research team to ensure full understanding by everyone listed within this AUP.

As per your declaration within this approved AUP, you are obligated to ensure that:

1) Animals used in this research project will be cared for in alignment with:
   a) Western's Senate MAPPs 7.12, 7.10, and 7.15
   http://www.uwo.ca/univsec/policies_procedures/research.html
   b) University Council on Animal Care Policies and related Animal Care Committee procedures
   http://uwo.ca/research/services/animalethics/animal_care_and_use_policies.html
2) As per UCAC's Animal Use Protocols Policy,
   a) this AUP accurately represents intended animal use;
   b) external approvals associated with this AUP, including permits and scientific/departmental peer approvals, are complete and accurate;
   c) any divergence from this AUP will not be undertaken until the related Protocol Modification is approved by the ACC; and
   d) AUP form submissions - Annual Protocol Renewals and Full AUP Renewals - will be submitted and attended to within timeframes outlined by the ACC. http://uwo.ca/research/services/animalethics/animal_use_protocols.html
3) As per MAPP 7.10 all individuals listed within this AUP as having any hands-on animal contact will
   a) be made familiar with and have direct access to this AUP;
   b) complete all required CCAC mandatory training (_training@uwo.ca); and
   c) be overseen by me to ensure appropriate care and use of animals.
4) As per MAPP 7.15,
   a) Practice will align with approved AUP elements;
   b) Unrestricted access to all animal areas will be given to ACVS Veterinarians and ACC Leaders;
   c) UCAC policies and related ACC procedures will be followed, including but not limited to:
      i) Research Animal Procurement
      ii) Animal Care and Use Records
      iii) Sick Animal Response
      iv) Continuing Care Visits
5) As per institutional OH&S policies, all individuals listed within this AUP who will be using or potentially exposed to hazardous materials will have completed in advance the appropriate institutional OH&S training, facility-level training, and reviewed related (M)SDS Sheets, http://www.uwo.ca/hr/learning/required/index.html

Submitted by: Copeman, Laura
on behalf of the Animal Care Committee
University Council on Animal Care

Appendix. 3 Human Tissue Ethics Approval

Western Research

Date: 17 July 2020

To: Dr. Lauren Flynn

Project ID: 105426

Study Title: Tissue Engineering with Adipose-derived Stem Cells

Application Type: Continuing Ethics Review (CER) Form

Review Type: Delegated

REB Meeting Date: 04/Aug/2020

Date Approval Issued: 17/Jul/2020

REB Approval Expiry Date: 13/Aug/2021

Dear Dr. Lauren Flynn,

The Western University Research Ethics Board has reviewed the application. This study, including all currently approved documents, has been re-approved until the expiry date noted above.

REB members involved in the research project do not participate in the review, discussion or decision.

Western University REB operates in compliance with, and is constituted in accordance with, the requirements of the TriCouncil Policy Statement: Ethical Conduct for Research Involving Humans (TCPS 2); the International Conference on Harmonisation Good Clinical Practice Consolidated Guideline (ICH GCP); Part C, Division 5 of the Food and Drug Regulations; Part 4 of the Natural Health Products Regulations; Part 3 of the Medical Devices Regulations and the provisions of the Ontario Personal Health Information Protection Act (PHIPA 2004) and its applicable regulations. The REB is registered with the U.S. Department of Health & Human Services under the IRB registration number IRB 00000940.

Please do not hesitate to contact us if you have any questions.

Sincerely,

The Office of Human Research Ethics

Note: This correspondence includes an electronic signature (validation and approval via an online system that is compliant with all regulations).

Appendix 4. Permissions and Requests

Figure 1.1 Permission

JOHN WILEY AND SONS LICENSE
TERMS AND CONDITIONS

Jun 25, 2021

This Agreement between Univeristy of Western Ontario -- Yehia Moharrem ("You") and John Wiley and Sons ("John Wiley and Sons") consists of your license details and the terms and conditions provided by John Wiley and Sons and Copyright Clearance Center.

License Number	5070871128771
License date	May 16, 2021
Licensed Content Publisher	John Wiley and Sons
Licensed Content Publication	Stem Cells
Licensed Content Title	Concise Review: Cell Therapy for Critical Limb Ischemia: An Integrated Review of Preclinical and Clinical Studies
Licensed Content Author	David A. Hess, Mohammed Al-Omran, Subodh Verma, et al
Licensed Content Date	Jan 3, 2018
Licensed Content Volume	36
Licensed Content Issue	2
Licensed Content Pages	11
Type of use	Dissertation/Thesis

Figure 2.1 Permission

SPRINGER NATURE LICENSE
TERMS AND CONDITIONS

Jun 25, 2021

This Agreement between Univeristy of Western Ontario -- Yehia Moharrem ("You") and Springer Nature ("Springer Nature") consists of your license details and the terms and conditions provided by Springer Nature and Copyright Clearance Center.

License Number	5076801278281
License date	May 26, 2021
Licensed Content Publisher	Springer Nature
Licensed Content Publication	Springer eBook
Licensed Content Title	Decellularized Adipose Tissue Scaffolds for Soft Tissue Regeneration and Adipose-Derived Stem/Stromal Cell Delivery
Licensed Content Author	Pascal Morissette Martin, Arthi Shridhar, Claire Yu et al
Licensed Content Date	Jan 1, 2018
Type of Use	Thesis/Dissertation
Requestor type	academic/university or research institute
Format	electronic
Portion	figures/tables/illustrations

Figure 2.2 Permission

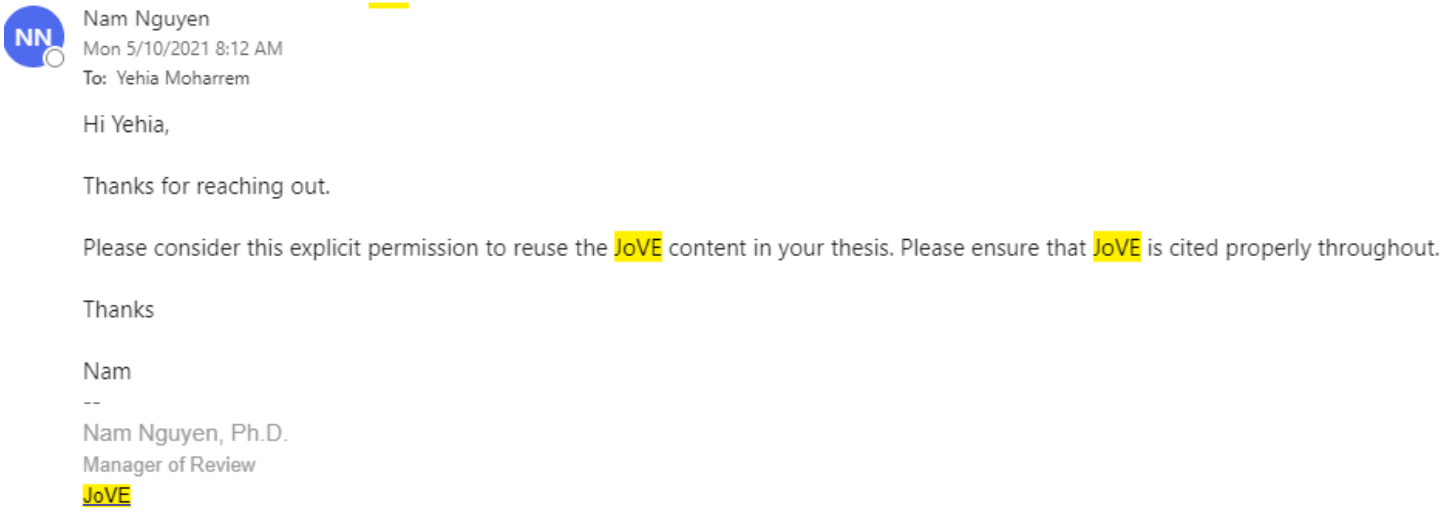

Nam Nguyen
Mon 5/10/2021 8:12 AM
To: Yehia Moharrem

Hi Yehia,

Thanks for reaching out.

Please consider this explicit permission to reuse the JoVE content in your thesis. Please ensure that JoVE is cited properly throughout.

Thanks

Nam
--
Nam Nguyen, Ph.D.
Manager of Review
JoVE

Curriculum Vitae

EDUCATION BACKGROUND

Western University, Physiology and Pharmacology, London, ON 2019 - Present

Master's of Science

Thesis Title: Characterization of mesenchymal stromal/stem cells on decellularized adipose tissue constructs for the treatment of critical limb ischemia.

Western University 2018

Bachelor of Medical Science (Honours). Interdisciplinary Medical Science

CONFERENCE PRESENTATIONS

Abstract Poster Presentation, **Moharrem, Y.,** Flynn, L., & Hess, D. (2020 October 26 – 28) *Characterization of Mesenchymal Stromal/stem Cells on Decellularized Adipose Tissue Constructs for the Treatment of Critical Limb ischemia* [conference poster presentation]. Till & McCulloch (TMM) conference. Vancouver, Canada.

- Showed that biomaterial fabricated from decellularized tissue enhanced bone marrow stem cell viability and proliferation while maintaining regenerative markers.
- Conference was virtual due to COVID-19.
- Abstract Competition Award Winner: https://stemcellnetwork.ca/training/workshops/travel-award-winners/
-

Abstract Oral Acceptance, **Moharrem, Y.,** Jalali, A., Hu, J., Fox, S., Swinamer, S., Rayman, R., Chua, K., Harle, C., Phillip, J., Dobkowoski, W., Romsa, J., Vezina, W., Chu, M., Teefy, P., Menkis, A., Boyd, D., & Kiaii, B. (2020 June 4 – 6). *20-year Single-center Experience Of Robotic-assisted Coronary Artery Bypass Grafting: Long-term Follow-up And Graft Patency* [conference oral presentation]. International Society of Minimally Invasive Cardiothoracic Surgery (ISMICS). Warsaw, Poland.

- Postponed due to COVID-19.
- Work showed excellent long-term quality of life, survival, and graft patency of patients that underwent robotic-assisted CABG.
- https://meetings.ismics.org/abstracts/2020/C32.cgi

Abstract Poster Acceptance, Chua, K., **Moharrem, Y.,** Jalali, A., Fox, S., Harle, C., Jones, P., Iglesias, I., Lavi, S., Teefy, P., & Kiaii B. (2020 June 4 – 6) *Clinical outcomes of Robotic Assisted Hybrid Coronary Artery Revascularization with Graft Patency at 10 Years* [conference poster presentation]. International Society of Minimally Invasive Cardiothoracic Surgery (ISMICS). Warsaw, Poland.

- Postponed due to COVID-19.
- Work showed long-term benefits of robotic-assisted cardiac surgeries combining CABG and percutaneous coronary intervention.
- https://meetings.ismics.org/abstracts/2020/PC56.cgi

Abstract oral presentation, Chua, K**., Moharrem, Y.,** Jalali, A., Alukayli, M., Harle,

C., Teefy, P., & Kiaii, B. (2019 December 6 – 8) *10 Year Patency And Clinical Outcomes Of Robotic Assisted Hybrid Coronary Artery Revascularization* [oral conference presentation]. International Coronary Congress (ICC), New York, NY.

- Presented in place of first author due to flight cancellation.
- Work showed superiority of hybrid robotic-assisted CABG combined with percutaneous coronary intervention.
- https://internationalcoronarycongress.com/program/2019/29.cgi

RESEARCH EXPEREINCE

2019 – Present. Masters Student. Dr. David Hess & Dr. Lauren Flynn. **Characterization of mesenchymal stromal/stem cells on decellularized adipose tissue constructs for the treatment of critical limb ischemia**. CIHR and NSERC.

- Collected and decellularized human adipose tissue.
- Optimized bone marrow stem cell growth on bio-scaffold.
- Showed that adipose tissue scaffolds enhance stem cell proliferation and viability while maintaining the conserved stem cell functional marker aldehyde dehydrogenase using flow cytometry.
- Collected conditioned media and assayed for *in vitro* pro-angiogenic capacity.
- Generated surgically induced limb ischemia in mice to assess *in vivo* revascularization potential.

2016 – Present, Clinical Research Associate. Dr. Bob Kiaii and Dr. Jonathan Romsa. **Long-term efficacy of robotic-assisted coronary artery bypass grafting.**

- Coordinated cardiac surgery and nuclear medicine departments.

- Showed excellent long-term graft and stent patency outcomes of robotic-assisted CABG.
- Recruited patients and organized MIBI and CT scans to assess graft and stent patency.
- Administered quality of life questionnaires and assessed patient response.
- Analyzed, interpreted, and presented CT and MIBI scan results.

2016 – 2018, Undergraduate Researcher Assistant. Dr. Chil-Yong Kang. **Ebola antibody neutralization assay.** CIHR.

- Performed molecular cloning to insert Ebola glycoprotein in VSV viral vector containing GFP.
- Performed PCR, bacterial transformation, and plasmid isolation.
- Transfected human cells lines with VSV vector with lentivirus to generate recombinant particle expressing GFP and Ebola surface protein.
- Quantified virus infectivity by infecting cells with different doses.

2016. Summer Research Student**.** Dr. Christopher Brandl's Lab in **Biochemistry**.

- Various projects examining how protein mistranslation and tRNA variation leads to cell malfunction and cancer.
- Performed bacterial and yeast culture, transformation, PCR, and DNA isolation.

2014 – 2015. Neurosurgical Biomedical Research Assistant**,** Dr. Roy Eagleson & Dr. Sandrine De Ribaupierre, **Human-Computer interface design for surgical skills.**

- Researched software for neurosurgery simulation training.
- Compiled, analyzed and presented brain CT scans to team.

RESEARCH-SPECIFIC AWARDS & SCHOLARSHIPS

$200, Ontario Institute of Regenerative Medicine Abstract Competition Award	2020
$3'000, Cardiac Surgery Research Grant	2020

- Travel award for presenting at ISMICS conference in Poland.
- Award granted but not received due to conference cancellation (COVID-19)

$2'000, Cardiac Surgery Research Grant	2020

- Travel award for presenting at the ICC conference in New York.

$3'000, Western Graduate Research Scholarship	2019-2020
$2'000, Western Entrance Scholarship of Excellence	2014-2015